Ocean Energy

The Waves of the Future

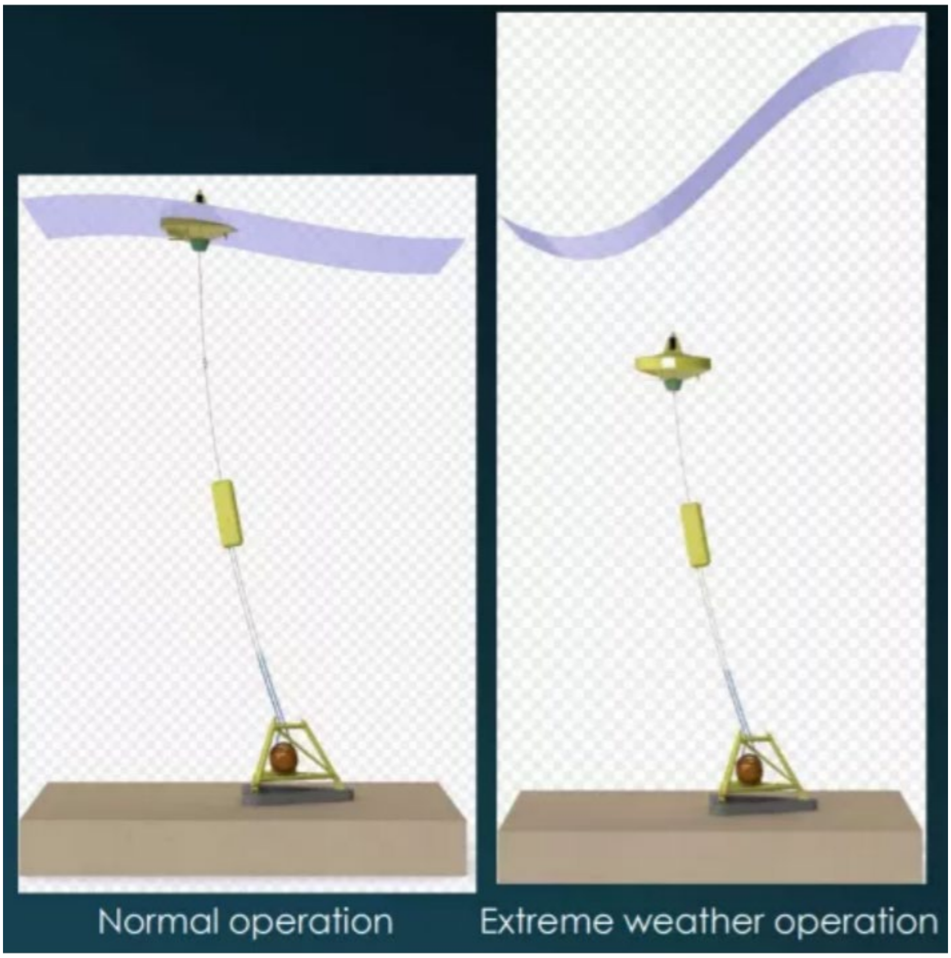

Aksjonærbrev 2022/03

Dato: 11. desember 2022

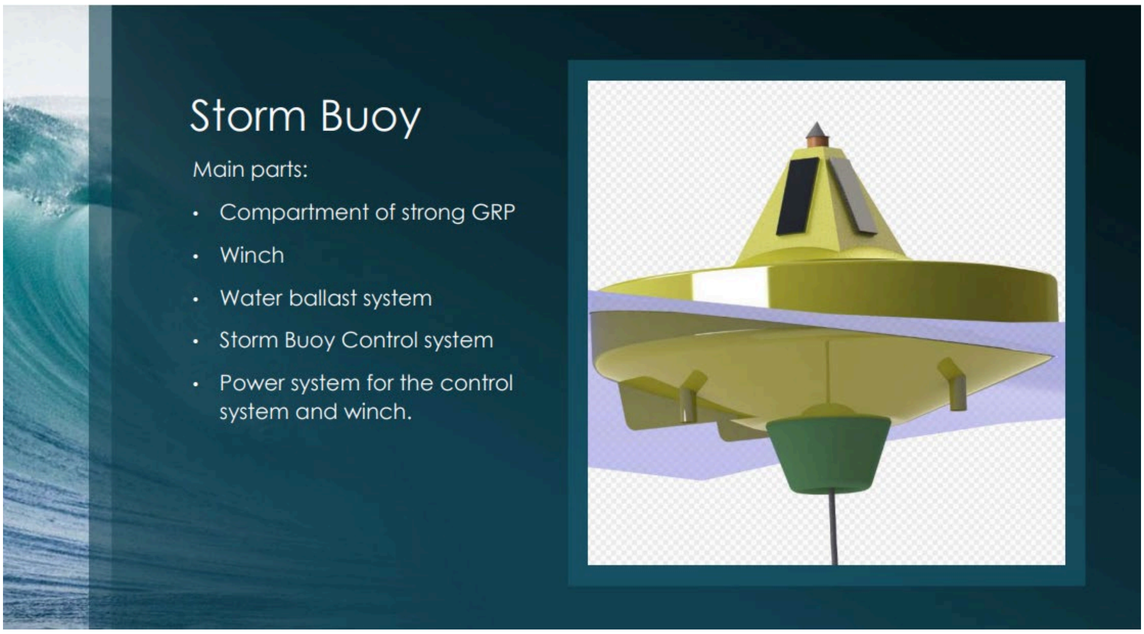

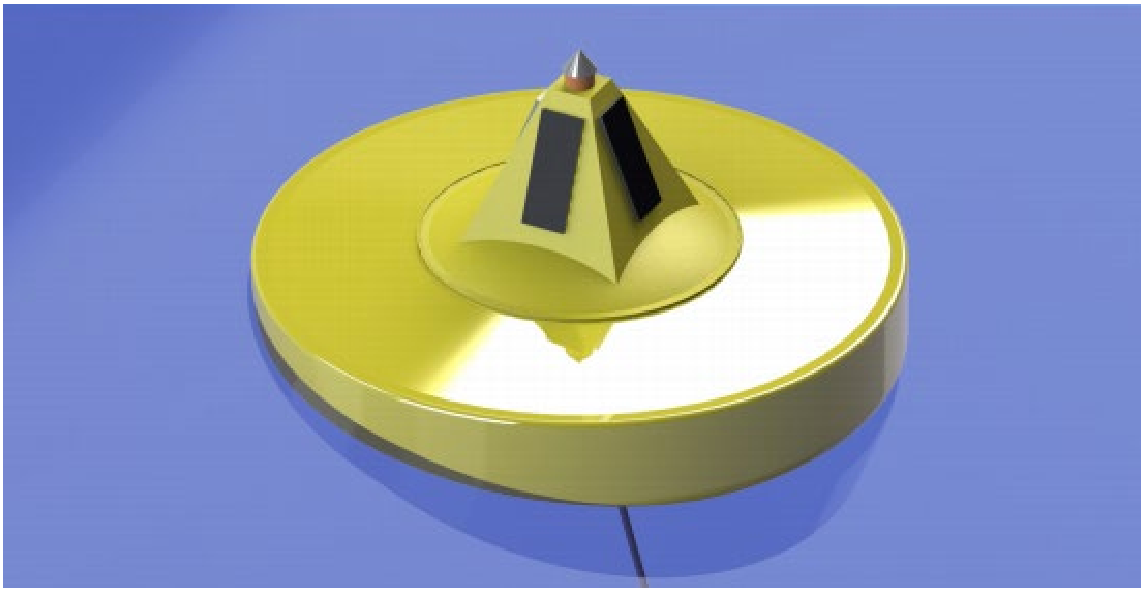

«All truths go through stadies. First, they are ridiculed. Thereafter strongly opposed. At last, they are accepted as completely evident. »

Arthur Schopenhauer (1788-1860)

Ocean Energy AS

Aksjonærbrev 2022/03

Dato: 11. desember 2022

Til: Selskapets aksjonærer.

Informasjon om nyheter før Jul og Nyttår 2022.

Vi vil her ta en kort oppsummering før Nyttår 2022 – det blir en oppsummering etter samme mal som ved forrige aksjonærbrev og kun aktuelle nyheter omtales.

Norsk meglerhus engasjert for å innhente penger til Hellas-Avtalen.

Som omtalt tidligere ble den første store anledning som virkelig viser hvilket fokus vi nå har fått på bølgekraft ***i utlandet*** vårt offisielle besøk i Hellas denne våren hvor vi under en offentlig seremoni på ONEX Nerion Shipyards på øya Syros med endog Hellas sin statsminister og ditto presse til stede signerte en general-avtale om samarbeid for Hellas og noen omliggende land for å satse på disse sårt tiltrengte nye energiløsningene med følgende representanter:

Fra venstre vår partner professor Nikos Milonas, styreformann Egil Holland, adm. sekretær Siv Vågsholm, industrialist, nå partner og verfts-eier: gresk-amerikaneren Panos Xenokostas, guvernøren av South Aegean Region Georgios Hatzimarkos – co-oppfinneren av systemene Tov Westby stående i ivrig samtale med statsministeren av Hellas - Keikos Mitsotakis – som en uvanlig hyggelig og genuint bølgekraft-interessert kar med svært teknisk innsikt nest til høyre ved bordet. Resten er statsministerens sekretærer og livvakter.

Som tidligere nevnt og for å kort oppsummere igjen så har denne utviklings- og produksjonskontrakten vært i en prosess over lengre tid og gjennom en lang evaluering. Ikke minst er konseptets revolusjonerende CO2-tall (CO2-koeffisient på kun 7,5) kombinert med de omtalte skremmende FN-rapportenene med «Kode Rød». I tillegg har vi opplevd at Europa eksploderer med et skrikende og akutt behov for ny grønn energi (se bare strømprisen i Norge nå – i Hellas er den enda høyere!). Dette påvirket konsernets markante gründer – Panos Xenokostas – til å nå personlig å gå inn for vårt konsept!

Med denne tunge partneren på plass forsatte vi så prosessen med Innovasjon Norge iht. deres tidligere anbefalinger om å finne en «tung» lokal partner i Hellas for videre fremdrift.

Søknaden ble derfor innlevert sammen med partnerne ETB og ONEX og det overaskende svaret kom først nå i høst.

Det viste seg igjen å være «negativt» i den forstand at Innovasjon Norge nå etter nye retningslinjer – nå krever at man har hele «egenkapitalen» for vår 50% andel av prosjektet på plass – da ikke kapitalkomponenten som før bare regnskapsmessig i selskapets øvrige verdier og i Aksjekapital samt partnere bak med stor tyngde – men nå i form av ren «cash – eller bankgaranti» stående på egen konto for formålet!

Man kan altså ikke som i mange prosjekter vi har forsert tidligere **først** søke og få en godkjent søknad fra Innovasjon Norge – og **så** gå ut og hente den «private andelen» av pengene i det åpne markedet med Innovasjon Norges «approved» som en garanti for meglerhuset…

Men – nå må man altså først skaffe egenandelen av finansieringen FØR Innovasjon Norge vil gi en godkjenning av søknaden - ut fra nye krav til «gjennomføringsevne»!

Dette gjør jo en velkjent og innarbeidet prosess – (som har vært så grei i andre tidligere prosjekter) - noe mere vanskelig og ble da dessverre en «forsinkelse» i det vi nå følte var en «stright forward» prosjektfremdrift med Hellas gruppen på plass…

Siden vårt budsjett samlet for en endelig utvikling av en full scale operativ prototype og uttesting av denne i Hellas gjennom 1 helt driftsår er på 20 Millioner kroner – må vi derfor «hente inn» minst 10 millioner kroner i markedet for å møte disse kravene.

Den prosessen er da igangsatt i høst og ett Norsk meglerhus er på saken og vi er i dialog med ytterligere ett mere internasjonalt meglerhus i disse dager etter rådgiving fra en «gammel rev» i megler-bransjen vi har tilknyttet oss som konsulent for å finne den rette partner snarest mulig.

Det må tillegges at vi i dag har en meget god dialog med Innovasjon Norge – og at vi bare må få disse formalitetene på plass – enten via et meglerhus i Norge som vi har igangsatt – eller ved at våre partner i Hellas over Nyttår får en mere sentral rolle samlet i denne finansieringen. En prosess som vi også diskuterer i disse dager…

Bølgekraft er i alle fall i ferd med å bli tatt inn i varmen nå – også på hjemmebane …

Etter suksessen i Hellas i mars ble det nye takter da vi ble invitert på Innovasjon Norge og Utenriksdepartementet sitt Svensk-Norske seminar i mai. Her i Gøteborg under meget hyggelig treff med to energiske og inspirerende herrer fra Innovasjon Norge og Regjering.

På bildet er:

Sjefen for Innovasjon Norge Håkon Haugli (fra venstre), Co-founder av Ocean Energy Tov Westby, adm. Sekretær Siv Vågsholm og Næringsminister Jan Christian Vestre.

Den potensielt nye partner i Malaysia! Meget suksessfullt besøk der i november med flere potensielle partnere og mulighet for finansiering.

Ut fra våre erfaringer i Hellas denne våren om at enthusiasmen for bølgekraft er langt større utenfor Norges grenser på grunn av de mange tidligere mislykkede bølgekraft-forsøk her hjemme på 80-tallet - så prøver vi mere og mere å «søke ut» for å finne potensielle investorer og partnere.

I denne sammenheng har vi lenge hatt et spor til Malysia som vi har ønsket å følge opp straks vi kunne reise ditt problemfritt igjen for Corona – og den muligheten åpnet seg i november.

Dette sporet dit er ganske unikt pga. en gammel kontakt gründerne har hatt i mange år med en McKinsey mann som jobbet der nede tidligere i over 30 år med store prosjekter som bla. bygging av Kuala Lumpur flyplass, bygging av 500 KV linjen mellom Singapore og Thailand hvor han fikk inn Statnett og Linjebygg fra Norge som deres første store utenlands-jobb – samt at han introduserte Køfri-systemet fra Trondheim inn i hele Kina (over 16 kontrakter) og forøvrig over hele Asia. Videre var han også i den tiden Chief Representative for Volvo Construction i Malysia og i det senere Adm. Dir for Volvo Equipment AB Central Europe. Denne karen har et unikt nettverk der nede fortsatt på absolutt høyeste plan – og sogar var den tidligere Kongen der nede hans forlover i sin tid når han giftet seg der inn i de kretsene. Så hans kontaktflate og nettverk der nede er derfor helt unikt.

Den gode kontakten med denne konsulenten ble som nevnt etablert allerede i 2010 i forbindelse med at Gründerne fra Ocean Energy da var engasjert i en større shipping-avtale i Malaysia sammen med bl.a. Pareto Corporate Singapore den gangen – og at denne kontakten og interessen for havenergi nå har modnet siden det.

Han tok derfor kontakt med oss for en tid tilbake og tilbød seg å introdusere oss til omtalte selskap YTL, men nå også flere andre alternativer – eller paralelle spor - og vi reiste da ned nå i november når Corona-begrensningene var helt fjernet.

Målet vårt med dette initiativet var da å få signert et «Letter Of Intent» etter noen lignende retningslinjer som Hellas-avtalen og med målsetting om å bygge – helt parallellt og uavhengig – en alternativ 1:1 prototype der nede også.

Dette for å ha flere parallelle spor fremover som vil øke den etterlengtede fremdriften mot å komme i mål med et endelig industrielt masseprodukt for vårt selskap raskest mulig.

Forskjellen på avtalene vi da ønsket å inngå der nede - i forhold til Hellas-avtalen - er at partnerene der nede skal stå for den vesentlige delen av finansieringen av denne prototypen alene – mot å tilsvarende å få en «50/50 partneravtale» på produksjon og salg av produktet der nede i regionen sammen med vårt selskap.

Turen gikk over all forventing og mens vi ventet på møtene med YTL og hans kontakter der og flere andre potensielle kontakter i Kuala Lumpur fikk vi ganske tidlig i prosessen helt overraskende «audiens» og besøk av selveste Prinsen av Malaysia(!) (ja - tro det eller ei!...) – altså sønnen av den tidligere Kongen der nede – Tunku Mahmud - og gode venn av Knut Regenius Pettersen (som McKinsey mannen heter) – som med et meget behagelig og diskret sikkerhetsoppbud kom helt uformellt «slentrende» i fritidsklær inn på vårt hotell i en avlukket lobby avdeling, som først ble meget sikkerhets-sjekket!

Vi ble selvssagt helt «starstruck» av dette og trodde dette kun var en gest fra Pettersen bare for at vi skulle få ta «en selfie» med selveste Prinsen – men nei:

Prinsen er teknolog og var genuint iteressert i vårt prosjekt! – fordi han hadde fått masse forhåndsinformasjon fra Pettersen (som vi ikke var klar over og var en overraskelse til oss!...) og hadde tydligvis selv vært engasjert i et tidligere prosjekt i Malakka-stredet som hadde blåst bort – og Prinsen forklarte ivrig at Storm-Bøyen vår – det var svaret for å løse Bølgekraft-gåten det(!)…..

(Du verden – endelig «noen som skjønner det»!…. Det måtte altså intet mindre enn «Prinsen av Malysia» til for endelig å få full aksept for vårt konsept!... 😊😊).

Så fra å være noe som vi trodde var et kort besøk for å hilse på «Uncle Knut» som han kaller Knut Pettersen! – endte dette med et lenger møte hvor han konkret sa at dette var noe han ville engasjere seg personlig i og at han er beskytter for et Universitet der nede ved Mallakka som har Maritim avdeling og «skipstank med bølgesimulator» og at han faktisk selv plutselig under presentasjonen faktisk kom med forslaget om at vi satte opp et felles selskap der nede og laget et «joint venture» med vårt selskap med Storm Bøyen, samt han, Universitet og Tenaga Berhard!... Og han kunne skaffe finansiering – sa han!

(Tenaga er som «Statnett og Statkraft» i Norge hvor Prinsen er sentral…)

Se selskapet her: https://www.tnb.com.my/

Så vi hadde fruktbare diskusjoner i flere timer – både teknologisk og finansiellt og ble enige om å følge opp denne tråden straks vi kom hjem.

Og den prosessen og dialogen er nå i gang og ledes fra vår side av Egil Holland og Tov Westby med Knut Regenius Pettersen som rådgiver – direkte med Prinsen nå daglig!

Så vi regner med å ha et «Letter Of Intent» og en kontraktuell struktur her på plass før Jul! Da igjen med de betingelsene at vi stiller med patentene og teknologien og de stiller med finansieringen – og vårt felles selskap får da enerett for dette i Malaysia. Og det «skader» jo da ikke å ha med Prinsen der nede som entusiast og pådriver – som også blir Konge der om 10 år!...

En særs uformell Prins av Malaysia - her i behaglig samtale først i møtet med sin «Uncle Knut», adm. Sekretær Siv Vågsholm og Co-founder av Ocean Energy Tov Westby.

Det viste seg jo at Prinsen er «Data-mann» han også som Gründer Tov Westby så de fikk en meget god tone og dialog rundt konseptet og teknologi som sådan! Han er «beskytter» av et Universitet som driver med maritim teknologi som kan bli engasjert i et nært samarbeide med våre ingeniører – når vi får på plass ett avtaleverk.

Svært behagelig møte med en fantastisk hyggelig, smart og uformell Prins som sa til oss at han ønsket å bli partner rundt bølgekraft for Malaysia!

Hans navn er intet mindre enn:

Sultan Tenku Muhamad Firdaus Mahmood Tenku Zambri

Dette kan jo bli en meget spennende partner for selskapet.

(Og selvsagt er det fotball i bakgrunnen – de er jo helt VM gale der nede…).

Det neste sporet – som var det originale sporet som bragte oss ned i første omgang – det er det store konglongmerat-selskapet YTL Berhard.

Den svært gode kontakten med YTL ble som nevnt etablert allerede i 2010 i forbindelse med at impliserte fra Ocean Energy da var engasjert i en større shipping-avtale i Malaysia – og at denne kontakten og interessen for havenergi nå har modnet siden det. Men den bygger selvsagt primært også på Pettersens mangeårige kontakter med denne familien lenge før det.

Se mer om selskapet på:

https://www.ytl.com/

Vår kontakt i YTL er en meget sentral person i selskapet som i dag er «nestor» i selskapet som er børsnotert - men styres som et familidynasti som har flertallet der.

Vår mann - Joe Seaton - sin far var den som hjalp Gründeren av YTL i 1954/55 med start-finasieringen av selskapet og har siden det vært helt sentral i selskapet gjennom «nesten 3 generasjoner» – og han er da også veldig nær denne gründerens etterkommer Dato Sri Francis Yeoh som styrer selskapet i dag:

Se video av han:

https://www.youtube.com/watch?v=6kg5T2Rta9Q

Han var dessverre på reise – men Joe Seaton er altså på en måte hans «Consigliere/rådgiver» - så han fikk da lett satt opp møte med den som er sentral i YTL Power og ny teknologi – P.K. Chin.

Vi fikk da møte hos han med noen andre ingeniører ut og inn og selvsagt Joe Seaton selv – men selve essensen av møtet var at han kom inn – snakket kjapt på «Amerikansk dialekt» og sa rett ut:

Dette har jeg tro på - for dette vil virke(!)

Så hadde han «klippet og limt» voldsomt sammen av alt jeg har sendt over tidligere og laget en hel mappe på dette og samstemt det mot andre «ikke storm sikre» prosjekter» som har vært kjørt der nede i Malakka stredet tidligere og blåst bort.

Så hele møtet gikk egentlig først ut på å forstå mere av den tekniske «storm sikrings løsningen» og så til selve essensen vår:

Kunne YTL tenke seg å delta i dette og finansiere en utvikling av noe slikt!?

Og svaret ble da på en måte både nedslående og oppløftende ved at han svarte og forklarte – om at det akkurat nå var på gang et generasjonsskifte i ledelsen så vi måtte «lirke oss inn» på disse nye i familien med ideen «pø om pø» og at disse nye nå neppe kastet seg over «nye utviklingsprosjekter» på sparket akkurat helt med det første….

Men, JA - dette er hyper interessant for YTL – på litt sikt – rundt Singapore hvor de «har et problem» med tilgang på energi – men at dette ikke kan gjøres over natten ….

Så kort fortalt ble vi enige om at vi måtte ta sporet mot YTL «step by step» og ikke påregne noe konkret akkurat med de FØR vi hadde en mere ferdig prototype og pris/produksjon og vise til – og at de da vil kunne bli en betydelig kunde!

Men på den annen side, sa han – hvis vi fikk i gang et utviklingsprosjekt der nede lokalt (som med Prinsen) da kunne de muligens «kaste seg på» ganske hurtig.

Dette fikk vi da formalisert med et «Letter Of Understanding» - og så får vi gå derfra og har da YTL absolutt med på lag – selv om de da kommer med «litt om litt» - men at konseptet nå er «tuftet» på topp plan og at vi holder løpende kommunikasjon fremover!...

Nestor og «7 far i huset» i YTL – Joe Seaton møtte oss utenfor den nye YTL-skyskraperen deres. En eldre og distingvert, uformell, stillferdig og behagelig mann som styrer meget mere enn man kan tro der i «butikken» - ja, dette er litt som et «pust» fra boken «Noble House» av James Clavell fra Hong Kongs Trading-familie dynastier … Joe Seaton er for øvrig av Portugisisk herkomst og hans familie var sentral i «Malaysia» (Malay den gangen) før det engelske imperiet tok over som kolonimakt fra Portugiserne og etablerte Øst Indiske Handelskompani der i 1824. Så her er det mye sus av fordums forfinede historier og diskret rikdom og kontinentets forandringer og en eventyrlig selskaps-oppbygging siden 1955 – da YTL starter som en liten sementfabrikk – med penger fra faren til Joe Seaton til Gründeren selv Yeoh Tiong Lay - og i dag er YTL Berhard blant Malysias største børsnoterte selskaper og driver med nær sagt alt.

Dagens lange møte ble avsluttet med en fantastisk like lang lunch i YTL sin elegante Direksjons Lounge, som var fornemt utformet i kinesisk høy-klassisk stil. Her spør man definitivt IKKE om kniv og gaffel(!), men «sliter» diskré med sine håpløse pinner i all høflighet og respekt! …

Interessen til Tekn. Direktør for nye prosjekter i YTL Power P.K. Chin (eller bare PK som han kaller seg) var upåklagelig og han hadde også gjort sin «hjemmelekse» som også Prinsen hadde gjort. Her hadde han utskrifter av vår hjemmeside med Patentene og våre tekniske dokumenter og klippet de ut og sammenlignet de med flere av de mislykkede forsøk der nede i Malakka-stredet som var blåst bort. Det er jo så artig å møte ledere som virkelig har interesse og engasjement og ser de store mulighetene i dette.

Fra venstre Knut Regenius Pettersen, Co-founder Tov Westby, Joe Seaton og tekn.sjef YTL Power P.K. Chin.

Så det tredje sporet – som også dukket overraskende postivt opp - fra gamle kjenninger av Gründerne i Ocean Energy fra shipping-prosjektet der nede i 2010.

Pettersen hadde også informert sin mangeårige partner - og faktisk gamle bekjente av oss - Dato Sri Eric Wong der nede, (Dato Sri – er det samme som Sir der nede når man blir adlet av Kongen …) - og hans nye høyre hånd Lucas Kong som er en super kjapp Engelsk-utdannet MBA og Siv.ing. (Tidligere CFO i en av de nest største bankene i Kuala Lumpur - så Eric Wong har virkelig klart å trekke inn topp folk i ledelsen siste årene).

Denne fornyede kontakten ble da initiert på grunn av våre tidligere forhold til disse og Eric Wong har til og med i sin tid besøkt Norge og Gründer Tov Westbys private familie-sæter tilbake tidlig på 2010-tallet – men har utviklet sin forretningsvirksomhet betydelig siden den gangen gjennom sitt private selskap MPF ASIA PTE. LTD som igjen er tungt involvert i flere noterte selskaper innen shipping, bergverk, olje og høyteknologi.

Ja – bare ved å dømme etter deres mange ansatte og kontoret rett ved «Petronas Twin Towers» midt i Kuala Lumpur har nok Eric Wong utviklet sin business betydelig siste 12 år…

Og når det da hadde alt ryktes om Ocean Energy sine møter med både Prinsen av Malaysia og med den sentrale ledelsen hos YTL… – vel så gjorde det også denne grupperingen meget ivrige og interesserte! (Her la jo Pettersen opp et smart spill…).

Vi tok derfor flere løpende møter med disse og presenterte igjen vår teknologi og ønske om finansierings- og forretningspartner der nede de siste dagene før hjemreise.

Så uten å utdype alle detaljene så fikk vi her også da et tilbud før avreise – etter samme lest som vi hele tiden har ønsket og samme forslag som fra Prinsen – nemlig at vi da eventuelt setter opp et felles selskap i Malaysia og at Wong-gruppen henter inn alle penger der nede i sitt miljø for utviklingen og uttestingen av en prototype og at vi stiller med Patentene, teknologi og våre ingeniører fra Norge der nede. Og at vårt felles 50/50 selskap der nede da får enerett til salg og produksjon for visse land. I dette case kan det være Indonesia og Japan.

Så vi kan altså fint kjøre dette parallelt med Prinsen og Tenaga Berhard og hans primære ønske om enerett i Malaysia -. og så senere YTL Berhard med tilsvarende ønske om enerett i Singapore …

To meget TUNGE aktører inn mot flere bølgekraft-markeder rundt Malaysia – Lucas Kong og Sjefen selv for Malyasia CSEEC (Stort Engineering selskap innen kraftverk og oljeindustri) - Ellis Lang - som de inviterte med på lag i møtene og som gjerne blir med i konsortiet - i ivrig diskusjon med Gründer Tov Westby – og disse KAN også mye om kystlinjene rundt i området pga. sin store aktivitet mot lokal oljevirksomhet.



Fantastiske disiplinerte, entusiastiske og kjappe super-ingeniører å diskutere med. Som skjønner problemets kjerne og rett på sak.

Så der står vi akkurat nå som dette skrives i kontraktuelle forhandlinger videre med disse direkte fra Norge og dette er jo et fabelaktig resultat å ende opp med flere «friere» etter en så kort tur til Asia – og dette må virkelig krediteres opplegget og kontaktene til Knut Regenius Pettersen – samt også den lille OCE-gruppens gode evne til å «kommunisere og selge» inn sitt konsept i møtene.

Andre potensielle kunder i utlandet – igjen gjenopptakelse av gamle kontakter fra den tiden Gründerne arbeidet inne oljebransjen World Wide..

Kort historikk

Vi har jo i tidligere aksjonærmeldinger så vidt nevnt dette med kontakten med Gambia, eller «The Gambia» som vel er den formelle betegnelsen på staten.

Gambia ligger i Vest Afrika et par timers flytur sydover fra Gran Canaria. Og merkelig nok er landet omsluttet av nabolandet Senegal på tre kanter. Gambia har en kystlinje på kun 54 km nord syd. Hovedstaden er Banjul, og landarealet er bare på 11.290 km2. (Og til sammenligning så er Norges landareal på 323.000 km2.) Innbyggertallet er på ca. 2,1 millioner og språket er engelsk.

Og bakgrunnen for denne litt merkelige statsdannelsen er at i slavetiden så erobret engelskmennene bare elvemunningen til elven som i dag heter Gambiafloden. Franskmennene erobret resten av det som er nabolandet Senegal. Men som sagt engelskmennene var bare interessert i ferskvannet fra elven, og ikke omlandet.

Gambia dealen:

Representanter for OCE har ved flere anledninger tidligere vært i Gambia, i endog flere ærender og da særlig tilbake på 2000 tallet under arbeide med å sikre en oljekonsesjon der sammen med partnere fra Calgary miljøet.

CEO Skotte var der forrige gang for ca. fire år siden. Og hadde faktisk ny flybillett dit den 30 mars 2020. Og alle vet jo at det ble en umulighet å gjennomføre den reisen pga. Corona utbruddet. Således ble det faktisk utsatt helt til nå før at denne planlagte reisen kunne gjennomføres, nå i oktober i år.

Gambia er jo et fattig land og strømmen kommer i hovedsak fra dieselaggregater og noen små gasskraftverk. Men dette er ikke tilstrekkelig til en sikker strømforsyning i landet. Så i perioder blir faktisk strømmen koblet ut i varierende bydeler, selv i hovedstaden Banjul. Prisen på lokal strøm er jo nærmest ekstrem i et så fattig land.

Så landet er meget interessert i enhver form for energi som kan forsyne innbyggerne med rimelig strøm og selvsagt da også miljøvennlig energi som en ekstra bonus – om ikke annet for ledelsen i landet.

Og som sagt så er kystlinjen mot Atlanterhavet, og det kommer nærmest «sinuskurvede» dønninger stabilt inn fra Atlanterhavet i vest døgnet rundt. Og det er meget sjelden at det er ekstremvær på denne kystlinjen. Så å plassere bølgekraftparker her er jo nærmest en perfekt lokalitet.

Og som sagt så er Gambia et fattig land, og den første finansieringen av en slik bølgekraftpark fra OCE, må nok delvis finansieres fra utlandet. Men det finnes jo flere slike latente finansierings- ordninger og institusjoner, for slik «u-hjelp» (i vid betydning).

Så vi skal nok medvirke til å kunne få realisert et slikt prosjekt – når OCE teknologien er ferdig utviklet.

Gambias Energiminister Kemo K Ceesay og OCEs CEO Asbjørn Skotte, under møtet i oktober 2022.

Målet er å inngå en eksklusiv rammeavtale for bølgekraft-konsesjoner langs landets korte kystlinje som enda et «Asset» for selskapet. Dette er nå i en positiv prosess og dialog.

Veien videre – Strategien videre

Vi har jo omtalt dette i tidligere Aksjonærbrev også – men vil gjerne dele noen av våre tanker med våre mange aksjonærer for veien og strategien videre.

Vi har sett for oss en bølgekraftpark med «Det Balanserte System» med Stormbøyen (DBS) med 100-150 bøyer som vil gi en installert effekt på 10 MW.

Og at denne parken vil bruke et areal ute i havet på ca. 800 x 800 meter. Og internt så har vi beregnet en produksjonspris pr Kw/t på Eurocent 5 eller tilsvarende 50-55 øre. Da vil en slik park kunne generere inntil Euro 8 Mill tilsvarende NOK 80 Mill pr år, om parken passerer ca. 5.000 driftstimer pr år.

Og når antatt kostnad på å etablere en slik park er på Euro 24 Mill, så er en inntjening pr år på ca. Euro 8 Mill gode måltall, for enhver økonom og investor.

OCE er nå kommet så langt i teknologiutviklingen at vi føler at vi kan levere et ferdig kommersielt produkt i DBS, innen kanskje 24 måneder.

Således har vi også påbegynt prosessen med å selge inn dette produktet – en komplett DBS park – til latente kunder Wold Wide.

Så derfor har vi også påbegynt et «road-show» for å begynne å markedsføre vårt snarlig ferdige produkt – DBS.

Denne aktiviteten vil fortsette ut over i 2023, og vi vil i de kommende aksjonærbrevene informere om denne aktiviteten.

Ting Tar Tid – dessverre – også for Hellas-sporet siden vi ble forsinket med selve prototype-finansieringen ved at Innovasjon Norge denne gangen satte dette kravet til egenkapital – men her arbeides det da videre med flere alternative spor mot meglerhus for å hente inn pengene i Norge og også etter hvert i utlandet.

Men - det nye og ferske sporet mot Malaysia åpner jo for helt nye muligheter med de forbløffende forbindelsene vi der klarte å få etablert gjennom vår McKinsey mann på topp nivå! – og dette gir vi selvsagt svært høy prioritet med å følge opp nå i det nærmeste – siden disse kontaktene også har midler selv til å finansiere prototype-utviklingen og gjennomføre selve testen av våre Patenterte-konsepter som jo er det vi Gründere av selskapet KUN har som vår primære målsetting og fokus nå!...

For gjennom all aktivitet og kontakter med større energiverk verden over vet vi jo at kundepotensialet synes å være meget stort – men vi MÅ bare fremvise en vel fungerende og samlet full skala prototype gjennom en vinter sesong – og det er hele vårt fokus nå med det nærmeste.

Avslutningsvis er vår erfaring gjennom alle disse møtene og presentasjonene siste året at mange – forståelig nok – gjentagende stiller det svært fornuftige spørsmål om det vitterlig er mulig å produsere 50 til 100 KW pr. enhet med vårt konsept!

Her laget vi en ganske omfattende «avhandling» rundt dette for energiselskapet Terna i Hellas for 3 år tilbake – som i dag er en mulig stor kunde når vi kan levere et ferdig produkt og den rapporten er også igjen senere grunnlaget for «Hellas avtalen» her denne våren.

Og det er ganske interessant å se hvordan denne rapporten «betrygger» enhver ny partner vi presenterer dette for.

Og siden vi i dag har fått patent-beskyttet alle våre løsninger og mye av rapportens mere akademiske informasjon i dag like fullt er tilgjengelig fra bibliotekene på Universitetet i Ålborg og Uppsala – er vi enige om at vi nå kan publisere denne rapporten til (ikke minst) våre egne aksjonærer!...

Rapporten bygger på 1 års innhenting av bølgedata utført av Ocean Energy AS selv rundt kysten ved Runde på Søndre Sunnmøre som er et typisk «bølgeområde» for det «Balansert system» og bøyer på opptil 6 meter.

Målingen ble utført ved hjelp av innleid målebøye og utstyr fra selskapet Oceanor AS i Trondheim. I dag en del av Fugro se:

https://www.fugro.com/about-fugro/our-expertise/technology/seawatch-metocean-buoys-and-sensors

Og etter at data var innsamlet over en sesong ble de så tolket og analysert av Sintef Ocean ved NTNU som en større konsulentjobb på vegne av Ocean Energy AS.

Med bakgrunn i alt det materialet vi har derfra samt en rekke avhandlinger vi har fått gjennom årene fra vårt tidligere samarbeide med Seabased AB og Universitetene i Skandinavia – har vi så klart å lage en ganske så nøktern og objektiv rapport som beviser at det er mulig å produsere – minst – 50KW med vårt konsept – men mere sannsynlig nærmere 100 KW i «daglige bølger» med en 6 meters bøye!...

Derfor har vi vedlagt denne – omfattende - rapporten til våre aksjonærer i dette Aksjonærbrevet som litt «interessant Jule-lektyre!» - og det er jo et voldsomt data-materiale og analyser fra Sintef som man (selvsagt) bare kan scrolle over hvis man ikke er spesielt interessert på «bit nivået» – men konklusjonen er meget interessant og positiv!

Den ligger da her vedlagt som Appendix 1.

Da vil vi gründere av selskapet med denne oppdateringen igjen takke alle tålmodige aksjonærer så meget for støtten og gratulere oss alle med den fantastiske aksepten og mottakelsen vi fikk for konseptet i Malaysia og at vi nå har ganske mange alternative spor frem videre med forskjellige finansielle partnere for å få sluttført prosjektet!

En Riktig God Jul ønskes alle aksjonærer fra Ocean Energy AS!

Direkte telefon og E-mail til ledelsen i Ocean Energy AS:

Tov Westby – 917 83 633 E-post: westby@oce.as

Asbjørn Skotte – 900 78 006 E-post: skotte@skotte.no

Egil Holland – 917 03 938 E-post: holland@oce.as

www.ocean-energy.no

E-Mail: oce@oce.as

… og en dag vil alle de naturens ustyrlige gaver – ikke bare fossefald – men kan hende også selve havet kunne temmes til glæde for menneskehedens økende behov for energi…

Gründer Norsk Hydro-Elektrisk Kvælstofaktieselskab (Norsk Hydro) – Ingeniør Sam Eyde

Fyr på den norske kyst, Peder Balke, malt ca. 1855 - Nasjonalgalleriet.

Bare Kapitaler, saa er det gjort. –
En Nøgle af Guld till Havets Port!

Peer Gynt – IV akt.

”Den bundne drage” – Naturens skjulte krefter – Th. Kittelsen, «Svælgfos» (1907). Laget på privatoppdrag av Sam Eyde – senere donert Norske Hydro A/S fra Generaldirektøren. I dag utstillet på Telemarksgalleriet.

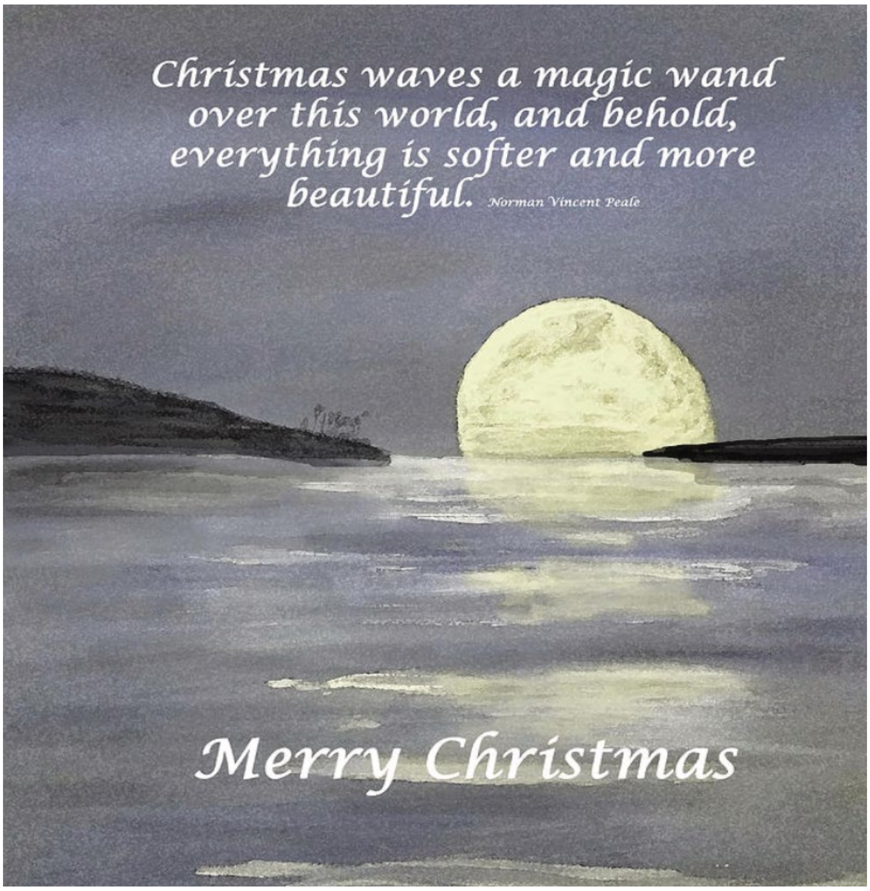
Christmas waves a magic wand over this world, and behold, everything is softer and more beautiful.
Norman Vincent Peale
Merry Christmas

APPENDIX 1

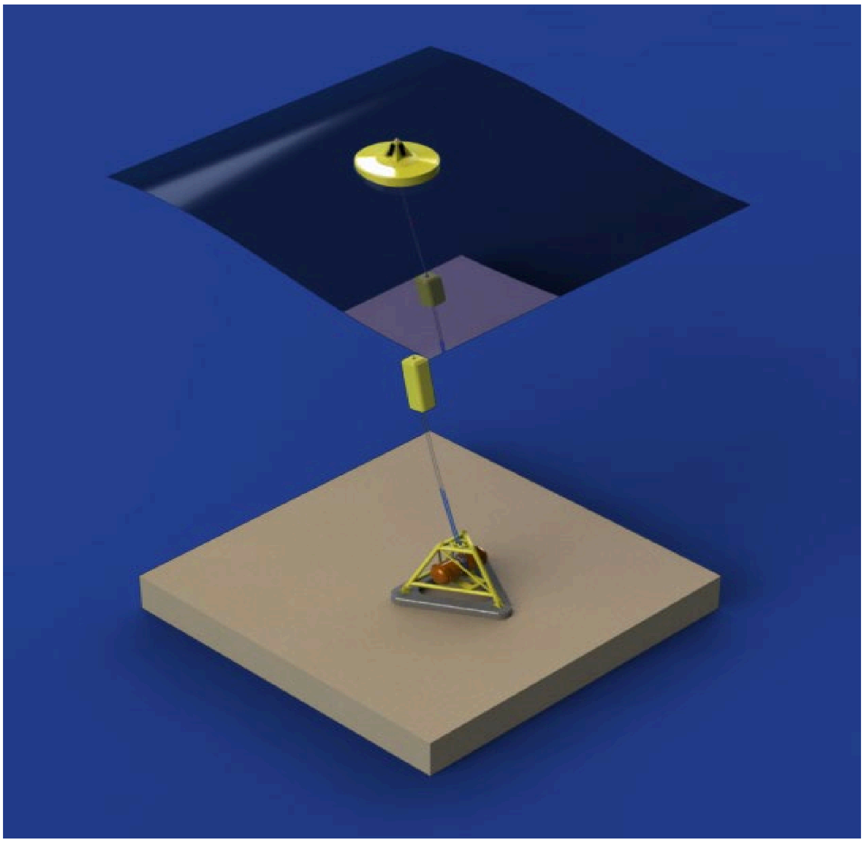

Project «The Balanced System» Wave generator prototype development and testing.

Developed for TERNA after meeting in Hellas and will be related to the coming Norwegian EEA Call.

Describing of the prototype-project and verification of the possibility to develop at least 50 KW with a 6-meter point absorber "Storm Buoy"!

CONTENT

1. Animation of the principle for «The Balanced System».
   Page 3

2. Examples and verifications from Research and Industry that proves it possible to produce minimum 50KW on each generator with a point absorber buoy in a wave climate like around the «Island».
   Page 4

3. Conclusion
   Page 25

Attachment 1:
The production simulation report from Sintef Ocean (NTNU - Norwegian University of Science and Technology): «Basic Dynamic Characteristics of the Balanced Wave Energy Converter – spring 2019»

Attachments 2:
Report from Uppsala University that refer to 170 KW production in the newest generators from the Angstrom Laboratory.

Attachment 3:
New report from Uppsala University (2019) that makes a small scale test of «The Balanced System» in the ship tank principle with very positive results.

Attachments 4 – 6:
Additional reports from Uppsala University.

Attachment 7:
Test results from Uppsala University which shows a production price of just 5 Eurocent per. kWh with the production price, the acquisition cost and depreciation of the plant included in the calculation.

Attachments 8:
All the drawings on the balanced system from West Maritime.

REPORT Version 1.4
AUTHOR(S) Tov Westby
Revised by: Egil Holland

1. Animation of the principle for «The Balanced System».

Point and click in the picture under to see the basic principle of the worldwide patented: “Balanced System”.

An overall solution that will solve the two biggest challenges associated with wave power - namely to be able to withstand extreme weather and at the same time cope with all types of variable wave heights during daily operation.

It’s a “must be seen” first to understand the whole logic in the simple and self-adjusting system.

Point at the picture over and click – together with the CTRL Key to start!

See also additional animations and much more information at

the company’s official WEB site: www.ocean-energy.no

Examples and verifications from Research and Industry that proves the possibility to produce minimum 50 kW on each generator with a point absorber buoy in a wave climate like at the Agios Georgios Island.

Ocean Energy has for many years collaborated with the Swedish company Seabased AB and followed their generator tests since 2006 also together with Uppsala University.

Since most of their production tests are internal, we cannot publish these reports in detail here, but we can refer to examples proving that today's commercial generators have been created for "Point Absorber Principle" which can produce - at least - 50 KW in a wave environment like around Agios Georgios Island.

We begin with our own research and simulations from 2019 carried out at Sintef Ocean in Spring 2019, confirming that (at least) 50 KW can be produced at this type of wave signatures as at Agios Georgios Island.

We then refer to the Sintef Ocean report attached at page 48, where the conclusion is that with a 4-meter buoy it can be produced at least 14 KW (real numbers are 28 KW but the researchers wanted to secure and halved the figure to only 14 KW).

The report concludes carefully with:

"the average power was found to be 14 kW – based on a 4 meter buoy.

(Sintef Report from Q1 2019 – page 48.

Since the effect will increase for each meter in diameter of the Buoy with a known factor - a 6-meter Buoy will according to the well-known hydromechanics formula: (Falnes/Bystrom/Aalborg University):

This gives a multiplication factor at 3.5:

$$Hmass = \frac{1}{2} * \frac{4}{3}\pi r^3 \text{ (ton)},$$

Will realistically give minimum 49 KW output power production for a 6-meter buoy in 1 – 2 meters waves with a rotation generator – like with "The Balanced System" solution.

This is the most realistic figures and the simulations showed that it most possible could be taken out even more energy – up against 100 KW with a 6-meter buoy.

Results that are also very similar to the proven production in the sea from the newest linear generators from Seabased AB and Uppsala University done in 2018 to 2020.

See their official technical sales-information from 2018 on the next page that also verifies the same production-figures in the rates between 50 to over 100 kW pr. generator:


TECHNICAL
OVERVIEW
Seabased
Wave Energy Converter
S2.7
SRS
OLE
GÖTEBORG
SEABASED

SEABASED
WAVE ENERGY CONVERTER
WEC S2.7

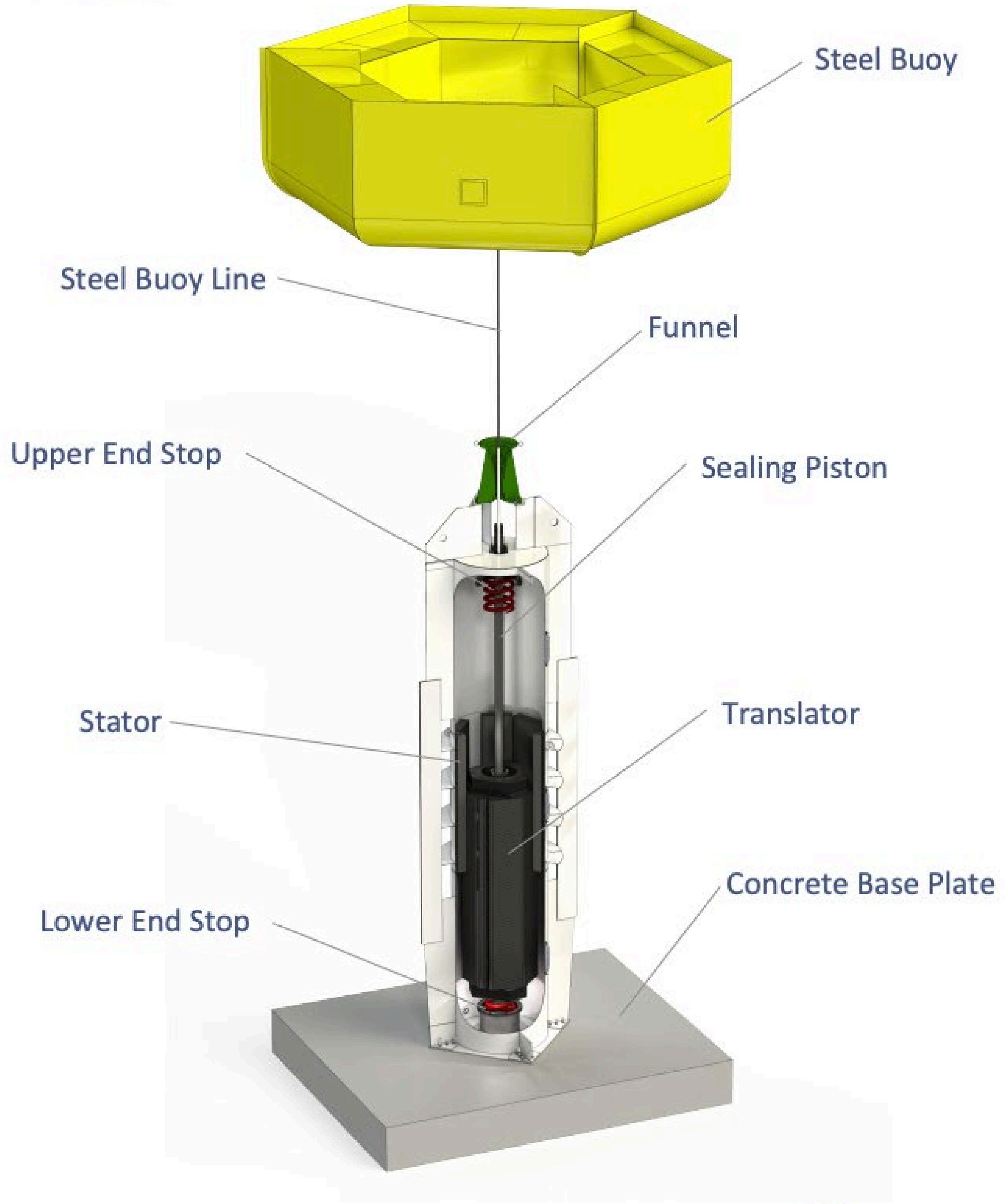

POWER GENERATION

SEABASED WEC S2.7

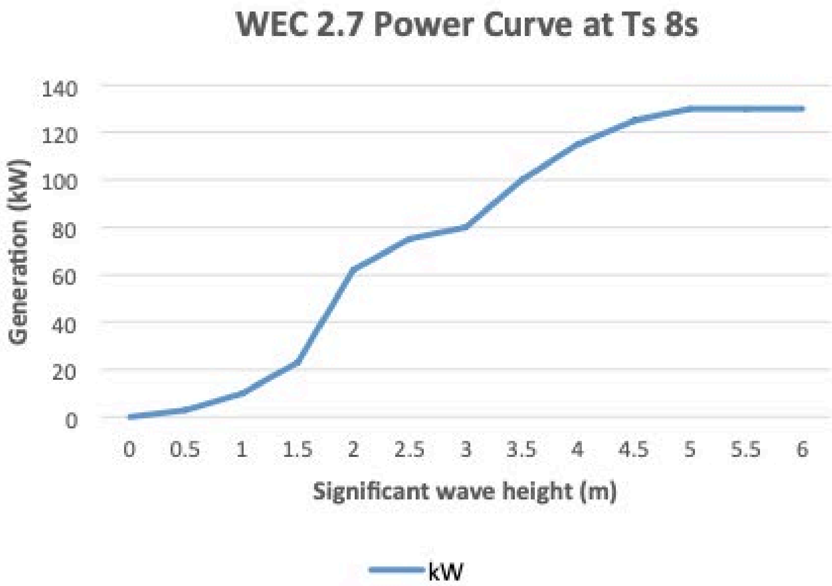

The Seabased Wave Energy Converter (WEC) S2.7 has been designed for a nominal rating of 100 kW. A unique feature, however, is that for brief periods it can extract more power than the nominal rating.

The cut-in wave height is 0.3m and there is no cut-out wave height.

ENERGY CALCULATIONS

Per MW installed, S2.7 WECs

Assumption: 90% operational time

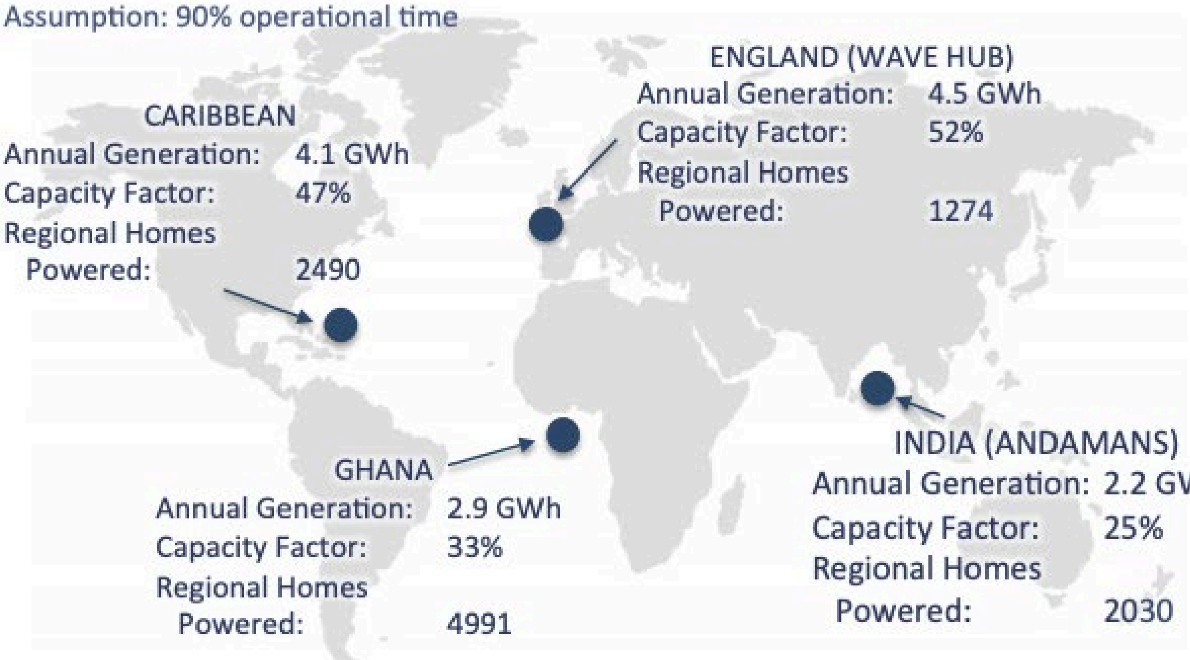

Souce: Seabased and World Energy Council 2014

COST-COMPETITIVE RENEWABLE ENERGY

The Seabased solution is already cost competitive in many markets.

Excellent Utilization Factor
Wave power offers excellent utilization per megawatt installed.

The sun sets, the wind stops, but waves essentially create energy essentially around the clock. Waves are quite predictable and can be forecasted 5 or more days in advance.

Stable Supply to Grid
The stable availability of wave energy results in a predictable supply of power to the grid, minimizing the need for expensive batteries.

Low Transmission Costs
Since a large portion of the earth's population live near the coast, transmission costs from wave power can be minimal, which in turn lowers the cost of electricity.

Small Footprint
Because of the high density of water, waves are a concentrated form of energy. This means that a relatively large amount energy can be harnessed in installations that take comparatively little space.

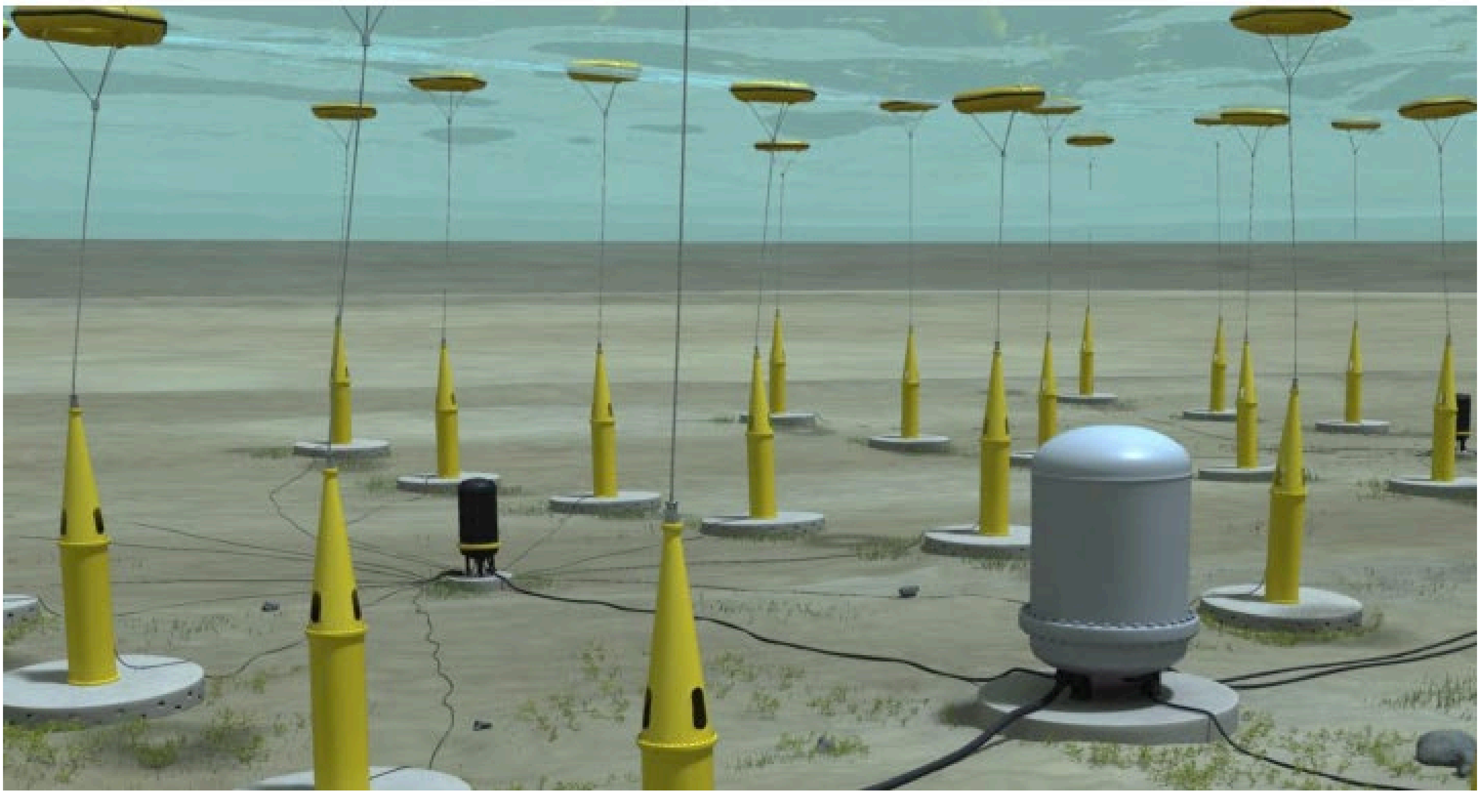

GENTLE ON THE ENVIRONMENT

Sustainable energy solutions need to strive for sustainability themselves. After all, we chose this business precisely because we believe in the amazing opportunities created when you work with, not against, the natural environment.

Seabased has been active in environmental research and testing from inception, in 2001. The development and design of Seabased's wave power technology is cradle to cradle in focus, minimizing negative environmental impact.

ARTIFICIAL REEF

A positive side effect of Seabased wave parks is that they create artificial reefs that provide a safe haven for both fish and other marine animals in the region.

We can add details to the installation for the sole purpose of making these reefs more attractive to marine life, including mussels, crabs and lobsters. Such a safe haven can provide excellent breeding grounds and help support a healthy marine environment.

NO TAKE ZONE

The area immediately surrounding the wave park becomes a "no take zone", with no fishing or trolling. The effect is similar to creating an underwater nature reserve.

KNOWN MATERIALS

We use only materials which are well-known and compatible with the environment. They are well tested and established as safe for saltwater subsea installation use. All components can be recycled.

BARNACLES? NO PROBLEM

Marine growth, including seaweed, barnacles and other invertebrates, is expected to occur – and welcomed. Rather than depending on regular cleaning to function properly, our wave parks are designed to be enjoyed by the local flora and fauna.

NO EMISSIONS

NO FUEL COSTS

NO MOVING PARTS
THAT COULD HARM ANIMALS

NO OILS THAT POLLUTE

NO LOUD NOISE

NO LAND AREA USE

NO EYESORES

LESS IS MORE

Sometimes it's what you don't do that's important.

Seabased lets you tap into the power of wave energy with no fuel costs or emissions. There are no underwater moving parts that could harm animals. Our solution uses an electromagnetic generator, and does not involve hydraulics that require oils that could pollute.

Studies show that the noise of the WECs and the LVMS is audible to nearby marine life, but does not disturb their behavior. Seabased wave parks require no significant land area use, other than what's needed to connect to the grid.

And as you can see below, the wave park is virtually invisible from a distance, so you can enjoy cost-competitive renewable energy and naturally beautiful views.

The picture below shows how a Seabased Wave Park might look to a person standing on shore.

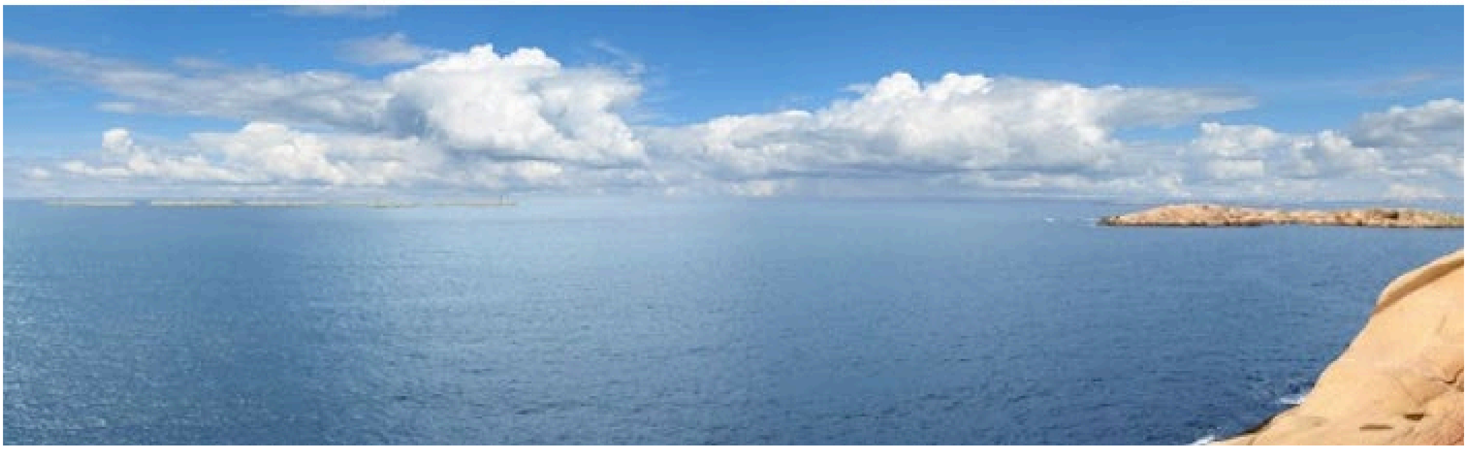

TECHNICAL SPECIFICATIONS
SEABASED WEC S2.7

OPERATING DATA	
Rated power	100 kW
Cut in wave height	0,3 m
Cut out wave height	NA
Sound level	50 dB
Installation depth	20 - 100 m
ELECTRICAL	
Generator	Seabased linear, direct driven generator
Grid feed	Subsea inverter, subsea transformer, land switch gear
Control sytem	Seabased SCADA
Power output	50/60 Hz AC
REGULATION	
Power regulation	Electrical regulated
Brake system	Electrical & mechanical
DRIVE TRAIN	
Force transportation	Rotational free steel line
DIMENSIONS & WEIGHT	
Generator height	8,3 m
Generator diameter	2,4 m
Generator weight	15 t
Buoy height	2 m
Buoy max width	6,1 m
Buoy weight	4,4 t
Base plate height	0,65 m
Base plate width	5,1 m
Base plate depth	4,1 m
Drive train	Steel line

SEABASED

Please also see the new report from the Ångstrøm Laboratory at Uppsala University about current cooling solutions in the generators where it now operates with a full 170 KW production at a point absorber buoy of 6 meters.

See the report here:

http://uu.diva-portal.org/smash/get/diva2:1049240/FULLTEXT01.pdf

In the abstract is stated:

"The comprehensive thermal study of the substation shows that the rated power in the present configuration is around 170 kW"

It is also interesting to note that the same Ångstrøm Laboratorium at Uppsala University has now got the "eyes up" for our own patented concept of "The Balanced System" and also made a first test of our solution – with rotating generator which shows astonishingly positive results compared to their "old" solution with static stroke length of approx. 2 meters and no protection against storms.

See the whole article at page, Attachment 3.

Conclusion:

Based on all these actual test results from Seabased AB and Uppsala University done with generators in the sea - and not at least our own simulation carried out at Sintef Ocean this spring, it clearly seems to be proven that it is realistic to develop - and later serial-produce - a generator which will be able to produce - at least - 50 kW based on a normal buoy size of 6 meters per unit.

In terms of cost, we have obtained some calculation on price for a total sea park from Seabased AB and the "price list" for today for a total 10 MW sea park - based on 150 units - including cabling and installation on approx. 20 Mill Euro all told.

The cost of the installation is thus calculated to a price of 2 Mill. Euro per installed 1 MW of wave power.

According to the calculations - both from Sintef Ocean and the first tests at Ångstrøm laboratory – “The effect and cost of using a *"Direct-Driven Wave Energy Point Absorber with High Inertia Rotatory Power"* seems to be far more economical – and that is the principle for our “Balanced System ” se the report on Page 83.

Compared to the above prices that are based on Linear Generators with extremely costly magnets we therefore believe that the cost of such a 10 MW wave park could be further reduced by using our solution with "The Balanced System».

And especially at locations such as Agios Georgios Island where the generators can be mounted close to shore and no additional scaffolding and transformations are required under the water.

A calculated real production cost on the units as a mass product is what should be highlighted during our upcoming prototype development for the first prototypes together.

We sincerely hope that these models and examples given above, will prove to you that it is realistic to produce at least 50 kW at one wave power unit. On your confirmation, we are looking forward to the continuation of the project, which if so, will coincide with the start of the important process of finalizing the EEA grant application together.

Oslo, 19/05 2019

Tov Westby

Co-founder Ocean Energy AS

Attachment 1:

The production simulation report from Sintef Ocean (NTNU - Norwegian University of Science and Technology):

«Basic Dynamic Characteristics of the Balanced Wave Energy Converter – spring 2019»

SINTEF

OC2019 F-044 - Restricted

Report

Basic Dynamic Characteristics of the Balanced Wave Energy Converter

Author
Karl E. Kaasen

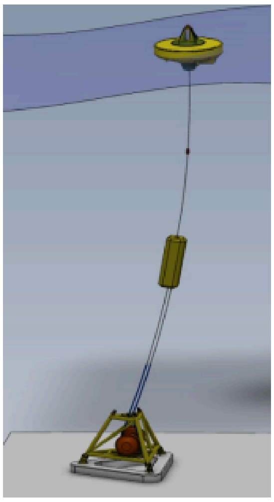

SINTEF Ocean AS

2019-03-07

SINTEF Ocean AS
Address:
Postboks 4762 Torgarden
NO-7465 Trondheim
NORWAY
Switchboard: +47 46415000

Enterprise /VAT No:
NO 937 357 370 MVA

Report

Basic Dynamic Characteristics of the Balanced Wave Energy Converter

REPORT NO.	PROJECT NO.	VERSION	DATE
OC2019 F-044	302004674	1	2019-03-07

KEYWORDS:
Hydrodynamics
Wave
Energy
Power
Converter
Simulation
Model

AUTHOR(S)
Karl E. Kaasen

CLIENT(S)
Ocean Energy AS

CLIENT'S REF.
Asbjørn Skotte

NUMBER OF PAGES/APPENDICES:
45 / 0

CLASSIFICATION	CLASSIFICATION THIS PAGE	ISBN
Restricted	Restricted	ISBN

ABSTRACT
A study of the basic dynamic properties of the Balanced Wave Energy Converter (BWEC) is carried out with a simple computer model. The model is based on temporary design data and is an approximation to the real system in that only the vertical wave-driven motion (heave) is considered. A comprehensive model will also include horizontal motion and angular components of motion. However, the vertical motion is expected to be the key component. The purpose of the study is to check the feasibility of the design principle and get some first figures for the systems motions, loads and power absorption. Simulation is carried out for eight regular and eight irregular sea states. Linear, speed-proportional power take-off is assumed. The parameters of the power take-off are optimised for each of the regular sea states and used in the simulations with irregular waves. The results are presented as tables and figures. The study shows that the principal design of the BWEC should work. For a more comprehensive study, the horizontal modes of buoy motion should be included, and also a realistic model for friction losses in the mechanical transmission.

PREPARED BY	CHECKED BY	APPROVED BY
Karl E. Kaasen	Ivar Fylling	Vegard Ø. Aksnes

This document has been approved according to SINTEF's approval procedure, and is digitally secured

Document History

VERSION	DATE	VERSION DESCRIPTION
1	2019-03-07	Initial version

Table of Contents

1 INTRODUCTION 4

2 MATHEMATICAL MODEL 5

3 SIMULATION RESULTS 7

3.1 Regular waves 7

3.2 Irregular waves 9

4 CONCLUSION 12

5 REFERENCES 12

6 FIGURES 13

6.1 Regular waves 13

6.2 Irregular waves 30

1 INTRODUCTION

This report gives a description of the essential properties of the Balanced Wave Energy Converter (BWEC) as a device to convert wave energy to electrical energy. Figure 1 shows the principle of the BWEC: A disc-like buoy moves in the waves. Attached to the underside of the buoy, a rope is extended to a unit on the seabed through a duct in the submerged buoy. The rope runs around a sheave on the seabed unit, its other end attached to the underside of a submerged buoy.

The sheave is connected to a pair of electrical generators and flywheels inside watertight compartments [2]. When the surface buoy moves in the waves the rope will make the generator rotate and produce an electrical current.

The purpose of the work presented herein is to make a simplified dynamic model for the BWEC and study its behaviour for a range of sea states.

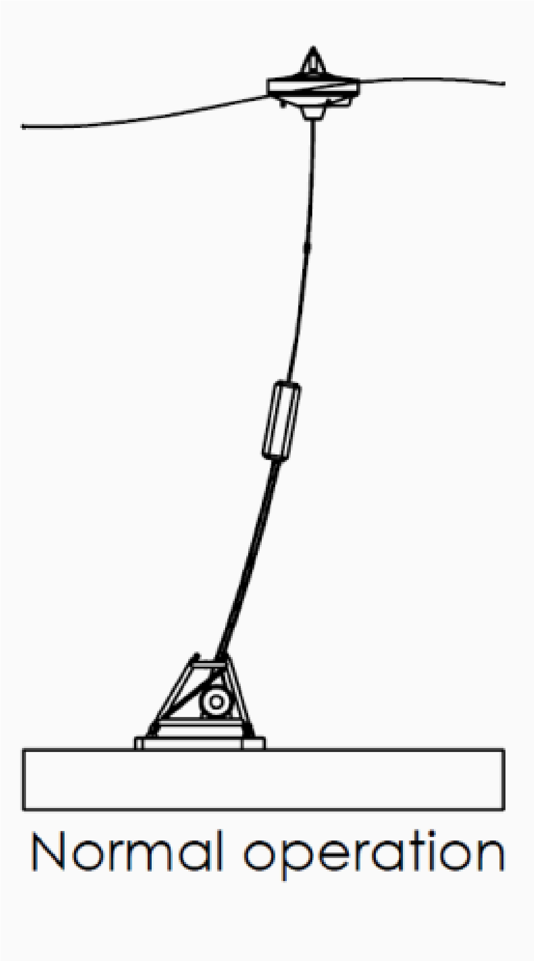

Figure 1 Balanced Wave Energy Converter (from [1])

2 MATHEMATICAL MODEL

It is assumed that the essential properties of the BWEC can be modelled by a description of the vertical component of motion. The main driver of the generator will be the buoyancy force on the surface buoy. In addition, there will be effects of hydrodynamic damping and inertia. Various sources of energy loss will exist: Hydrodynamic damping of the two buoys and friction in the duct through the submerged buoy and in the machinery in the seabed unit. The hydrodynamic damping has been estimated, but friction forces are neglected.

The electrical generator and flywheel are modelled as rotating inertia plus linear damping to represent the power take-off (Linear damping means that the power output is proportional to the rotating speed of the generator).

It has not been considered what revolving speeds the generator should have to produce electrical power efficiently. However, it seems likely that a gear of a certain ratio will be needed between the sheave and the flywheel (As a comment, this may add unnecessary cost if the dual arrangement of generator and flywheel is retained).

Table 1 shows the parameters estimated for the model. Although some of the parameters have uncertain values, the uncertainty is not so large that it will affect the system's behaviour significantly.

In general, it is difficult to calculate the hydrodynamic properties of a body moving up and down with varying cross section at the water plane. Some simplifying assumptions must be made: For the surface buoy the added mass is estimated as the mass of a water-filled hemisphere having the radius of the cross-section of the buoy at the water line. When the cylindrical part of the buoy is partly submerged the added mass has the value shown in the table, i.e. 14 725 kg. When the top of the cylindrical part is submerged one meter or more below the surface, the added mass is doubled. Between 0 m and 1 m submergence the added mass is given a linear increase. When the bottom of the cylinder is above the water surface the hemispherical model is used based on the radius of the cross section at the water surface. Thus, the added mass approaches zero gradually as the buoy rises and gets out of the water.

Figure 2 shows the buoyancy of the surface buoy as a function of the buoy's vertical position. Fully submerged, the buoy has a buoyancy of about 90 kN

For the submerged buoy constant added mass is calculated according to formulae in [3], which is also used for the coefficients of square damping of either buoy.

The varying added mass of the surface buoy may give rise to slamming force. In the model, this kind of force is considered relevant only when the buoy is moving downward and calculated only in this case.

Although approximate, the varying mass model is expected to add realistic limitation to the driving ability of the surface buoy.

The driving force from the waves have three components:

1. Buoyancy or hydrostatic force. This force is given by the function in Figure 2 when the buoy position is taken to be the position relative to the instantaneous water surface
2. Hydrodynamic inertia force (added mass force), which is proportional to the vertical relative wave acceleration
3. Hydrodynamic damping force, which depends on the vertical speed of the wave relative to the buoy. In the model only square damping is included.

In principle, the added mass will vary with the frequency of motion. This variation is not considered important at the precision level of the present model. Also, frequency-dependent linear damping will exist, but is neglected for the same reason.

Table 1 Parameters of mathematical model

		Surface buoy	Submerged buoy
Item	**Unit**	**Value**	**Value**
Mass	Tonnes	1.00	0.200
Weight	kN	9.81	1.962
Buoyancy	kN	See Figure 2	26.1
Hydrodynamic added mass	Tonnes	14.725	0.504
Linear damping coefficient	kNs/m	0	0
Square damping coefficient	kNs^2/m^2	3.894	0.347
		Power take-off	
Gear ratio		1:16	
Sheave diameter	m	1.0	
Linear damping coefficient (c_{PTO}) of generator	kNm s/rad	varying	
Moment of inertia (I) of generator + flywheel	kNm^2	varying	

The electrical loading of the system is assumed to be an ohmic load that represents so-called *active power* consumption, as opposed to *reactive power* which is the rate of change of non-dissipative energy stored in magnetic and electrical fields. In the model, reactive power is assumed to be negligible. Active power is associated with a speed-proportional moment of resistance from the generator shaft:

$$M = c_{PTO}\, \omega$$

Here, c_{PTO} is the PTO coefficient, and ω is the angular speed of the generator in radians per second. The instantaneous power dissipation ("active power" in the terminology of electrical machines) becomes

$$P = \omega\, M = c_{PTO}\, \omega^2$$

For maximum power output, we want both c_{PTO} and ω to be large. However, since the moment M acts back as a damping force on the surface buoy via the gear, sheave and rope, increasing c_{PTO} will slow down the motion of the buoy and reduce ω. Hence, it must be expected that there exists an optimal value for c_{PTO}, such that the active power P is maximized.

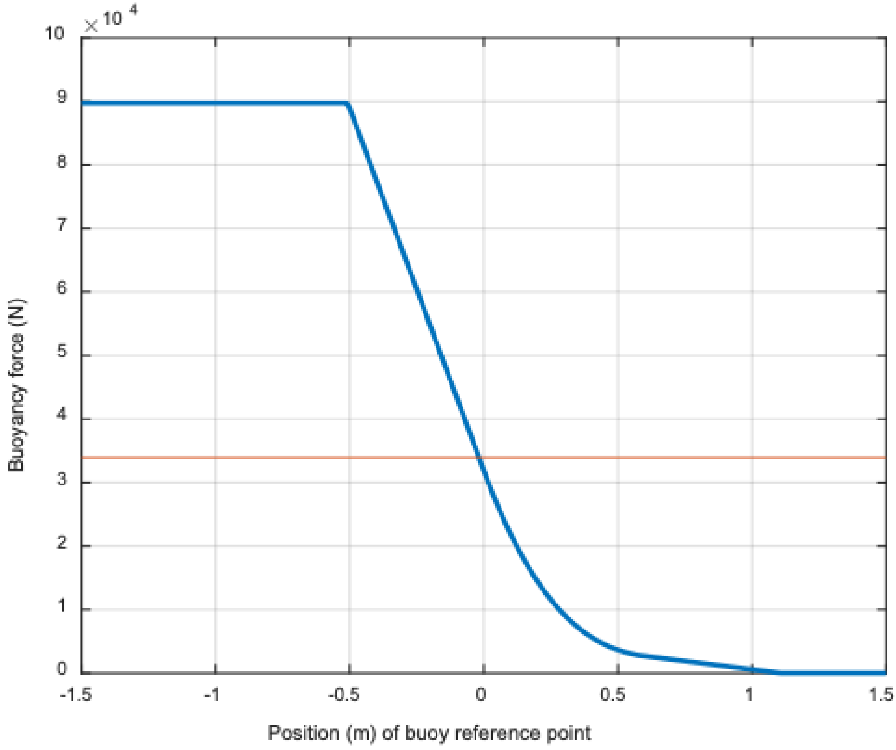

Figure 2 Buoyancy force on surface buoy as a function of vertical position. The reference point of the buoy is the centre of the imagined bottom plane of the cylindrical part. The horizontal line represents the opposing effect of the buoy's weight and the weight and buoyancy of the submerged buoy. Static equilibrium occurs when the draft of the cylinder is 1.8 cm.

3 SIMULATION RESULTS

3.1 Regular waves

Simulations in regular waves is valuable, as it gives good opportunity to study the details of the system's operation. Simulation is carried out for wave amplitudes A=1 m and A=2 m and periods T = 6, 8, 10 and 12 seconds. Note that wave height is defined as the distance from wave trough to wave crest, such that an amplitude of A corresponds to a wave height of 2A. The results are given in Table 2.

For each wave, the moment of inertia of the flywheel plus generator and the power take-off coefficient c_{PTO} have been adjusted for maximum mean power absorption.

In the table c_{PTO} and I are optimized for each wave by manual trial and error. The criterion for optimality is maximal mean power. One constraint was set on the optimum: The rotating speed of the generator should not go below *two revolutions per second* (rps) in the decaying phase, i.e. when no energy is transferred from the buoy via the sheave. This is an arbitrary limit, based on the assumption that an electrical generator must have some minimum speed of rotation in order to generate a significant voltage.

Note that the parameters represent the machines in *both* subsea compartments, i.e. one equivalent machine of double size.

Table 2 Results from simulation with regular waves. The moment of inertia is that of the flywheel plus generator.

Wave No.	Amplitude (m)	Period (s)	Moment of inertia (kgm^2)	PTO coefficient (Nm s /rad)	Mean power (kW)	Max power (kW)
1	1	6	90	20	9.2	17.6
2	1	8	120	19	6.1	11.6
3	1	10	170	14	3.7	6.0
4	1	12	170	7	1.5	2.2
5	2	6	90	8	17.9	24.2
6	2	8	90	20	18.5	34.1
7	2	10	90	20	15.1	36.0
8	2	12	150	25	13.4	30.5

While c_{PTO} can be changed by the generator's system for power control, I is a fixed constant representing the rotational mass of the PTO. Depending on the capability of the power control system, it may be possible to create artificial rotational mass by changing the reactive power. If this possibility does not exist, I should be optimised as the best average over the relevant range of wave states the BWEC will operate in.

The values for the parameters I and c_{PTO} in the table hold for the gear ratio n=16. Should a different ratio be wanted, e.g. n', the behaviour of the BWEC will remain unchanged provided the parameters are scaled by $(n/n')^2$.

Figure 4 - Figure 20 show results for the eight wave cases in Table 2, two figures for each case.

For the case A=1 m and T=6 s, the top plot in Figure 4 shows the wave elevation and the position of the buoy's reference point. After transient initial phase, the motion becomes periodic. The figure shows the two last cycles, which are identical.

The top plot shows that the buoy's lags behind the wave when the buoy moves upwards and follows the wave on the way down. This is a reasonable effect of the freewheeling action of the PTO system.

The second plot from the top shows the position of the buoy relative to the moving water surface. The dashed lines indicate when the buoy is fully submerged or out of the water. As is seen, the buoy gets under water in short periods, but is never lifted above the water.

The third plot shows the vertical velocity of the surface buoy in blue and an equivalent velocity of rotation in red. "Equivalent" here means the speed of the sheave periphery (in metres per second) that corresponds to the angular speed of the generator (in revolutions per second). Thus, when the blue and red curves coincide the surface buoy is driving the generator. This is the work stroke of the buoy, i.e. the (only) phase when energy is transferred from the waves to the PTO. During the work stroke the free-wheel ratchet is engaged, and the generator is accelerated. Eventually, the generator will "want to" rotate faster than the equivalent peripheral speed of the sheave. At this point the ratchet mechanism slips, and the blue and red curves depart. The stored energy in the generator and flywheel is now discharged in the dissipating load. The speed of rotation falls gradually until the buoy speed catches up as the buoy moves upward and the next work stroke starts.

Between the work strokes the buoy is seen to oscillate at the natural frequency as determined by the hydrodynamic stiffness of the surface buoy and the total mass of the two buoys. Stronger damping, like the unmodelled damping by friction in the gear transmission, will probably smooth out the oscillations.

The fourth plot in the figure shows the generator speed in revolutions per second.

The bottom plot shows the generated active power. It is proportional to the square of the speed of revolution. The dashed line shows the mean power.

Figure 5 shows some of the forces acting in the BWEC system. The top plot shows the hydrostatic force on the surface buoy. The flat parts of the curve correspond to full submergence.

The second plot from the top shows the force when the hydro*dynamic* force – i.e. force due to hydrodynamic inertia and damping - is added to the hydrostatic force.

The third plot shows the total of forces acting on the surface buoy. This force is equal to the force in the plot above plus gravity force, buoyancy and gravity of the submerged buy, and force from the PTO.

The bottom plot shows rope forces. "Rope 1" is the part of the rope that extends between the surface buoy and the bottom unit. "Rope 2" is the part between the bottom unit and the submerged buy. When the ratchet wheel slips and no moment is transferred to the generator, the tensions in Rope 1 and Rope 2 are identical (since friction in the rotating parts of the PTO has not been modelled). The tension in Rope 2 is almost constant at about 20 kN and equal to the net buoyancy force of the submerged buoy. The effects of inertia and damping is seen as small fluctuations. During the work stroke, the tension in Rope 1 increases to the force needed to drive the PTO.

The orange curve represents the sum of the tensions in Rope 1 and Rope 2. This is the lifting force that acts on the bottom unit. In the example shown in the figure, the lifting force is almost 100 kN at the largest.

The maximum differential rope force (blue curve minus red curve) acting on the sheave is about 50 kN. It is necessary that there is enough friction in the rope groove in the sheave such that the sheave can be rotated without slippage.

The 2 rps limit reduces the amount of energy that can be extracted. Without this constraint the power would be greater. As an example, the 2 rps constraint is removed in the case with A=2 m, T=12 s. The maximal converted power now becomes 7.4 kW. This is substantially more than the 1.5 kW in Table 2. The optimal parameters are in this case I = 120 kg m^2, C_{PTO}=100 Nm s/rad. See the motion responses and power in Figure 12 and compare with Figure 10.

3.2 Irregular waves

Irregular waves are much more representative of real wave conditions than regular ones. Eight cases of irregular waves were simulated. The waves were generated as random realisations of the JONSWAP spectral density function with different significant wave height and peak period, but common gamma parameter, γ = 3.3. See Figure 3 and Table 3. With respect to energy, the values 2.83 m and 5.66 m for the significant wave height (H_s) correspond to the amplitudes 1 m and 2 m, respectively of the regular waves in the previous section. The duration of the irregular wave realisations is one hour.

The parameters of the PTO that were "optimised" for the regular waves in 3.1 above are used also for the corresponding irregular waves. Comparing the mean power of Table 3 with the values obtained for the regular wave of similar wave energy, we see that we get electrical energy on the same level of magnitude from the irregular cases. The ratio of max power to mean power is significantly higher for the irregular cases, i.e. about 4-6 in comparison with about 2 for the regular waves. With longer duration, the ratio will increase

Plots of motion response and power are shown in Figure 21 - Figure 36. The figures correspond to the first figure ("Results (1)") for the regular waves and are shown in two versions: for the full 60 minutes duration and for a shorter duration around the time of the highest instantaneous power absorption.

Amongst the cases in Table 3 the largest average power capture (28 kW) is obtained for the shortest of the larger waves (T_p = 6 s, H_s = 5.66 m, cf. Figure 29 and Figure 30). However, this combination of significant height and peak period is very unlikely to happen (which is why the power figures are written in parentheses in the table. For the H_s values used in the study, i.e. H_s =2.83 m and H_s = 5.66 m the peak period is usually found in the range $T_p \approx 9 - 13$ s).

The largest rope force during the one-hour simulation is shown in the table. The maximum force is much larger than in the case of regular waves. This is also a quantity that will show considerable statistical variation from one 1-hour period to another. For longer durations, the expected maximum force will rise. It is probable that the force will be smaller in reality, since no elastic or geometric stiffness has been modelled.

On several occasions the surface buoy's reference point is pulled more than four metres below the wave surface. If this is not permissible, the loading of the buoy by PTO inertia and power extraction must be reduced.

It is pointed out that only one realisation of each sea state is made. Other realisations with identical parameters will give different results. It is expected, however, that the mean power will remain fairly constant from one realisation to another, but that the max values will differ more. The ratio of maximum power to mean power is much larger than for the regular waves, due to the characteristics of irregular waves. If large instantaneous power cannot be handled by the generator and associated power electronics, some limiting mechanism must be devised. Such a mechanism will also reduce the maximum load in the rope.

For the large waves (H_s=5.66 m), we see that the mean output power is 12 kW and 14 kW for T_p = 12 s and 10 s, respectively (which are typical periods). Like for the regular waves, the power capture will probably be greater if the constraint of 2 rps on the generator speed of rotation is removed. However, if it is feasible to remove the constraint, and thus allowing the generator speed to go to zero between the work strokes of the surface buoy, the question arises if there is any advantage at all in using a freewheel mechanism.

Note that the results in Table 3 are *examples* obtained for the assumed BWEC model parameters and the chosen wave states. The calculated power cannot be used as predictions of the energy capture of the final real system

Table 3 Results in irregular waves with JONSWAP spectrum and gamma=3.3

Wave No.	Significant height, *Hs* (m)	Peak period, *Tp* (s)	Moment of inertia (kgm^2)	PTO coefficient (Nm s /rad)	Mean power (kW)	Max power (kW)	Max rope force (kN)
9	2.83	6	90	20	10	60	233
10	2.83	8	120	19	6.9	39	138
11	2.83	10	170	14	4.9	24	126
12	2.83	12	170	7	2.6	12	116
13	5.66	6	90	8	(28)	(206)	(606)
14	5.66	8	90	20	19	112	319
15	5.66	10	90	20	14	88	228
16	5.66	12	150	25	12	58	204

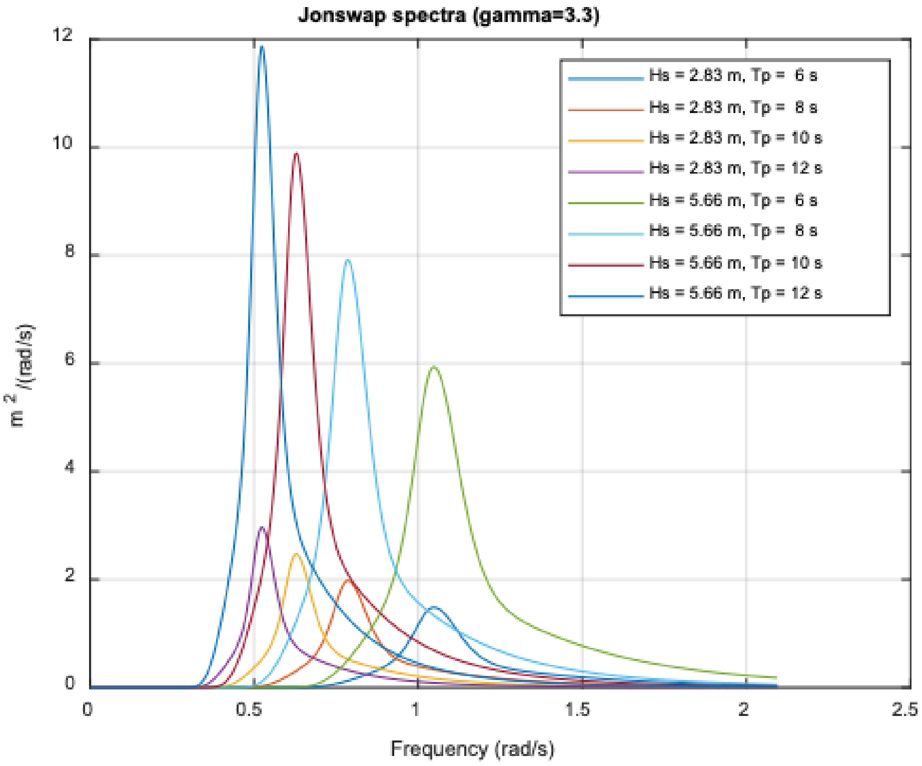

Figure 3 JONSWAP spectra

4 CONCLUSION

A simplified numerical model for simulation of the behaviour of the Balanced Wave Energy Converter (BWEC) has been made. The model only simulates the vertical component of motion of the BWEC, which is considered to be the key component with respect to energy capture.

The hydrodynamic properties are modelled by assuming draught-dependent hydrostatic buoyancy, added mass and damping. It is assumed that a gear transmission is necessary to convert the rope motion to generator rotational speed of sufficient magnitude.

Simulation is carried out for eight regular waves and eight irregular ones. Power capture is maximised for each regular case by adjusting the linear resistance coefficient of the Power Take-Off system and the total angular inertia of the flywheel plus the generator. In a real situation the inertia will have to stay fixed at a value to be optimised for the range of sea states the BWEC will operate in. It may in principle be possible to mimic variation in flywheel inertia by creating reactive power with the control system for the generator. In this case there could be some potential for adaptive optimisation as the sea state changes.

For the irregular cases, the PTO settings from the regular cases are used without further adjustment. In general, the power capture increases with wave height and decreases with the period. For the highest wave height (Hs=5.66 m) the average power was found to be 14 kW for a spectral peak period of 10 seconds.

A lower limit of 2 revolutions per second was set on the rotational speed of the generator. Optimising the parameters of the PTO without the speed constraint will probably give higher output average power, provided the generator can operate effectively at low speed.

The tension in the rope can reach high peak values in irregular waves. The rope must have sufficient strength. Further, the rope force must not become so large that it can lift the bottom unit.

The coefficient of friction between the rope and the sheave must be large enough that the sheave can be turned without slippage.

Apart from assumed reasonable hydrodynamic damping, no energy losses have been modelled. Friction loss in the transmission must be expected and should be included in a more comprehensive study. Such a study should also be done with a model that includes horizontal motion of the surface buoy.

5 REFERENCES

[1] Balanced Wave Energy Converter - Principal Sketch rev. P1 P101-CL903-000-00D (undated)
[2] Drawing "Seabed Unit" P101-CL903-300-01D (undated)
[3] Recommended practice – DNVGL-RP-N103. Modelling and analysis of marine operations. July 2017

6 FIGURES

6.1 Regular waves

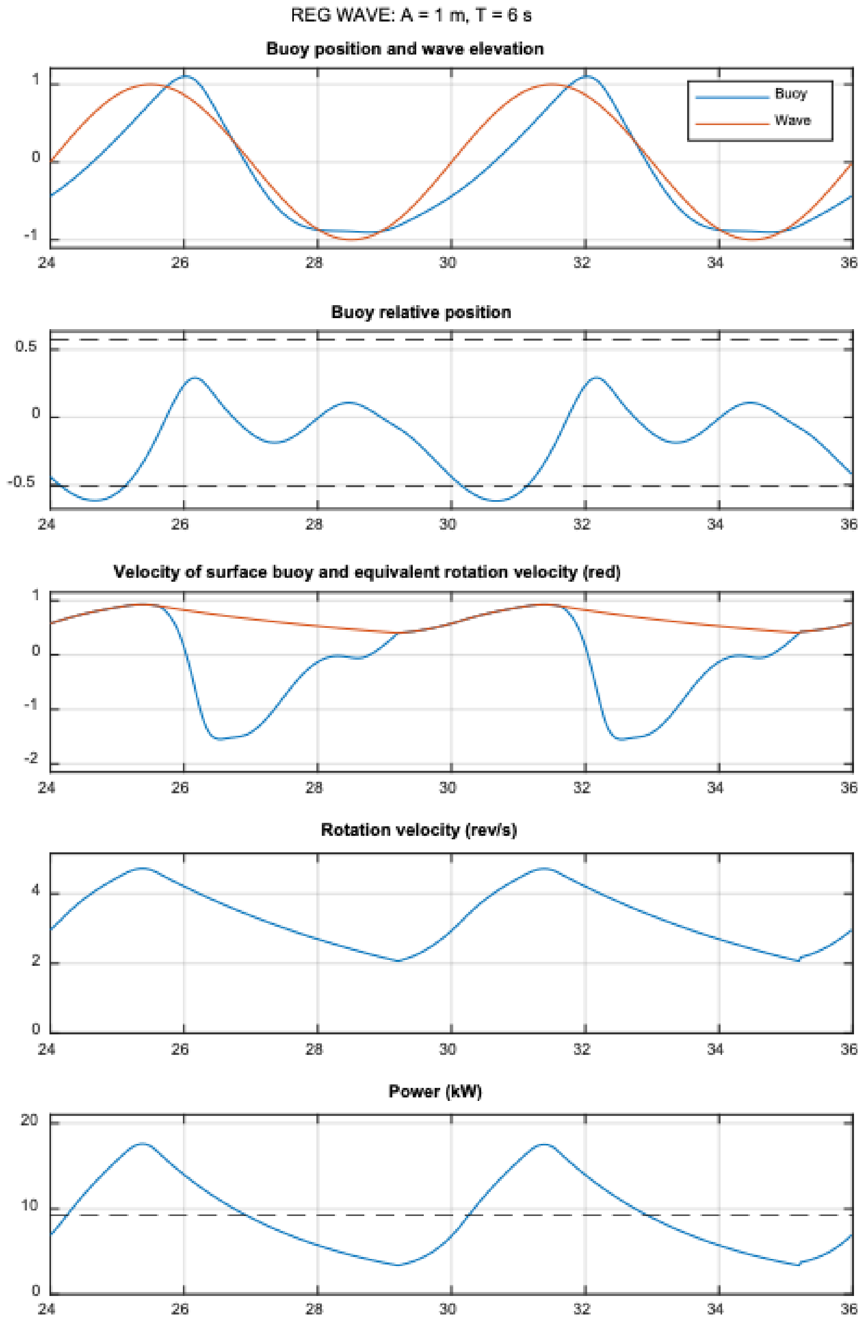

Figure 4 Results (1) for regular wave of 1 m amplitude and 6 s period

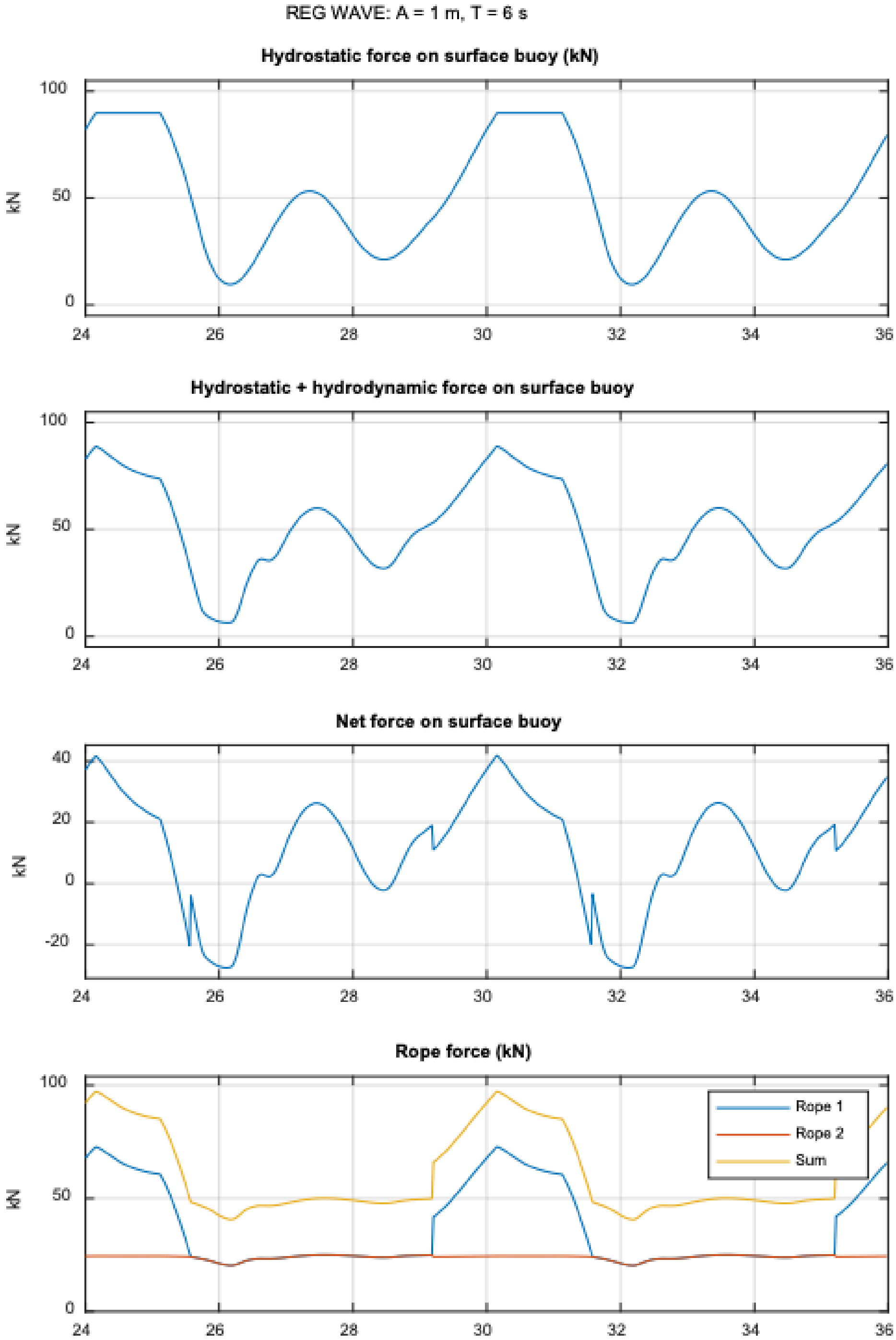

Figure 5 Results (2) for regular wave of 1 m amplitude and 6 s period

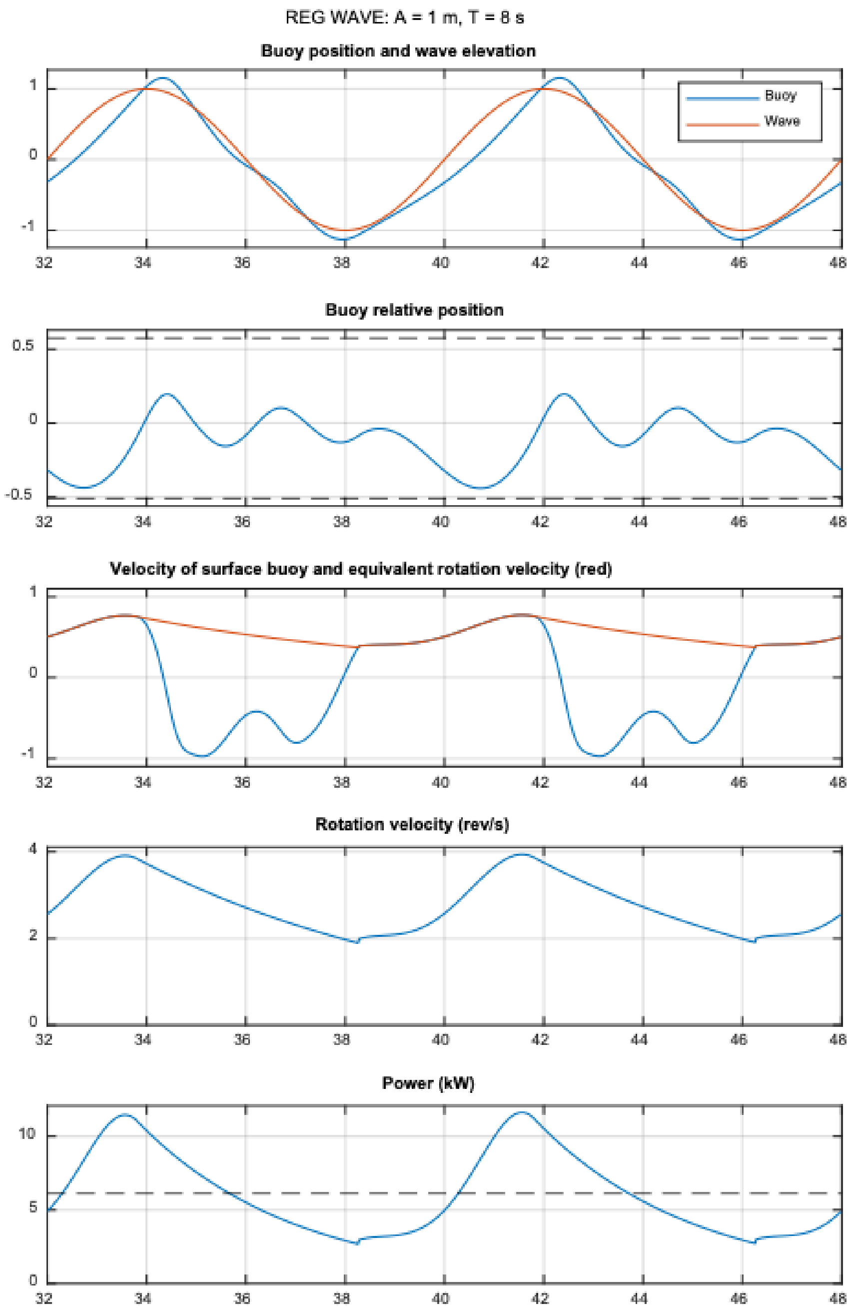

Figure 6 Results (1) for regular wave of 1 m amplitude and 8 s period

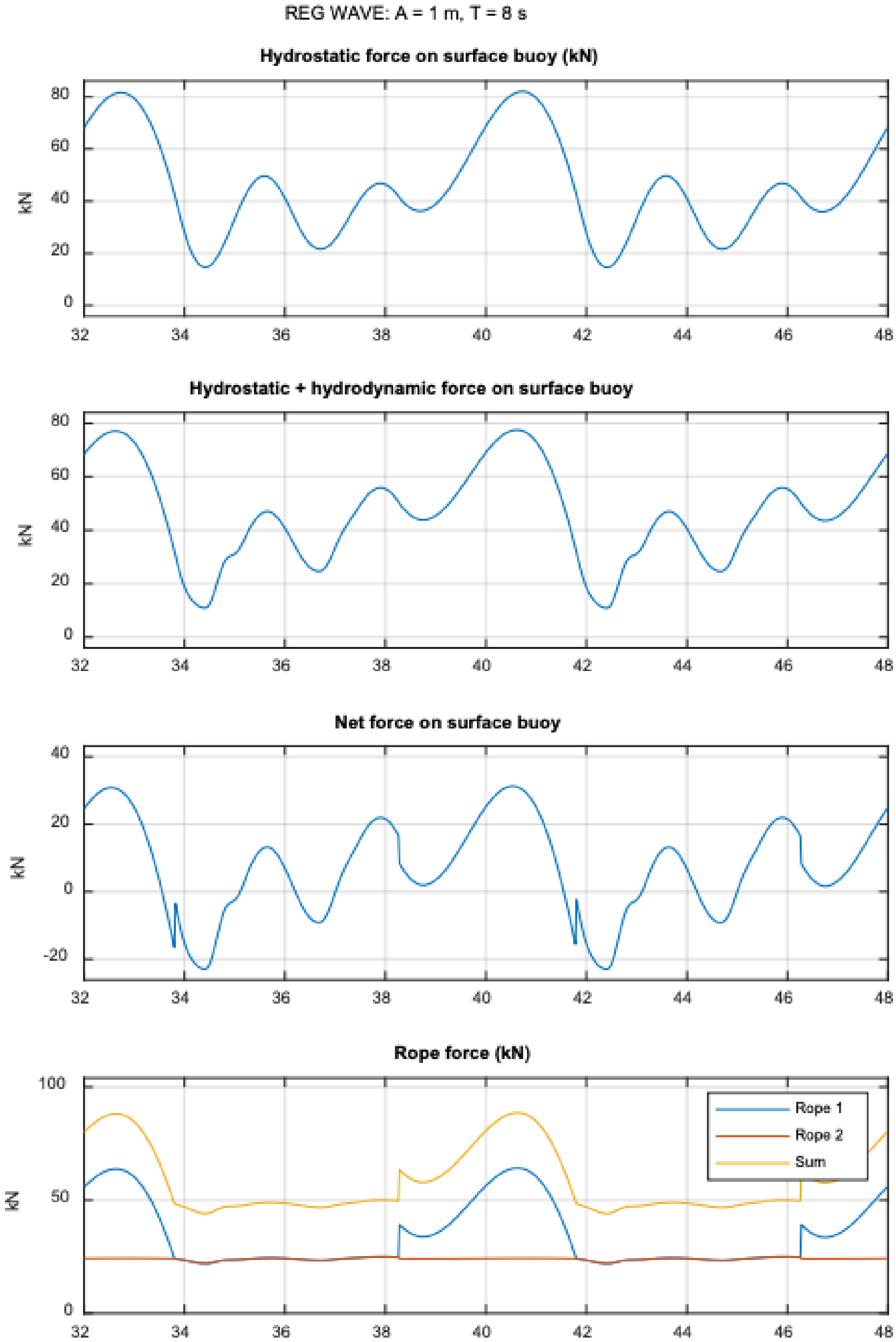

Figure 7 Results (2) for regular wave of 1 m amplitude and 8 s period

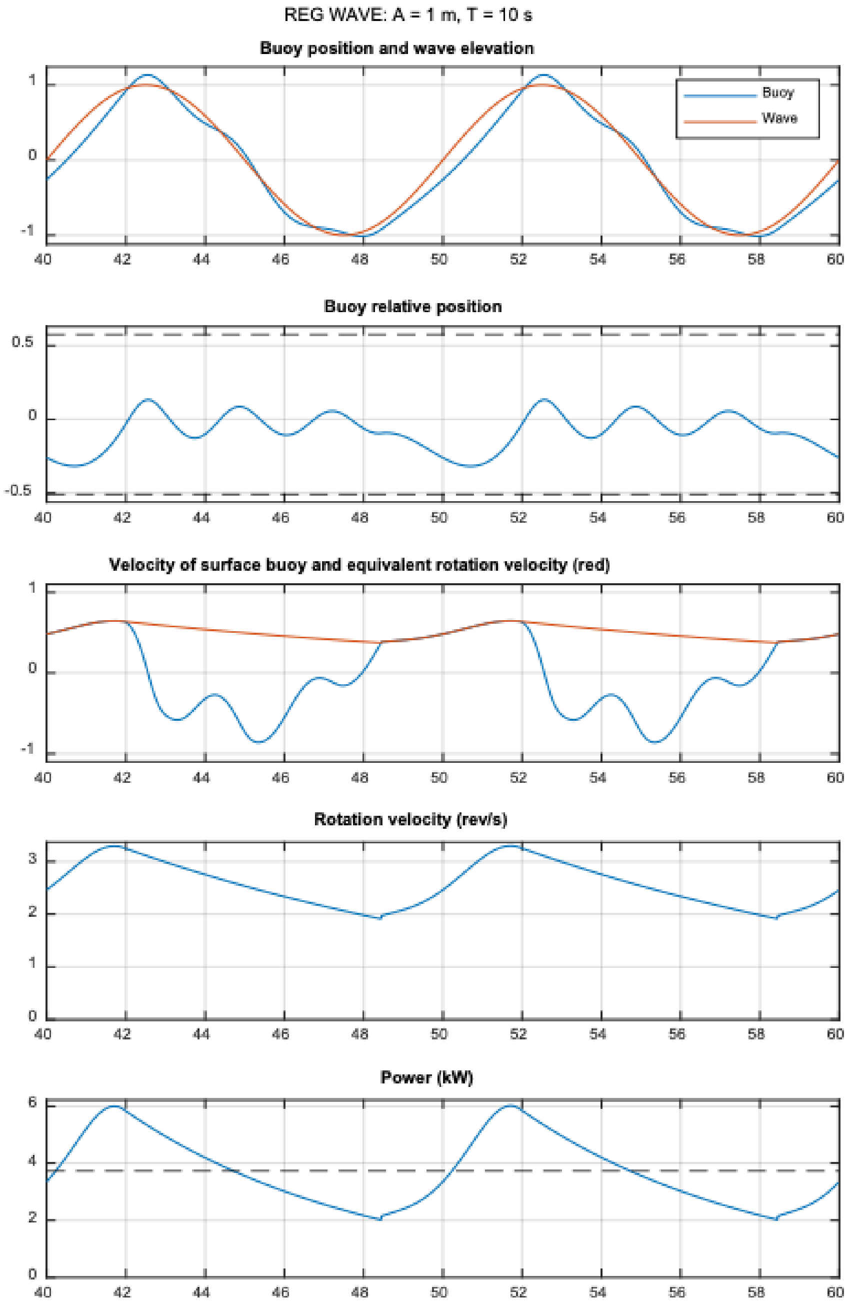

Figure 8 Results (1) for regular wave of 1 m amplitude and 10 s period

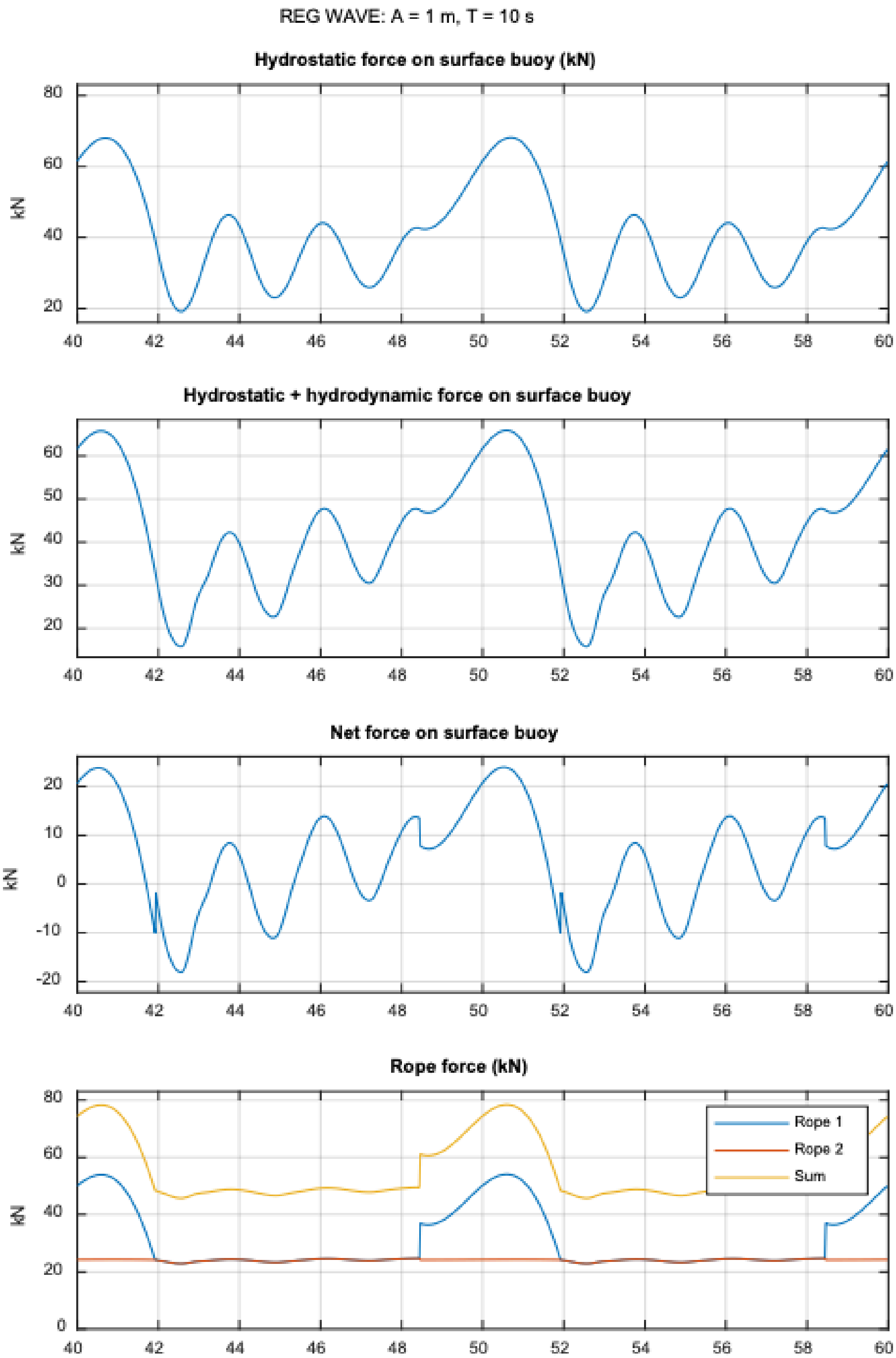

Figure 9 Results (2) for regular wave of 1 m amplitude and 10 s period

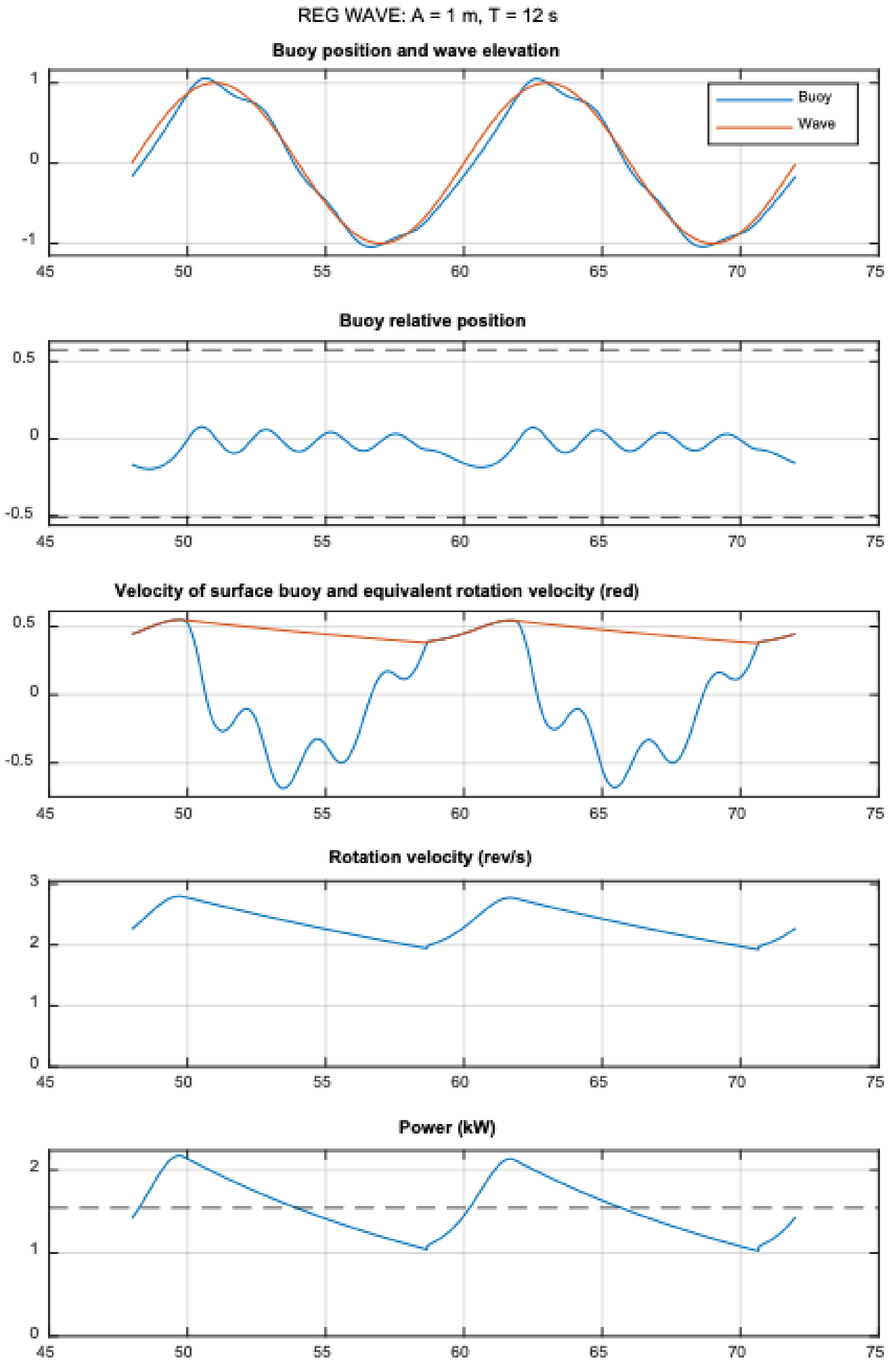

Figure 10 Results (1) for regular wave of 1 m amplitude and 12 s period

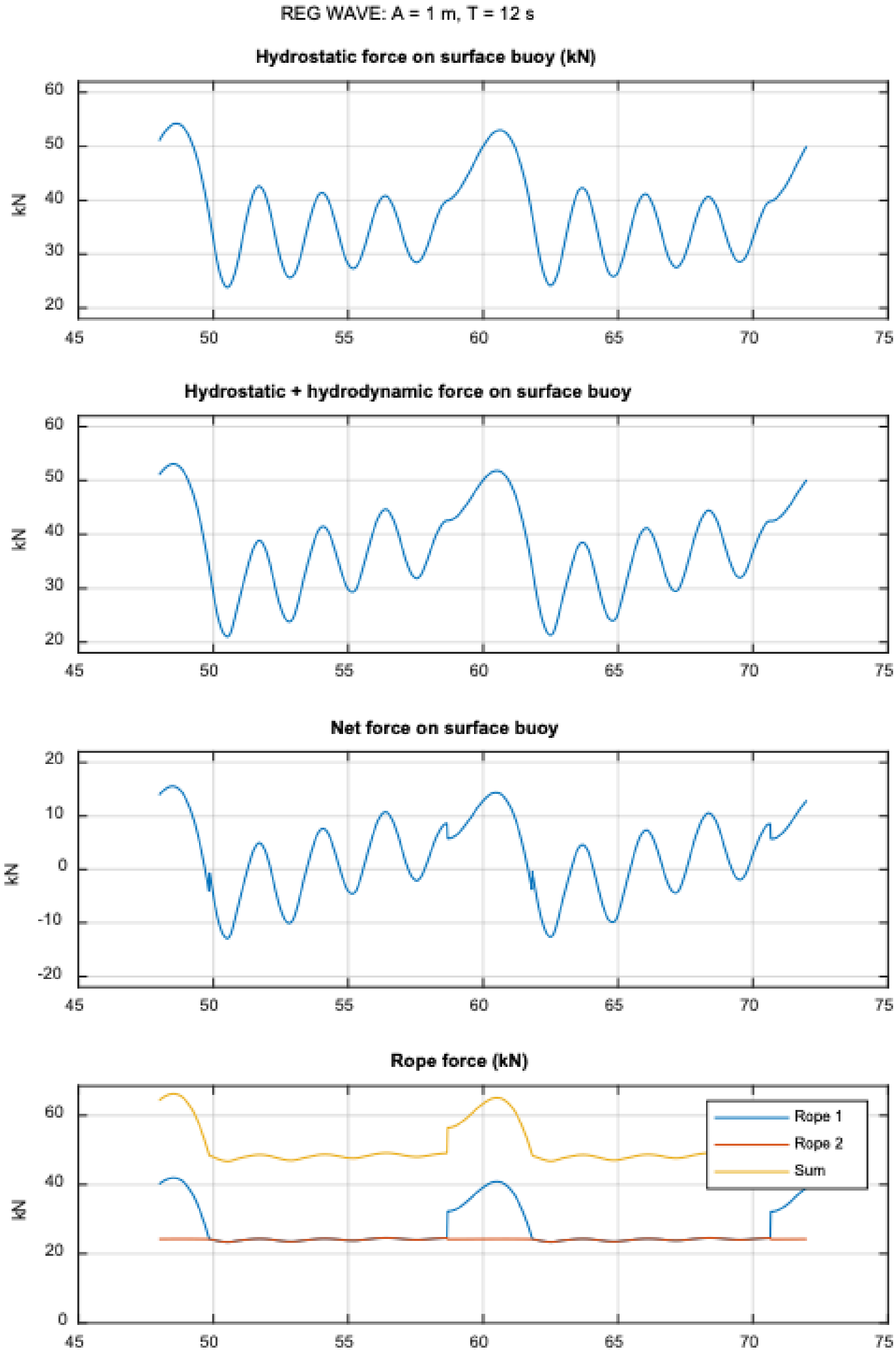

Figure 11 Results (2) for regular wave of 1 m amplitude and 12 s period.

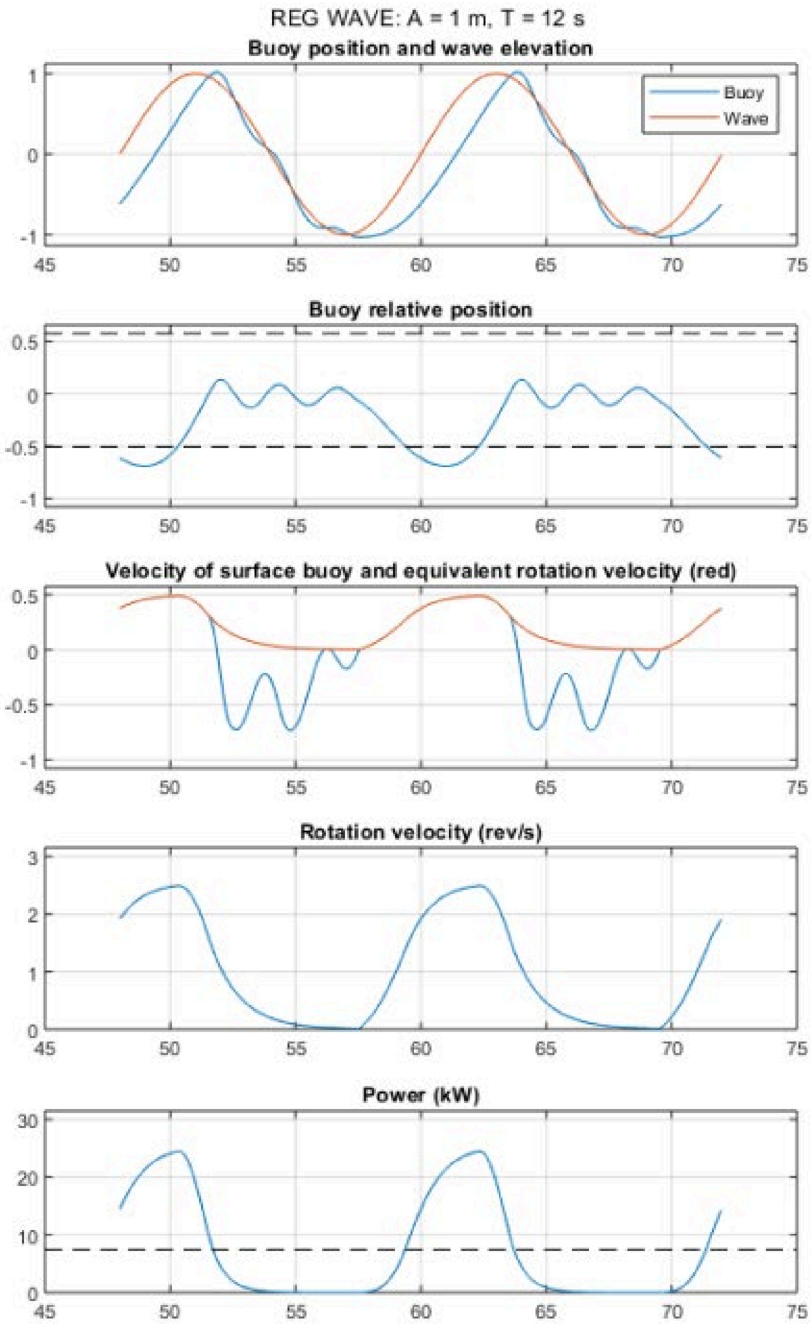

Figure 12 Buoy motion and power extraction with no constraint on generator speed. Dashed line shows mean power. C_{PTO} = 100 Nm rad/s, I = 120 kg m^2

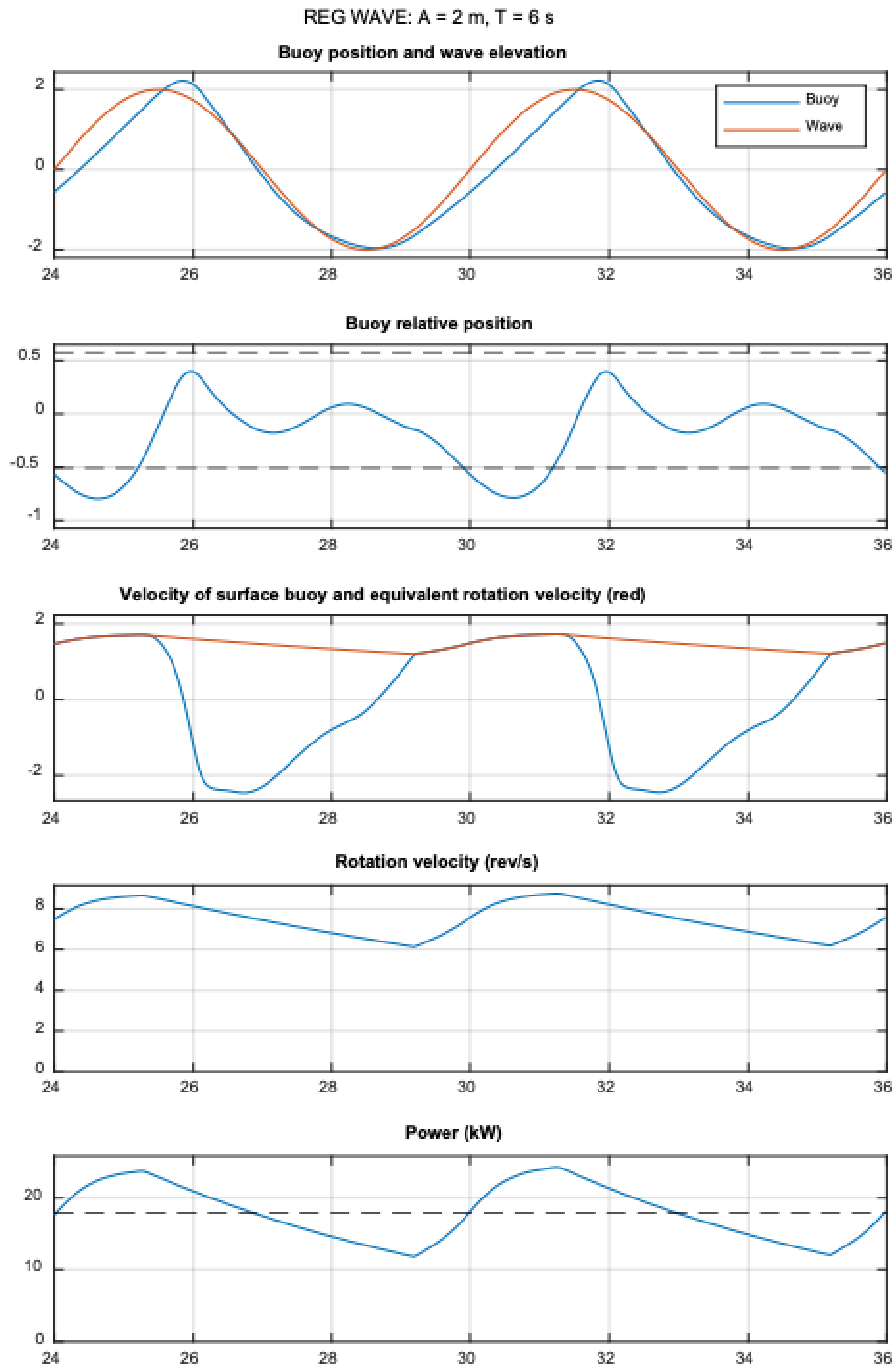

Figure 13 Results (1) for regular wave of 2 m amplitude and 6 s period

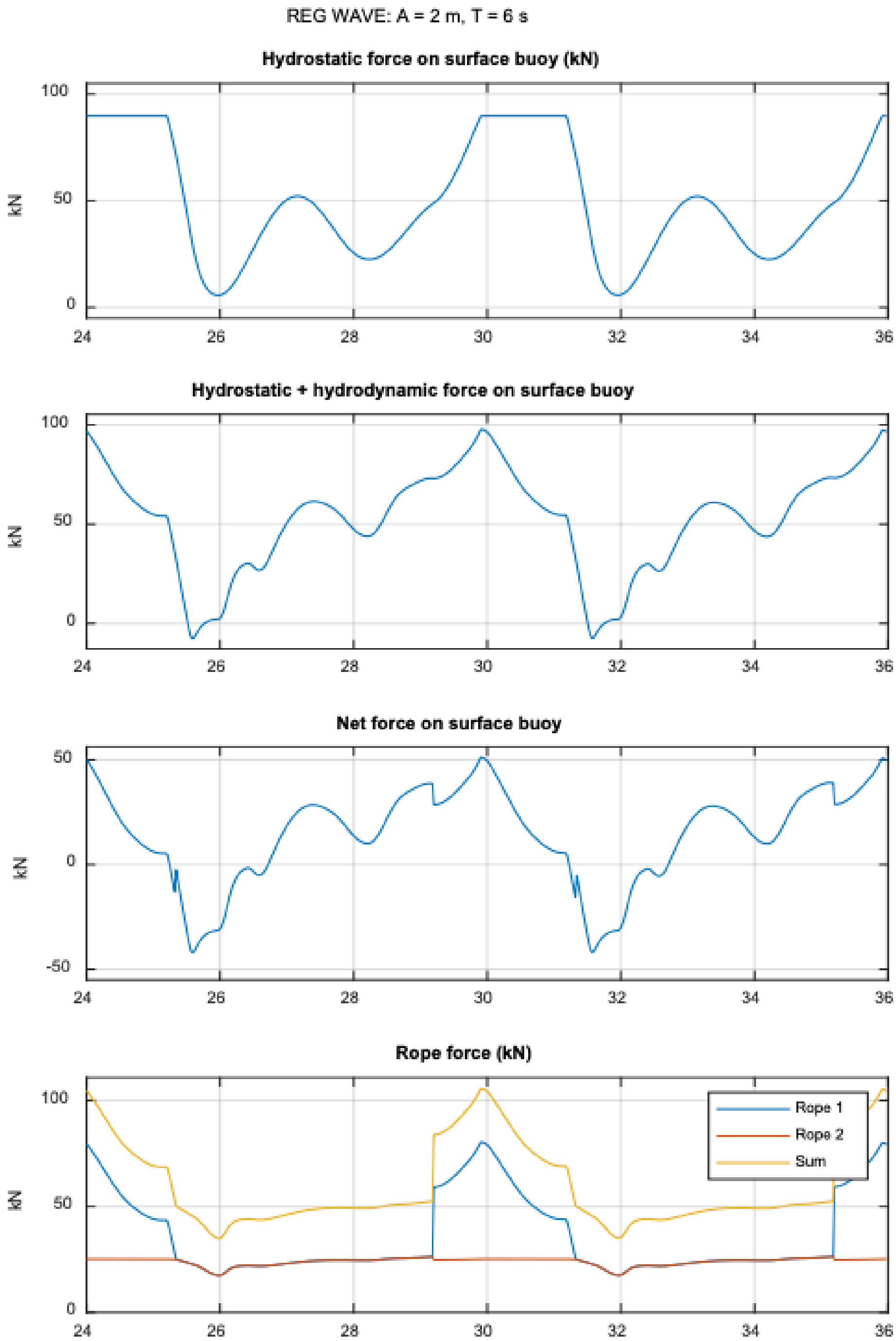

Figure 14 Results (2) for regular wave of 2 m amplitude and 6 s period

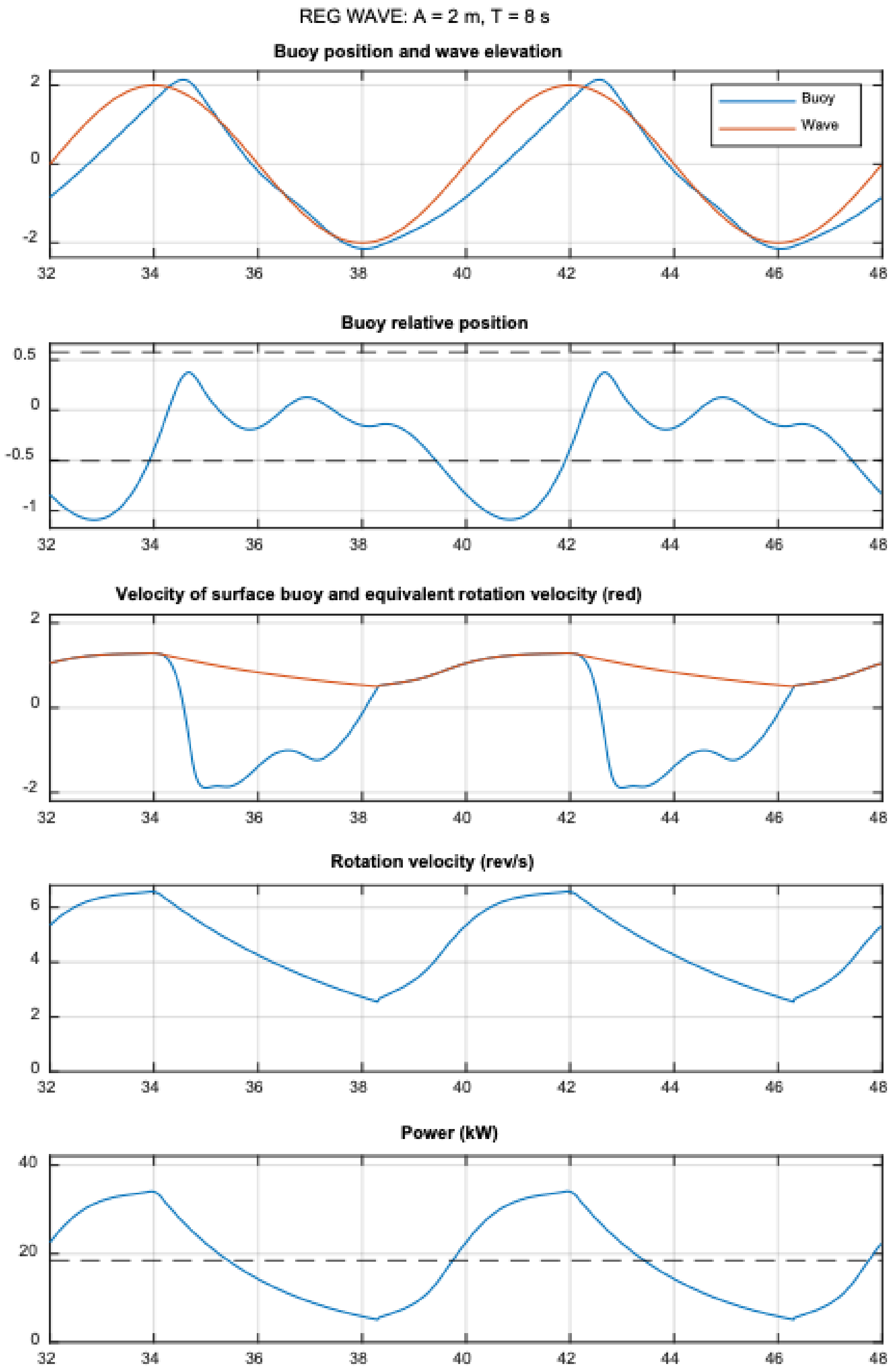

Figure 15 Results (1) for regular wave of 2 m amplitude and 8 s period

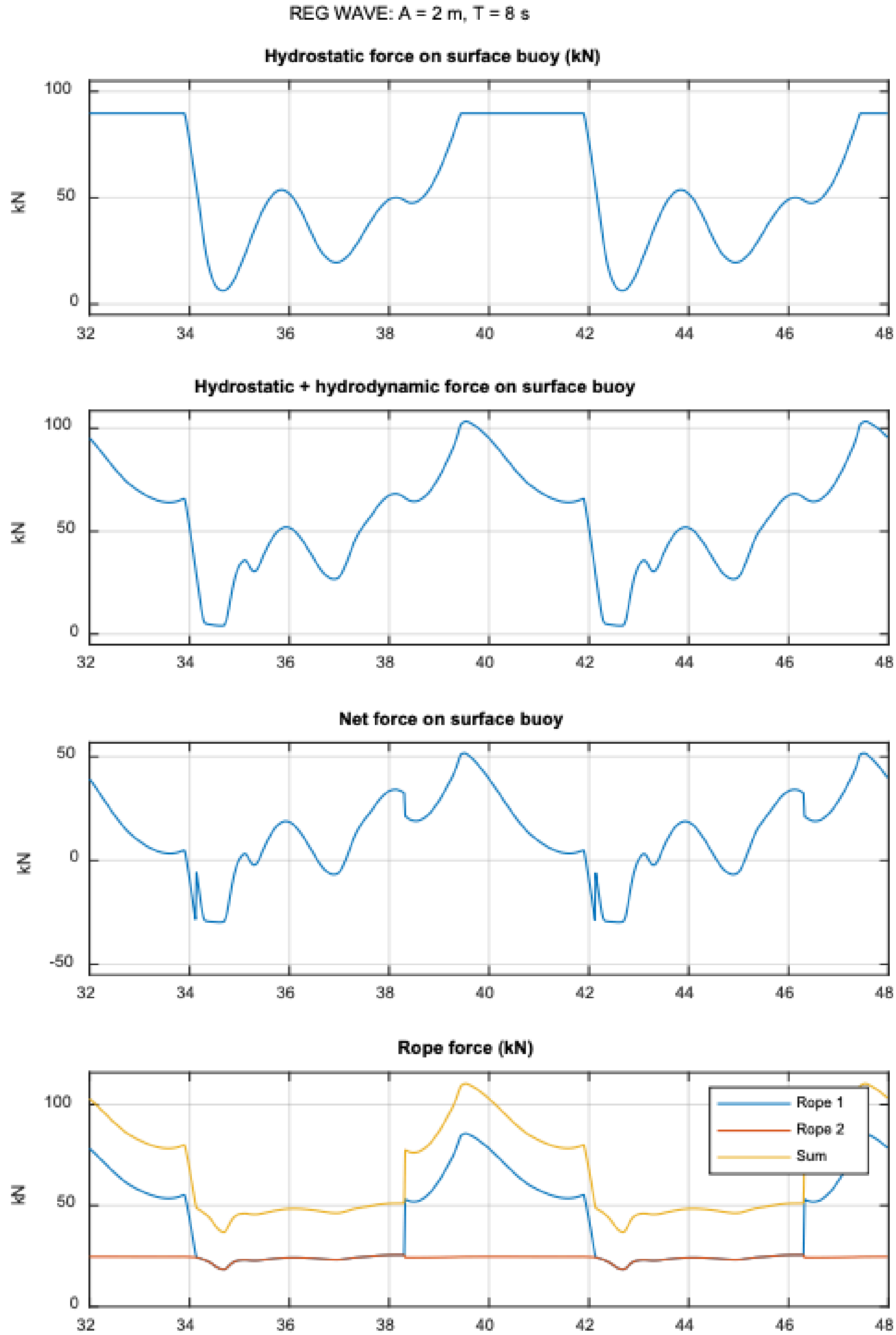

Figure 16 Results (2) for regular wave of 2 m amplitude and 8 s period

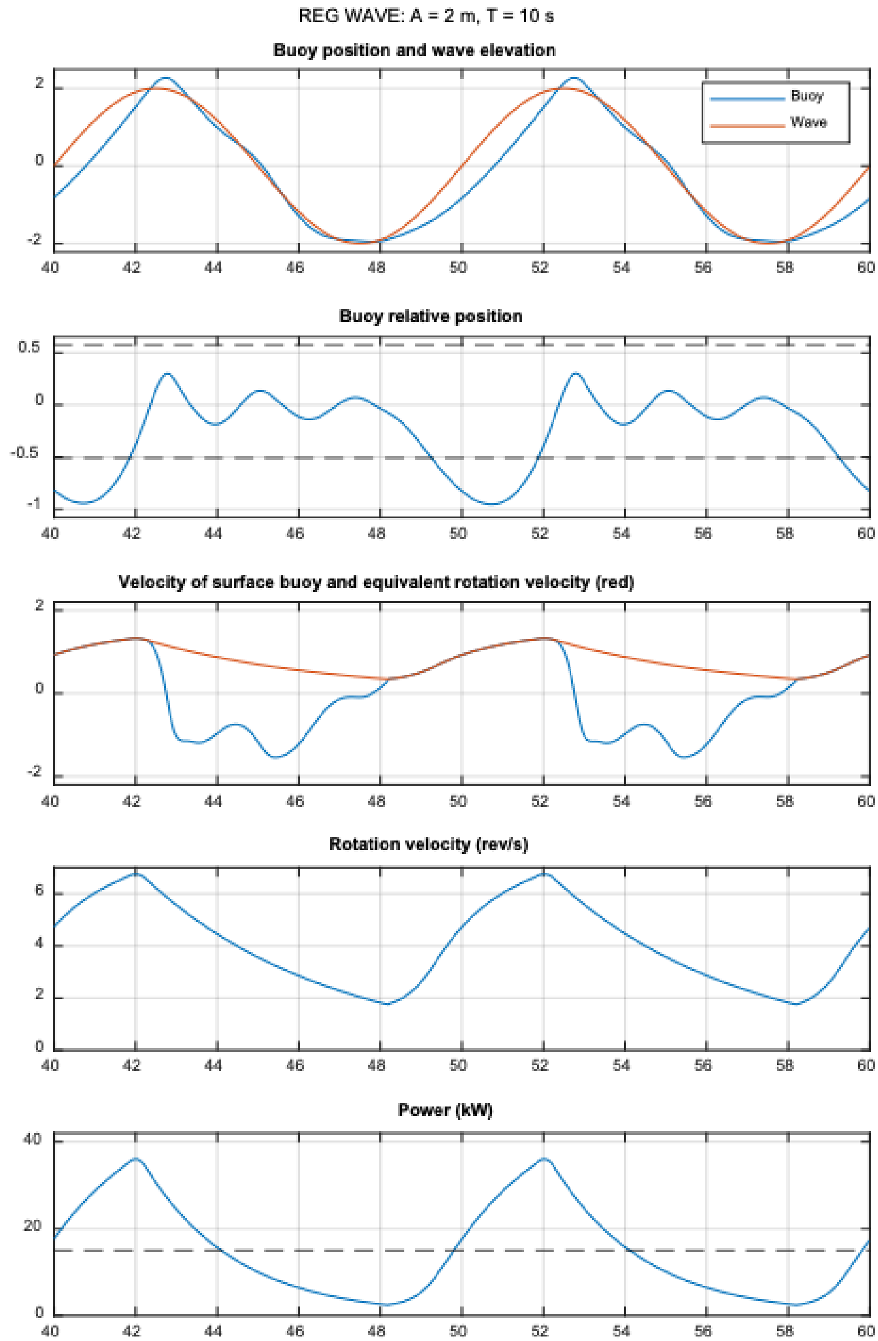

Figure 17 Results (1) for regular wave of 2 m amplitude and 10 s period

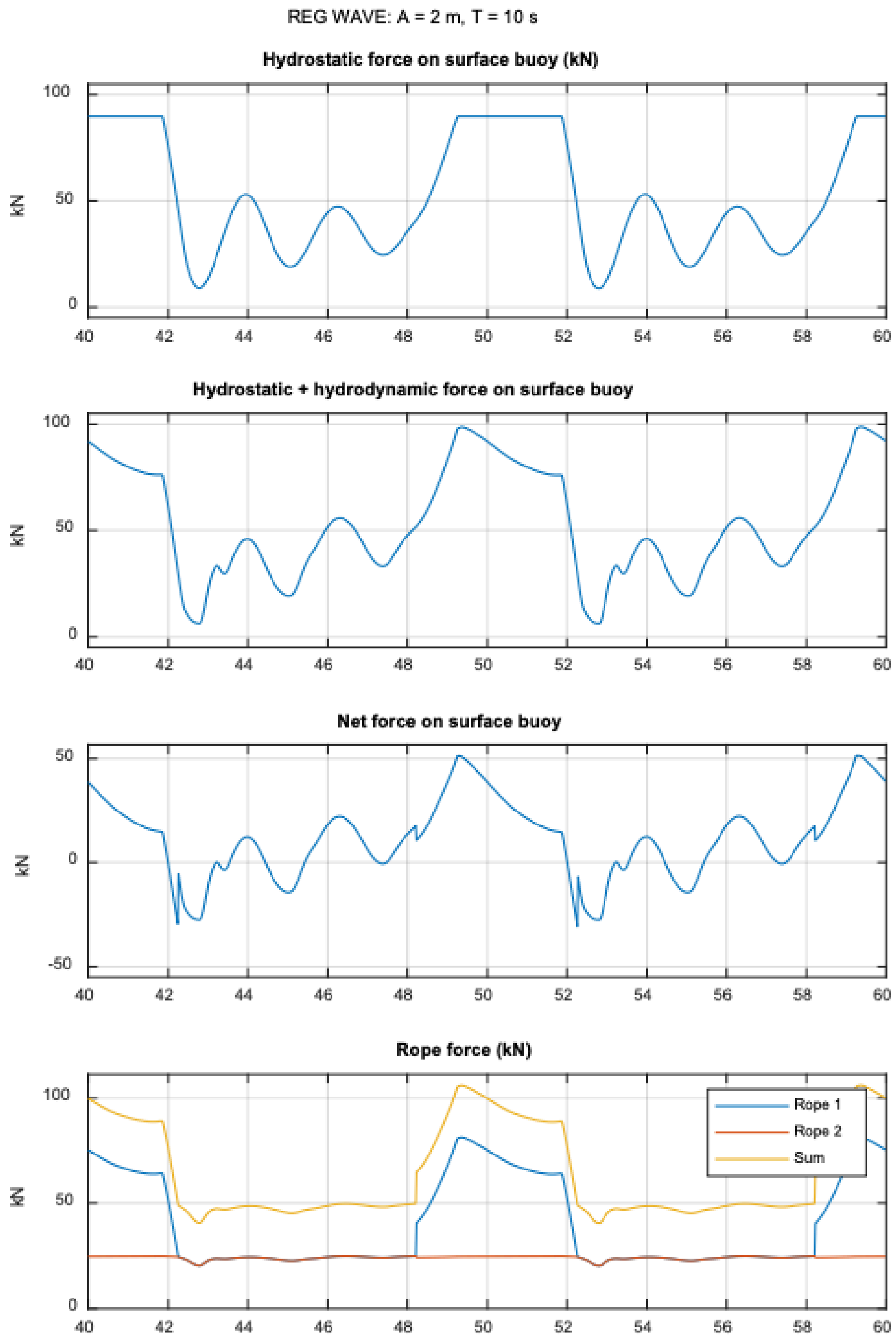

Figure 18 Results (2) for regular wave of 2 m amplitude and 10 s period

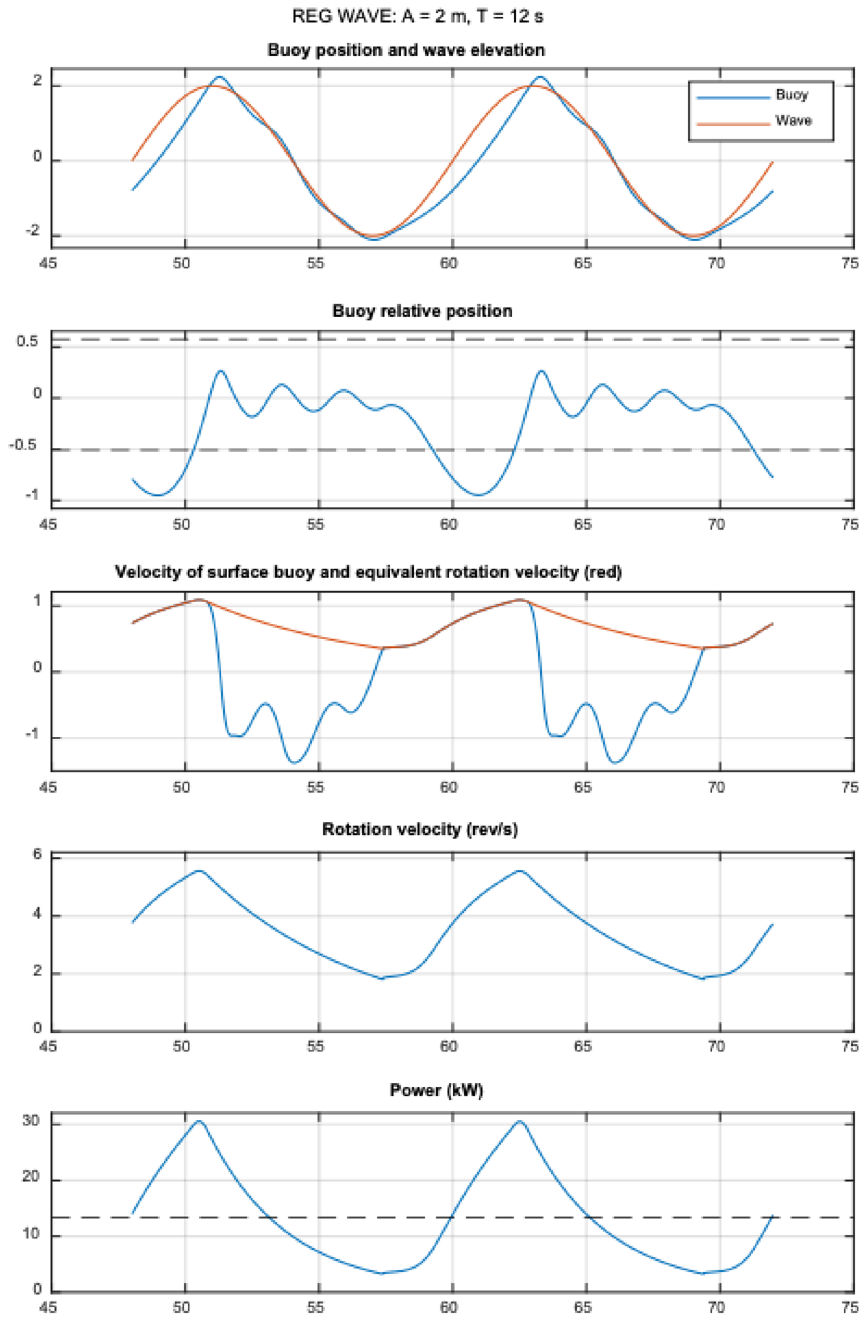

Figure 19 Results (1) for regular wave of 2 m amplitude and 12 s period

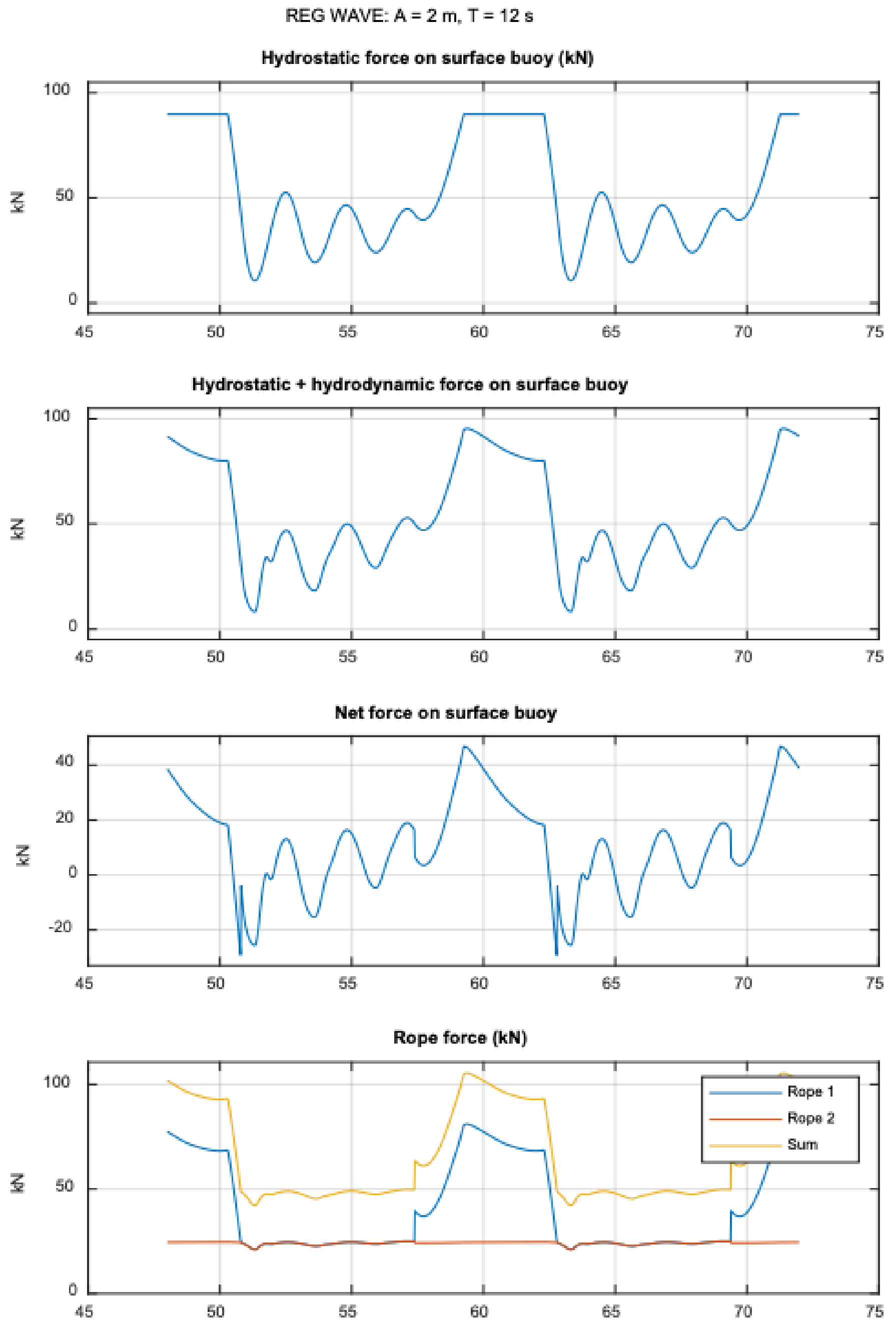

Figure 20 Results (2) for regular wave of 2 m amplitude and 12 s period

6.2 Irregular waves

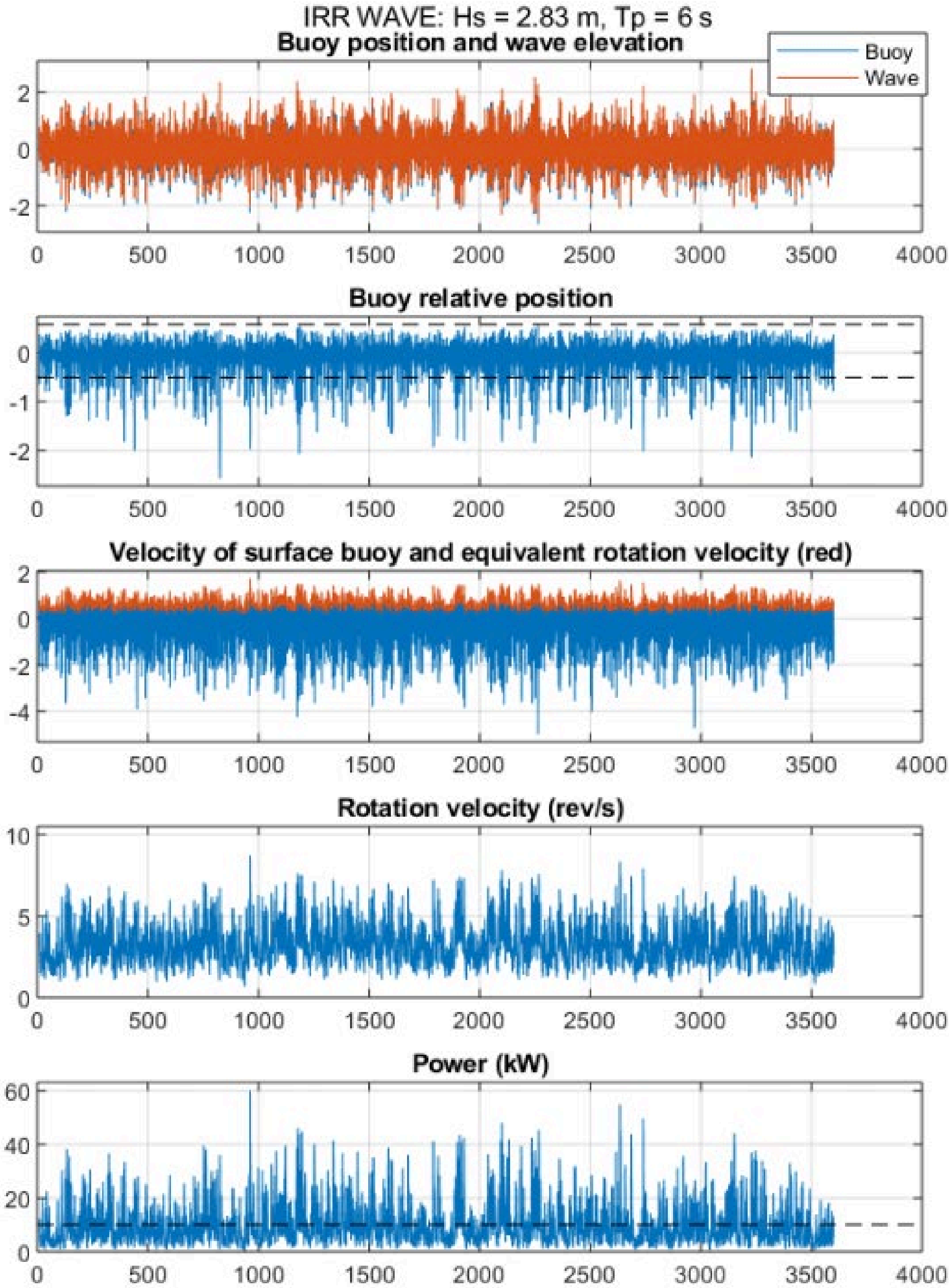

Figure 21 Results for irregular waves (Jonswap, Hs=2.83 m, Tp=6 s, gamma=3.3)

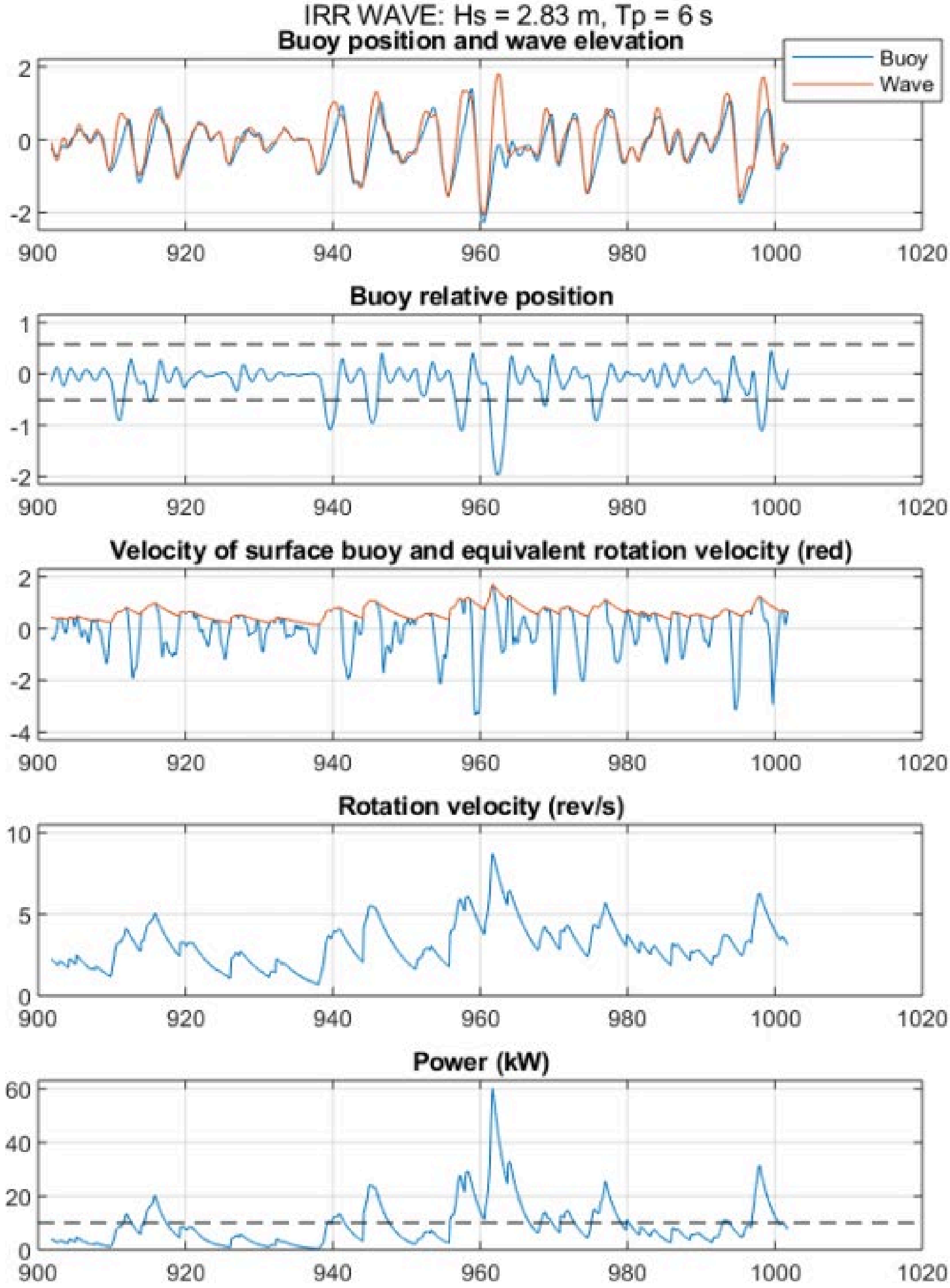

Figure 22 Results for irregular waves. Details around incident of maximum power (Jonswap, Hs=2.83 m, Tp=6 s, gamma=3.3)

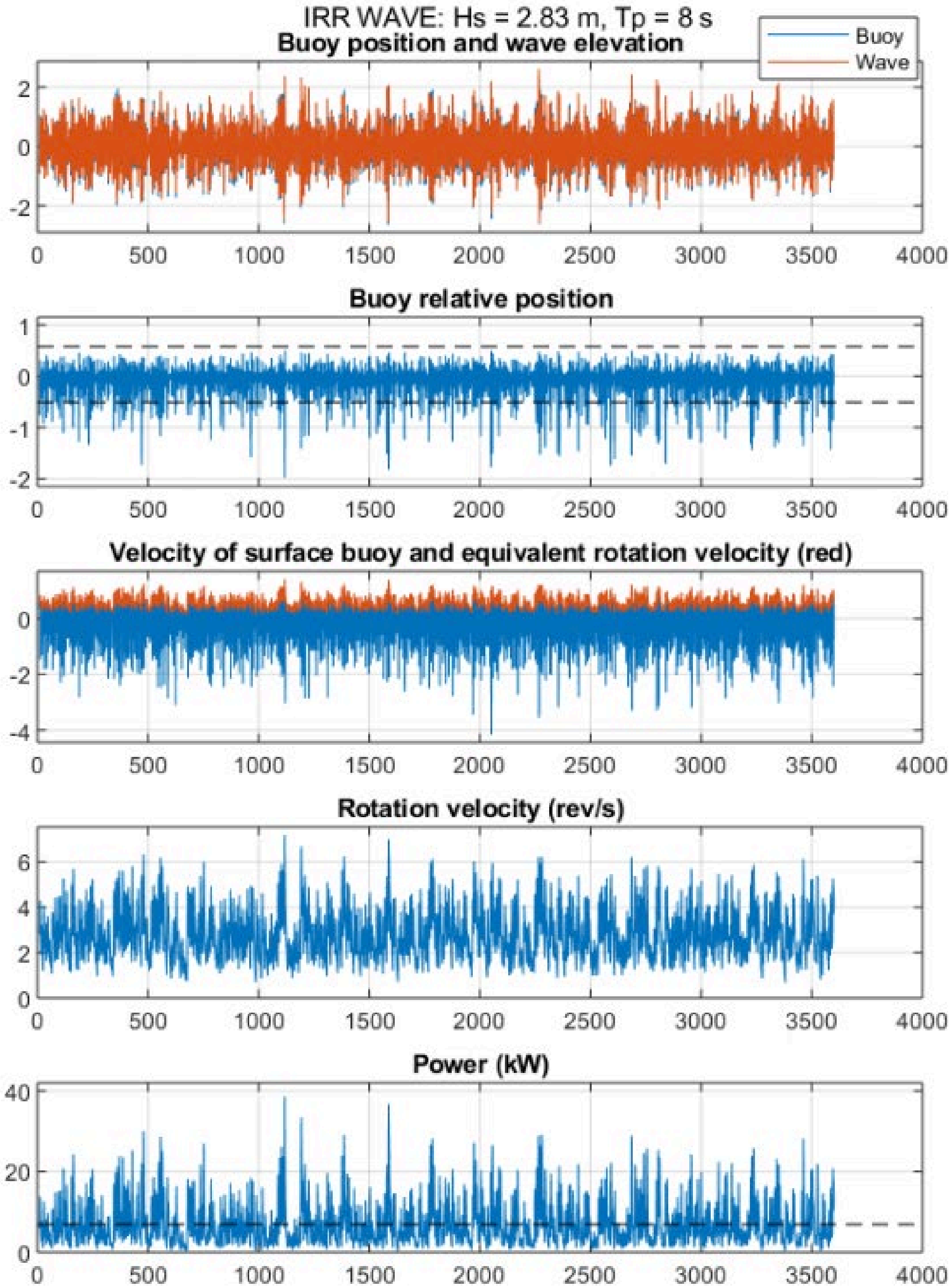

Figure 23 Results for irregular waves (Jonswap, Hs=2.83 m, Tp=8 s, gamma=3.3)

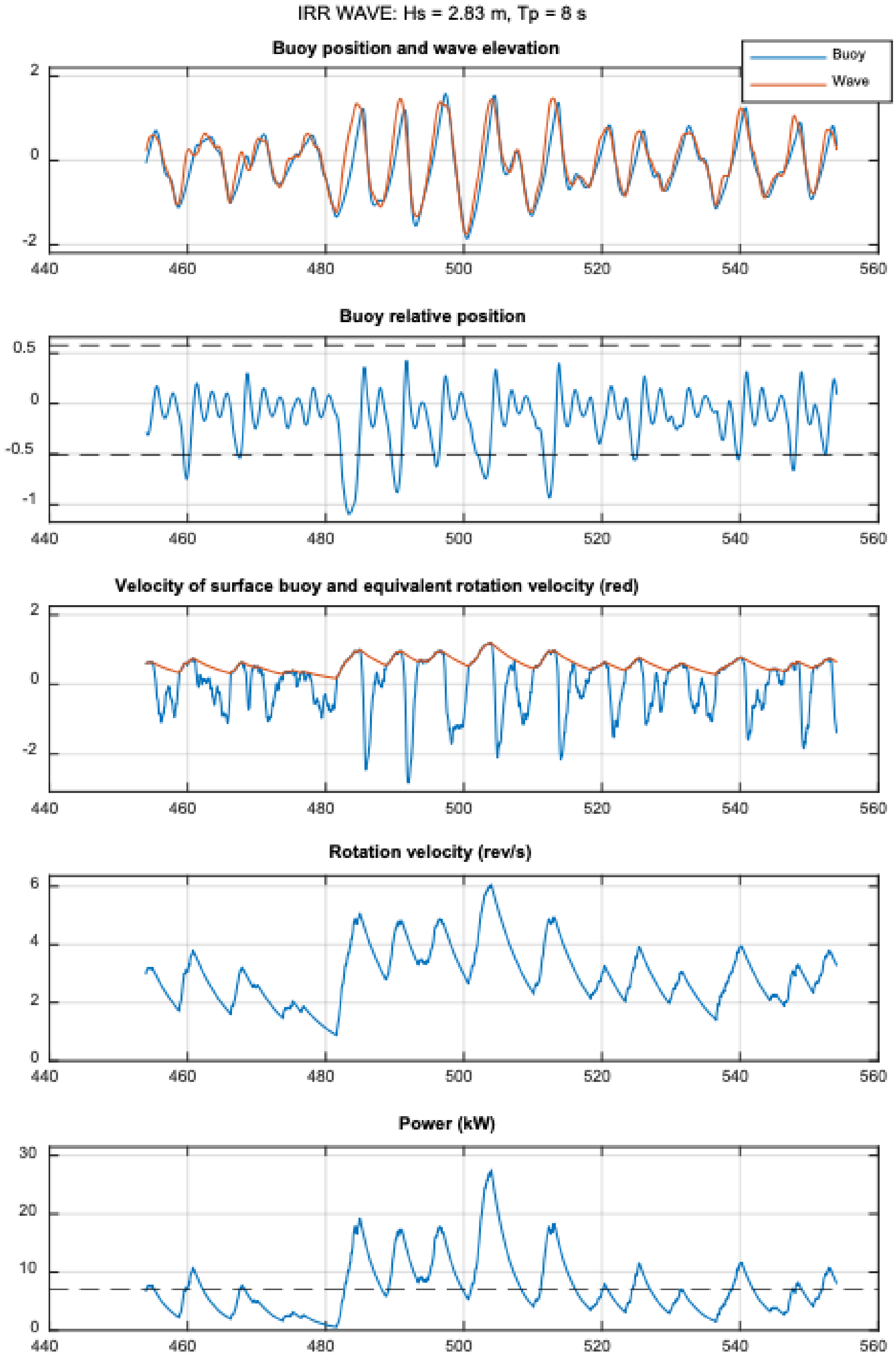

Figure 24 Results for irregular waves. Details around incident of maximum power (Jonswap, Hs=2.83 m, Tp=8 s, gamma=3.3)

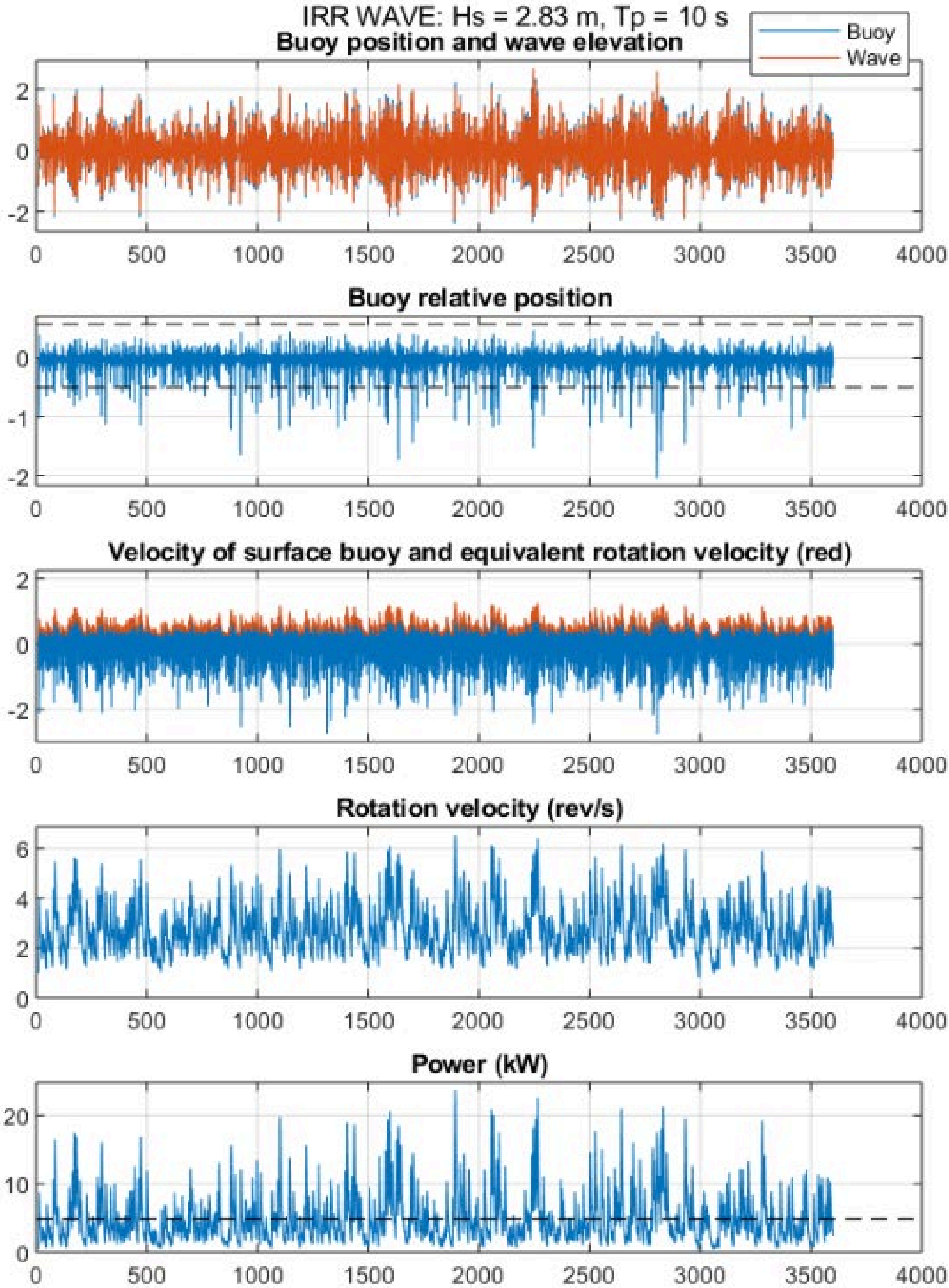

Figure 25 Results for irregular waves (Jonswap, Hs=2.83 m, Tp=10s, gamma=3.3)

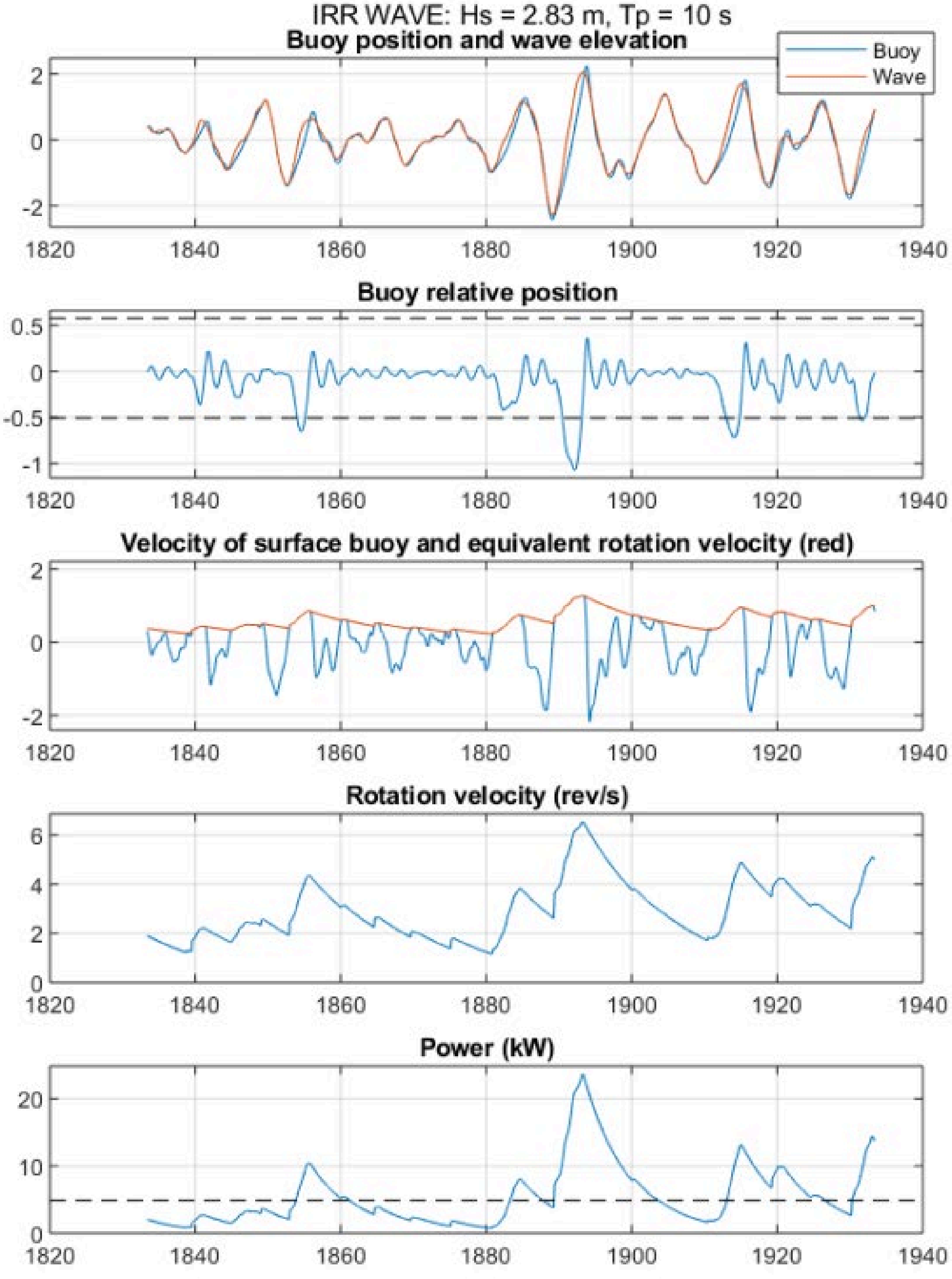

Figure 26 Results for irregular waves. Details around incident of maximum power (Jonswap, Hs=2.83 m, Tp=10 s, gamma=3.3)

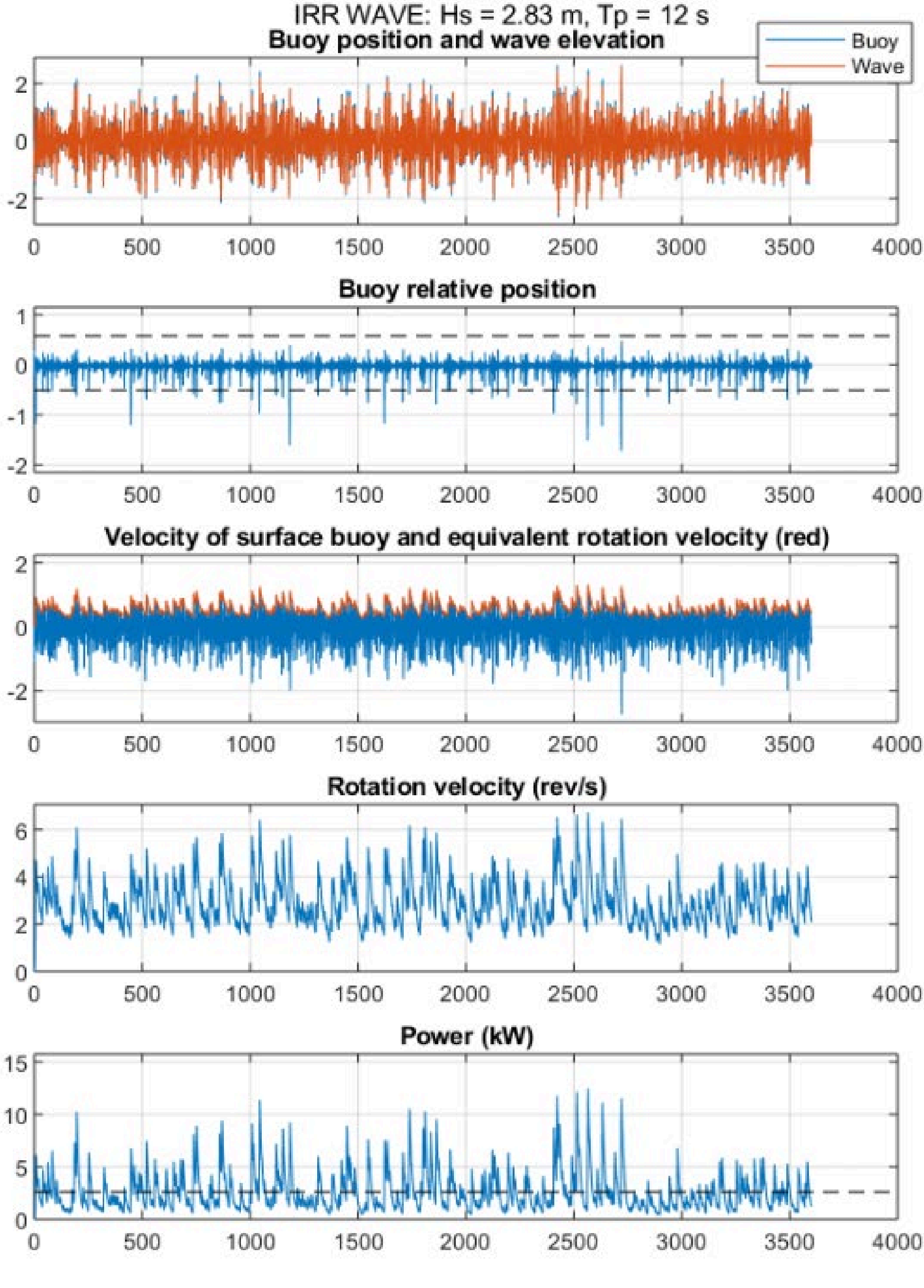

Figure 27 Results for irregular waves. (Jonswap, Hs=2.83 m, Tp=12 s, gamma=3.3)

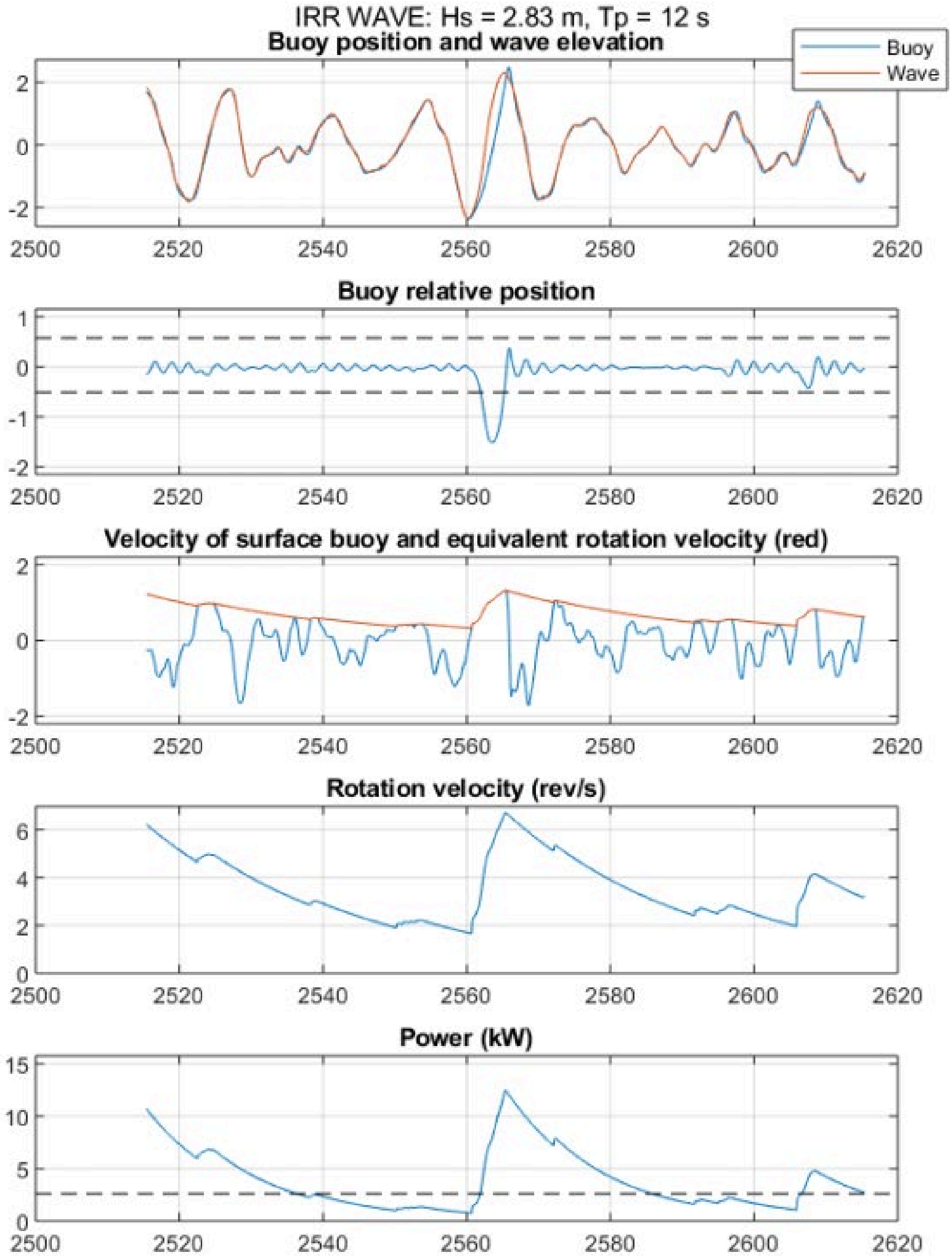

Figure 28 Results for irregular waves. Details around incident of maximum power (Jonswap, Hs=2.83 m, Tp=12 s, gamma=3.3)

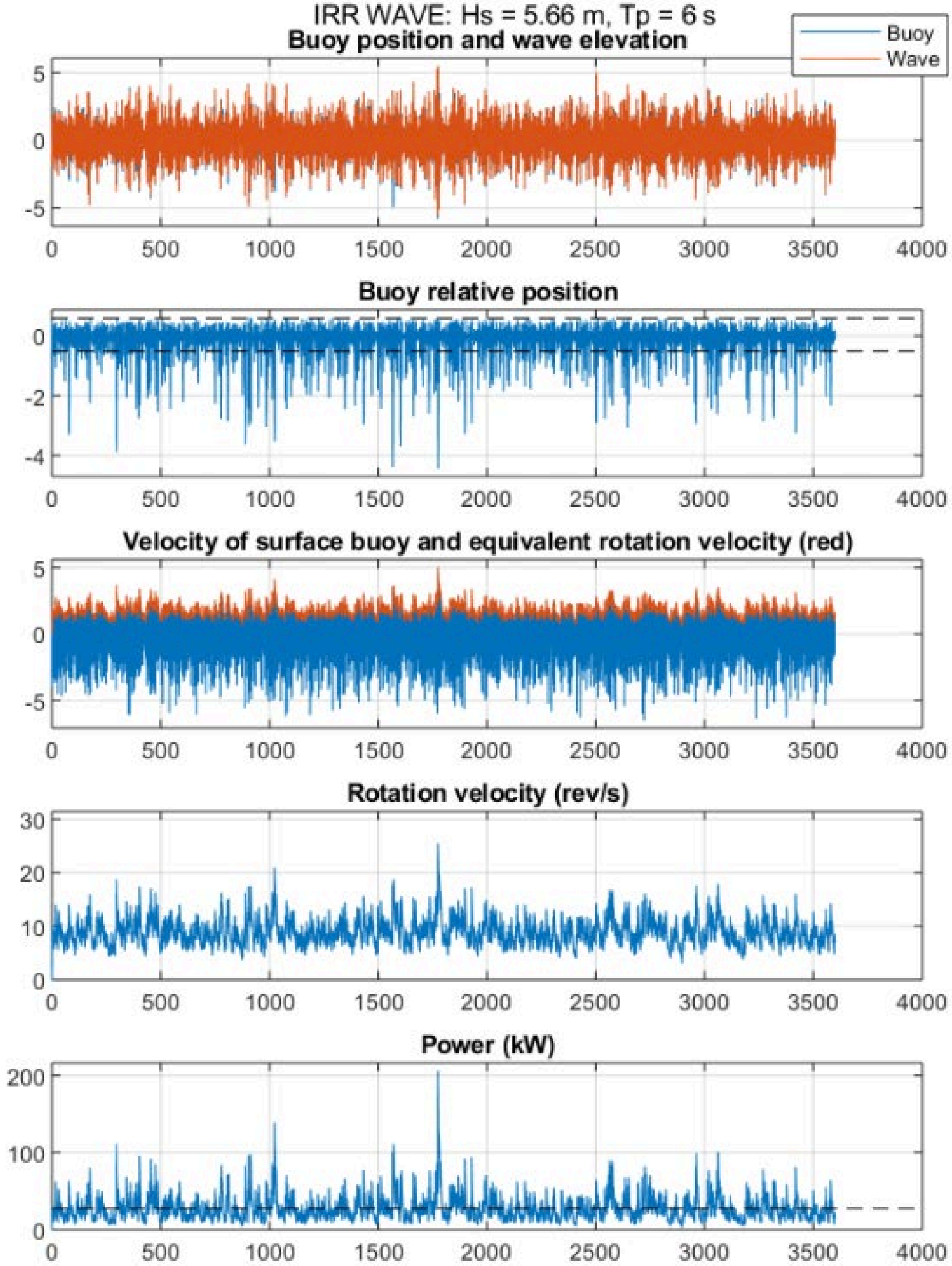

Figure 29 Results for irregular waves (Jonswap, Hs=5.66 m, Tp=6 s, gamma=3.3)

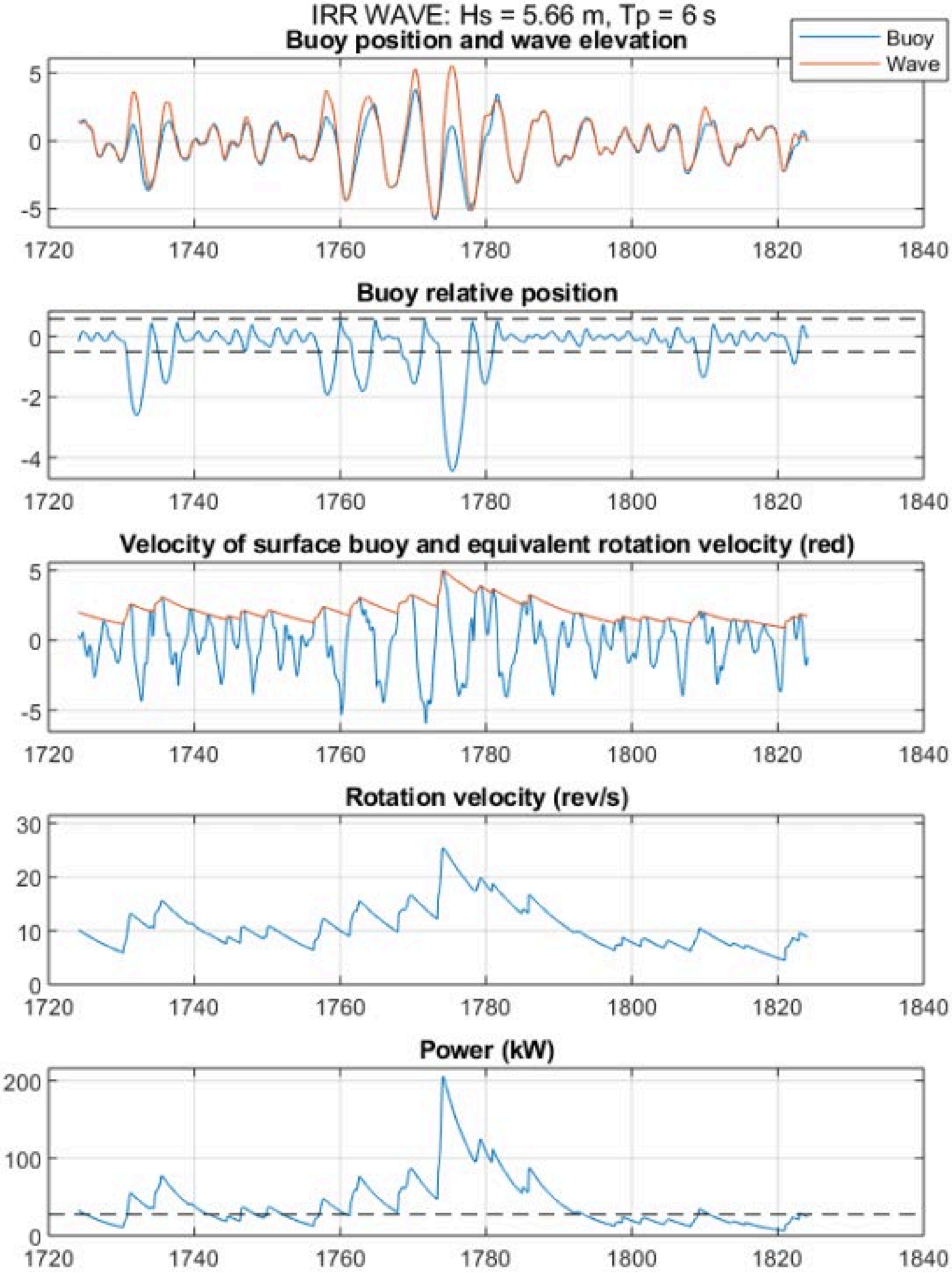

Figure 30 Results for irregular waves. Details around incident of maximum power (Jonswap, Hs=5.66 m, Tp=6 s, gamma=3.3)

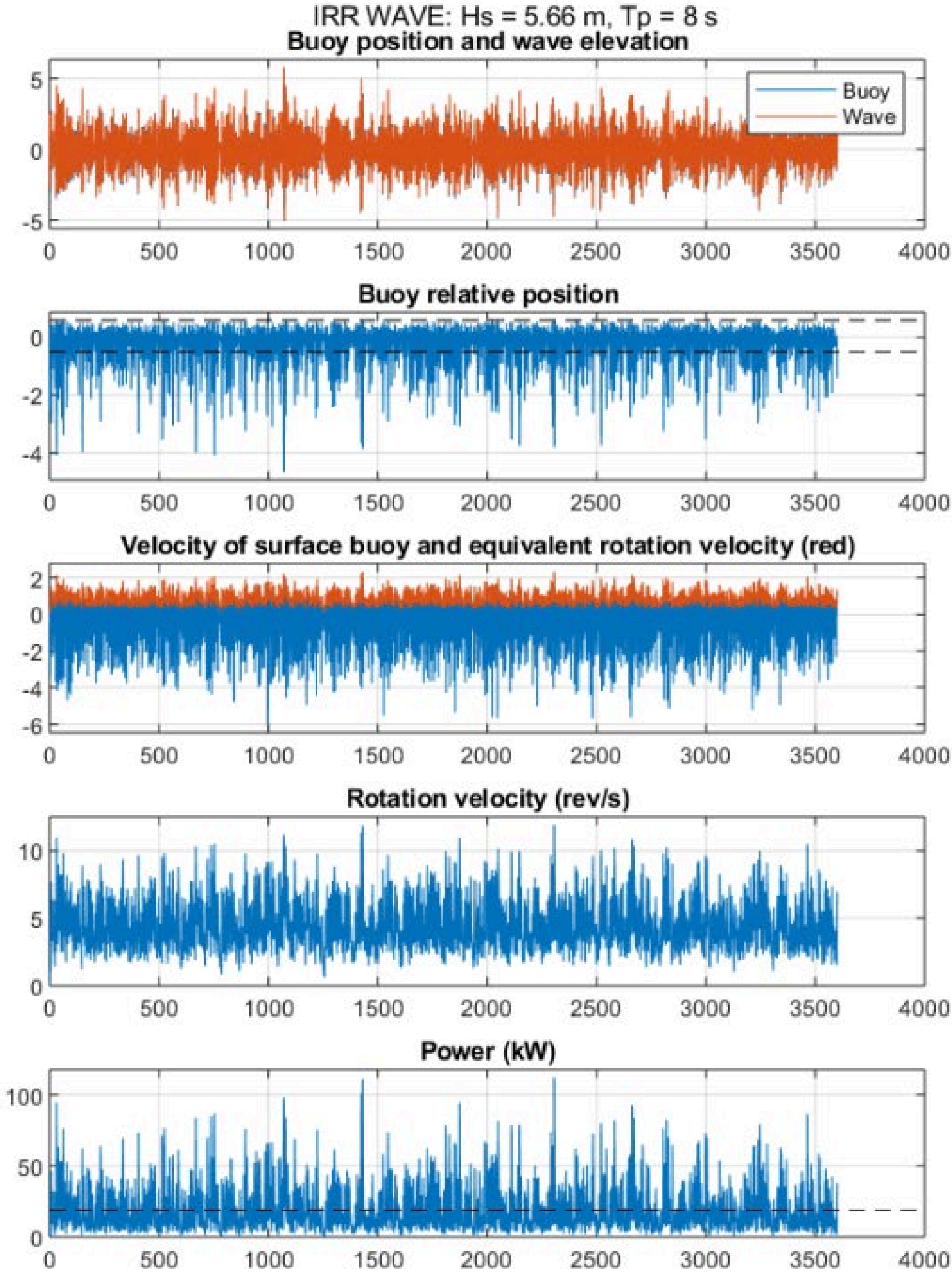

Figure 31 Results for irregular waves (Jonswap, Hs=5.66 m, Tp=8 s, gamma=3.3)

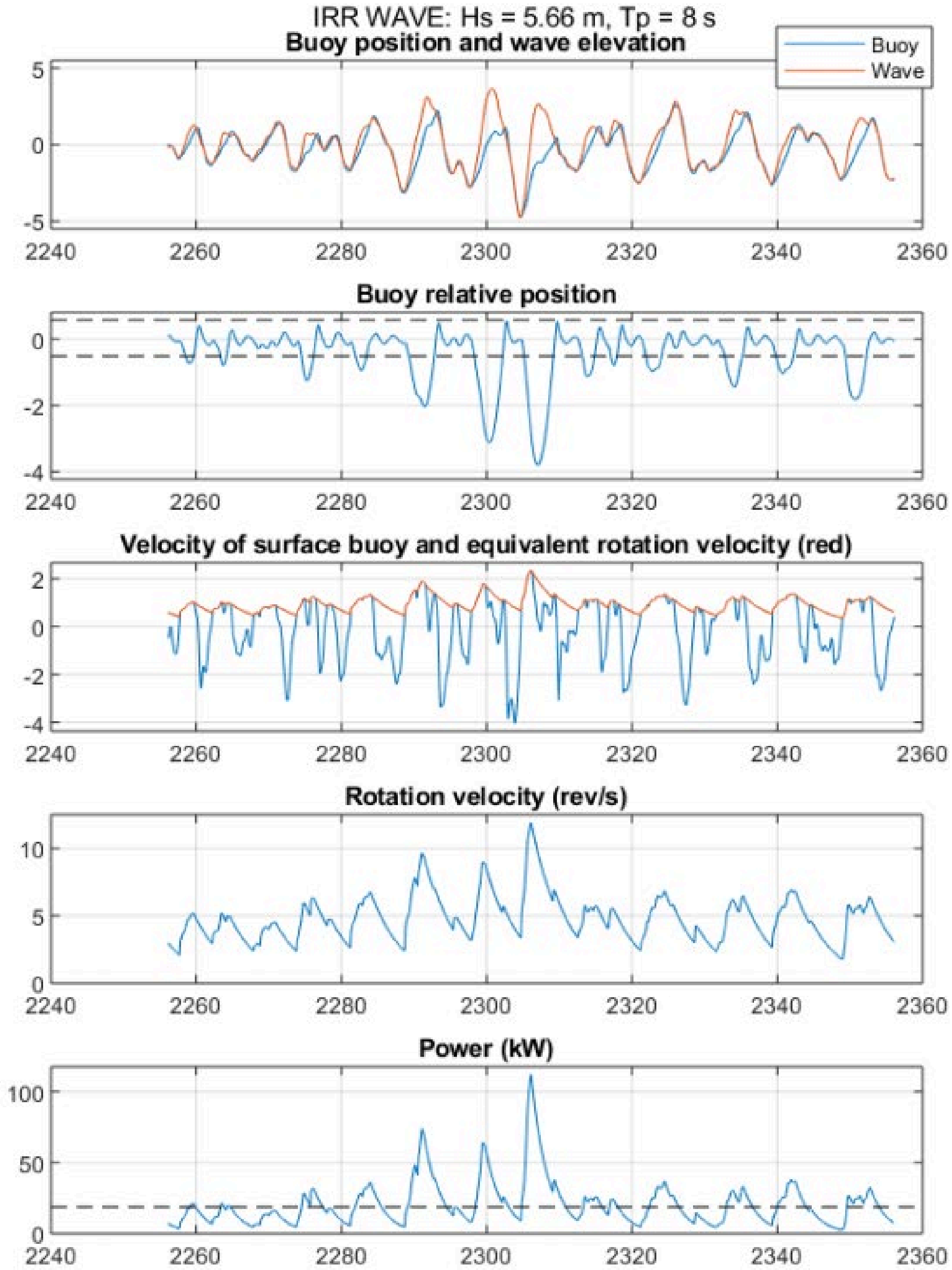

Figure 32 Results for irregular waves. Details around incident of maximum power (Jonswap, Hs=5.66 m, Tp=8 s, gamma=3.3)

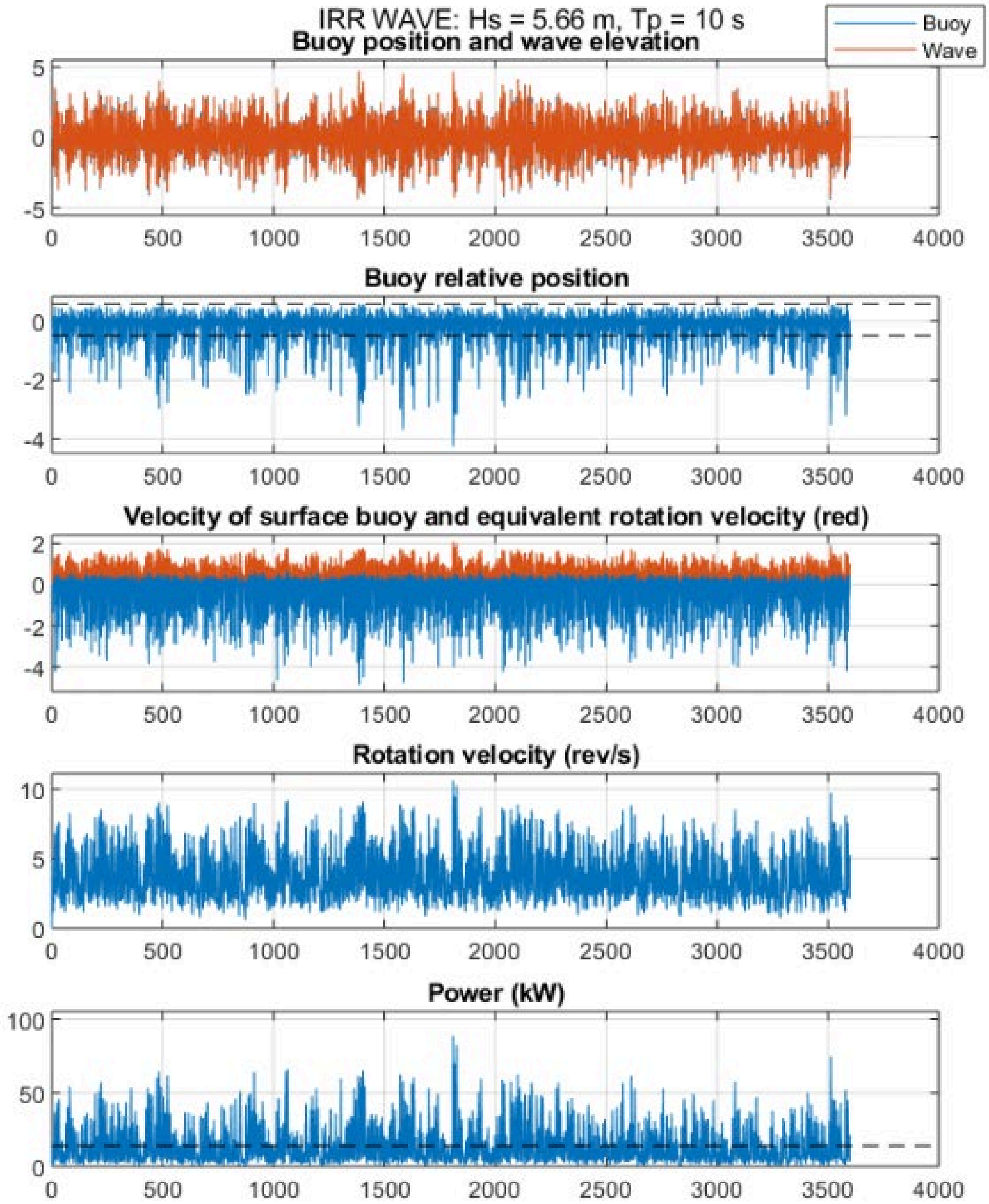

Figure 33 Results for irregular waves (Jonswap, Hs=5.66 m, Tp=10 s, gamma=3.3)

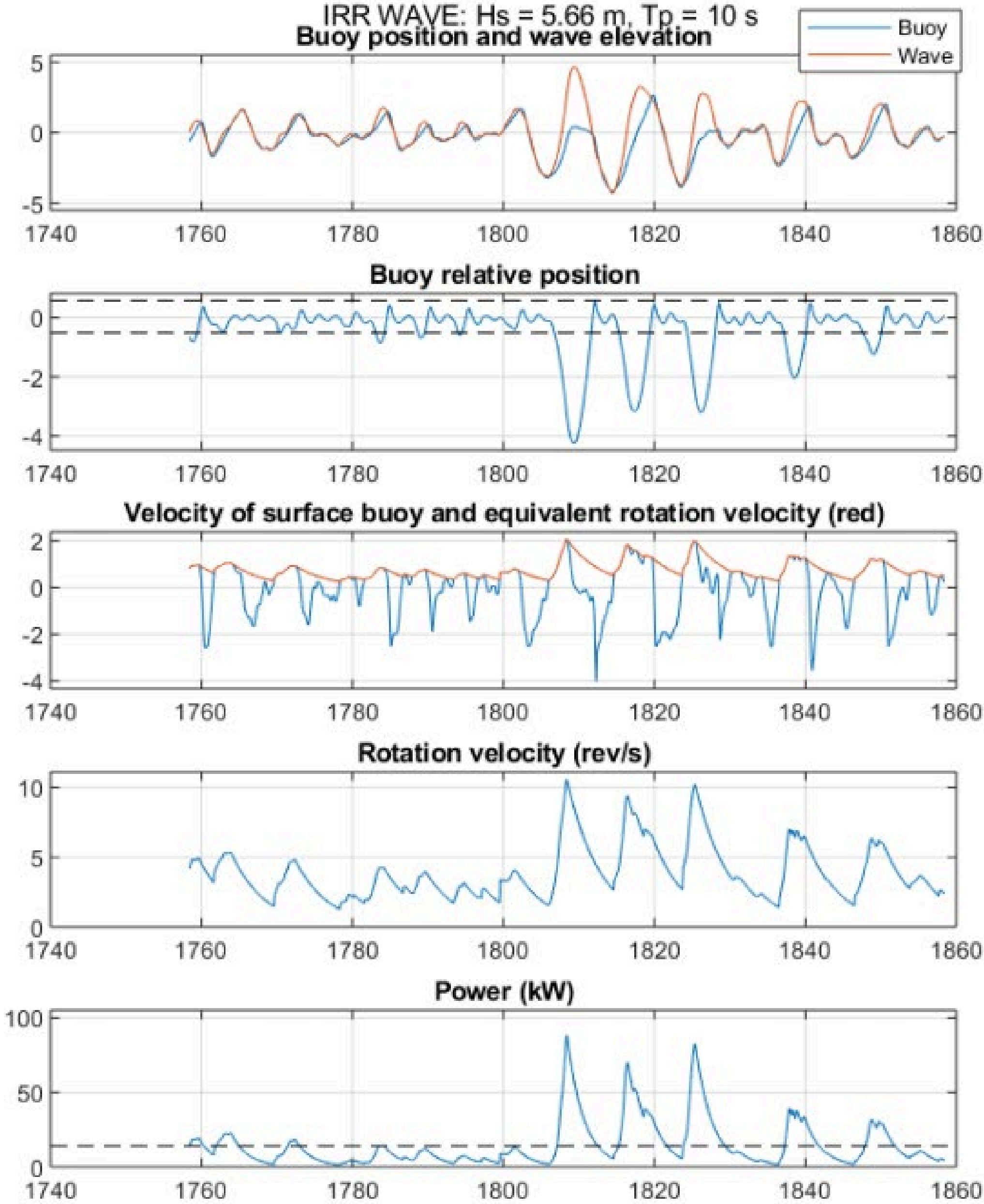

Figure 34 Results for irregular waves. Details around incident of maximum power (Jonswap, Hs=5.66 m, Tp=10 s, gamma=3.3)

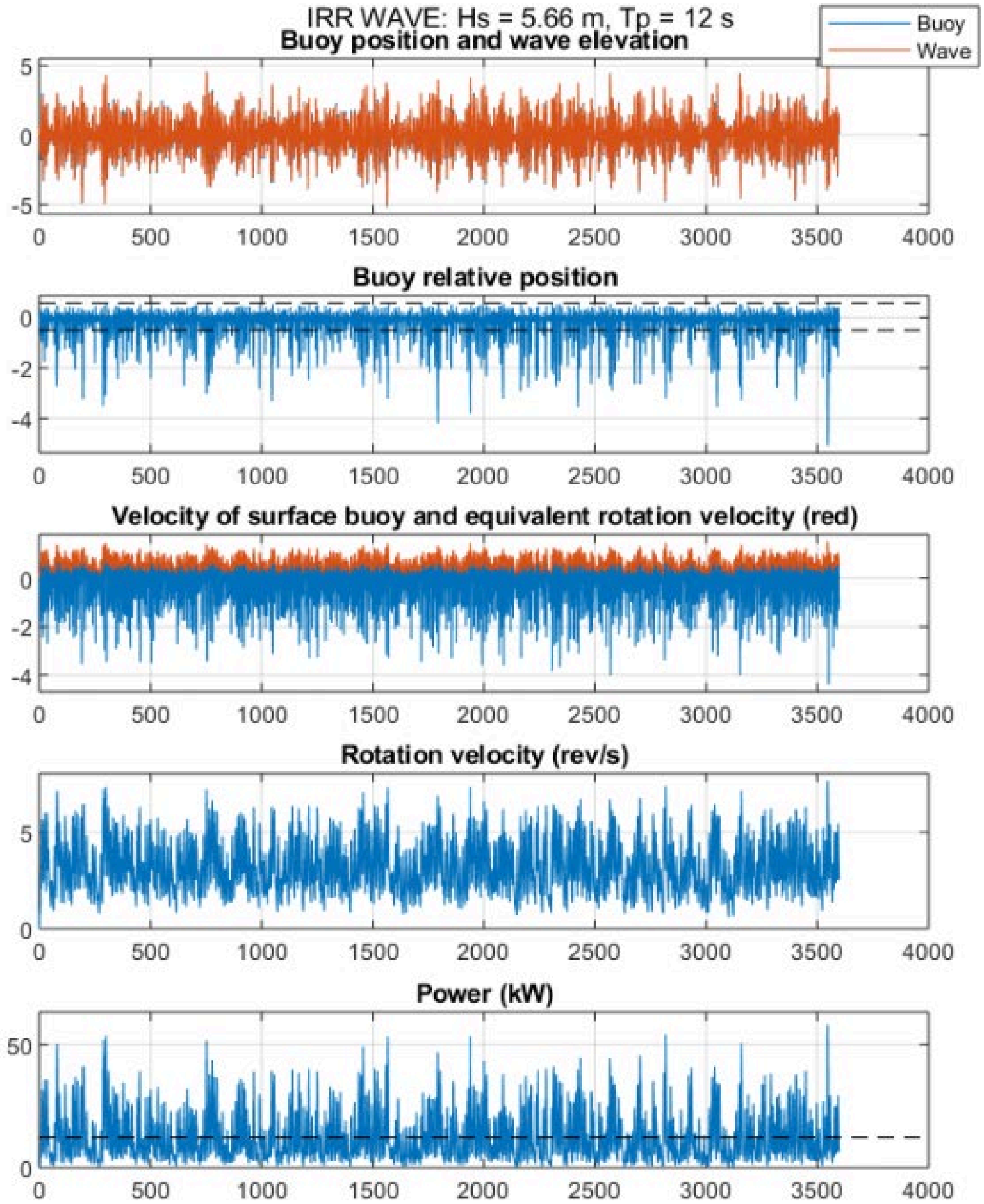

Figure 35 Results for irregular waves (Jonswap, Hs=5.66 m, Tp=12 s, gamma=3.3)

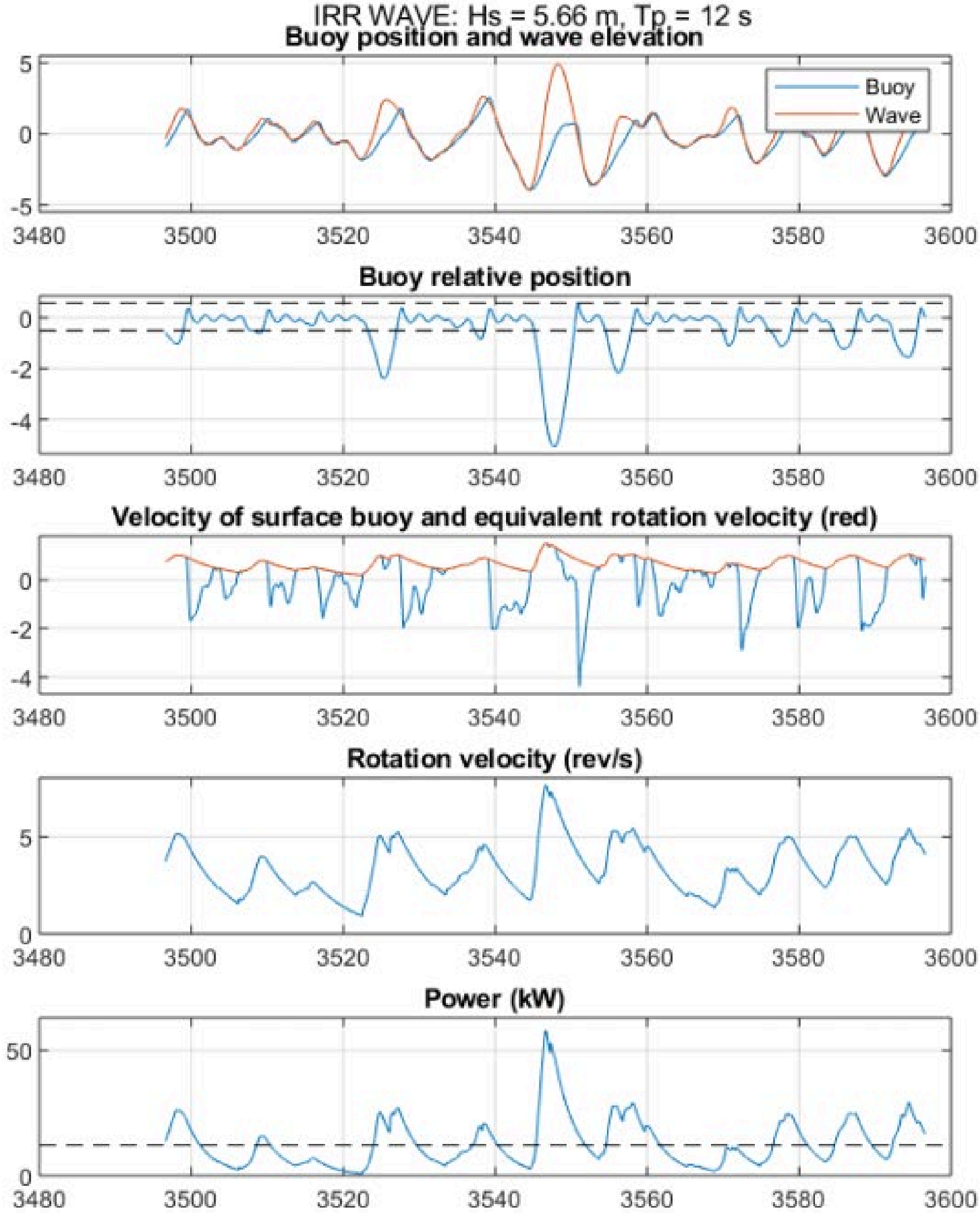

Figure 36 Results for irregular waves. Details around incident of maximum power (Jonswap, Hs=5.66 m, Tp=12 s, gamma=3.3)

Attachment 2

Report from Uppsala University that refer to 170 KW production in the newest generators from the Angstrom Laboratory.

See the whole report at:

http://uu.diva-portal.org/smash/get/diva2:1049240/FULLTEXT01.pdf

Attachment 3

New report from Uppsala University (2019) that makes a small-scale test of «The Balanced System» in the ship tank principle with very positive results.

energies

MDPI

Article

Performance of a Direct-Driven Wave Energy Point Absorber with High Inertia Rotatory Power Take-off

Simon Thomas [1,*], Marianna Giassi [1], Malin Göteman [1], Martyn Hann [2], Edward Ransley [2], Jan Isberg [1] and Jens Engström [1]

1 Lägerhyddsvägen 1, Division of Electricity, Angströmlaboratoriet, Uppsala University, 75237 Uppsala, Sweden; Marianna.Giassi@angstrom.uu.se (M.G.); Malin.Goteman@angstrom.uu.se (M.G.); Jan.Isberg@angstrom.uu.se (J.I.); Jens.Engstrom@angstrom.uu.se (J.E.)

2 School of Engineering, University of Plymouth, Drake Circuit, Plymouth PL4 8AA, UK; Martyn.Hann@plymouth.ac.uk (M.H.); Edward.Ransley@plymouth.ac.uk (E.R.)

* Correspondence: simon.thomas@angstrom.uu.se

Received: 1 August 2018; Accepted: 30 August 2018; Published: 4 September 2018

check for updates

Abstract: An alternating rotatory generator using an eddy current break is developed as a physical scale model of a direct-driven floating point absorber power take-off (PTO) for wave tank tests. It is shown that this design is a simple and cost-effective way to get an accurate linear damping PTO. The device shows some beneficial characteristics, making it an interesting option for full scale devices: For similar weights the inertia can be significantly higher than for linear generators, allowing it to operate with natural frequencies close to typical wave frequencies. The influence of the higher inertia on the power absorption is tested using both a numerical simulation and physical wave tank tests. With the increased inertia the PTO is able to absorb more than double the energy of a comparable direct-driven linear generator in some sea states. Moreover, the alternating rotatory generator allows the absorption characteristic to be tuned by changing the inertia and the generator damping.

Keywords: wave energy; power take-off; direct-driven; wave tank test; physical scale model; natural frequency tuning; floating point absorber

---

1. Introduction

Physical wave tank tests play an important role in validating numerical results and testing devices under realistic and repeatable conditions. They are an important, while cost efficient, step in the development of a wave energy converter (WEC) before going to full scale. In this paper a new power take-off (PTO) design for floating point absorbers is presented which has been developed especially for wave tank tests.

Despite extensive research on wave energy during the last decades [1], the levelized cost of energy is too high compared to other energy sources [2]. One way of lowering these costs is to simplify the mechanical design of the wave energy converter, and here especially the power take off (PTO) [3]. One notable WEC design, which was also the inspiration for the WEC presented here, is the floating point absorber with linear generator, for example developed at Uppsala University [4] (UU-WEC), CorPower [5] or the Archimedes Wave Swing [6]. A disadvantage of most of these devices, is the high natural frequency, leading to a poor capture width for sea states with long wave energy periods, if no additional control [7] or similar mechanism [8,9] is applied.

A simple way to increase the natural frequency occurred while developing a power take-off device (PTO) mimicking an ideal generator for model scale wave tank tests of WEC arrays. Existing physical scale models of WECs can roughly be divided into two groups: Simple and cost-effective models neglecting the generator force or replacing it with a constant friction [10], while advanced scale

Energies **2018**, *11*, 2332; doi:10.3390/en11092332 www.mdpi.com/journal/energies

models may use electric actuators mimicking the generator [11–14]. The latter may mimic the generator behaviour very well, but relays heavily on a good control system. For the purpose of working under time-constraints with several physical scale WECs, a motor-based approach, seemed too complex and too susceptible to faults. But on the same side, when concentrating on the absorbed power a high accurate generator model is indispensable.

The physical model presented here combines the simplicity and cost-efficiency of inaccurate models, whilst providing a nearly ideal damping force and an improved power absorption. This is done by combining two fundamental concepts used for PTOs: The alternating linear generator and the unidirectional rotatory generator. Using rotatory generators for wave power requires a gearbox (hydraulic, pneumatic [15] or mechanical [16,17]), transforming the linear alternating motion of the wave into a unidirectional rotatory motion. Direct-driven linear generators on the other hand generate the electric energy directly from the alternating motion without the losses of a gearbox, but require a rectifier for grid integration [15]. For the physical model presented here, a direct-driven alternating rotatory PTO is used, that does not require a complex gearbox and has a much higher inertia than direct-driven linear generators or unidirectional rotatory generator. Direct-driven rotatory generators converters for low speeds, but with unidirectional motion, play already a significant role in wind power [18,19] and were also tested for WECs [16]. Bi-directional direct-driven rotary converts however can be hardly found [20,21]. In this paper the characteristics of such a PTO, and especially the influence of the high inertia, compared to a direct-driven linear generator will be investigated. A similar analysis of the influence of the inertia on the absorbed power, but for a cylindrical bottom-hinged WEC was performed in [22], while the effects in resonance frequency between fixed and self referenced point absorber are discussed in [23].

PTO concepts using rotational electrical generators have been considered previously by a number of developers:

- An innovative approach using a rotatory generator for wave energy and tuning the natural frequency is discussed in [9], where a pendulum excited by the heave motion of the WEC turns a rotatory generator. The pendulum can be designed, so that it is in resonance at the frequency of the incident wave and so the power absorption is maximised.
- The dynamo presented in [16] converts the bi-directional movement of the buoy into a unidirectional rotation for the generator what might result in similar inertia effects as the PTO presented here. However, the design requires a complex gearbox and a rectifier to make the pulsed output of the WEC grid conforming. The effects of the increased inertia on the power absorption are not investigated.
- Concepts based on flywheels, like in [17] (and similarly in [24,25]) convert the linear bi-directional motion of the buoy into a bi-directional rotation, but the generator connected to a flywheel is run in uni-directional motion. A controllable clutch connects the generator with the buoy shaft whenever it might accelerate the generator shaft. In the meantime the generator is run by the energy stored in the flywheel. As the generator's angular velocity does not follow the buoy's velocity, it does not show the high inertia of the alternating generator and is only able to absorb energy while the buoy is moving downwards. The power output is very smooth and may need no or only little smoothing to be grid compatible, and so the peak-to-average power ratio is much lower than in conventional WEC designs.
- A bi-directional winch based design, similar to the concept presented here, but with a gearbox and the PTO placed in the buoy is used in the WEC described in [21]. The generator is a conventional electrical machine used in industrial servo applications. It only produces power while moving upwards and operates in motoring mode during downwards motion.

In this paper a numerical simulation and wave tank experiments were used to characterise the system. The numerical time-domain model uses linear potential flow theory to calculate the absorbed power of floating point absorber with ideal generator for different inertiae and damping coefficients.

The physical model is characterised with experiments in the Ocean Basin in the COAST Laboratory at the University of Plymouth are conducted to test the influence of the inertia in different sea states.

In the following section the scale PTO model will be presented, showing its characteristics in comparison to a linear generator PTO. Theoretical background on wave body interactions, used for the numerical simulation, is given in Section 3. In Section 4 the physical and in Section 5 the numerical test set-up are presented, the results and their discussion can be found in Section 6, before the conclusions are drawn in Section 7. Unless otherwise stated, all values in this paper refer to a full scale device, values obtained from the scale model are presented as full scale values using Froude scaling.

2. Design of the Physical Model PTO

The most important goal during the design of the physical scale PTO was a linear behaviour to ease the comparison of theoretical and practical results. High friction is often a problem in scale model tests and therefore it is necessary to aim for a low friction design. For the design of the PTO the issue is addressed by using a rotational generator, assuming that a low friction rotation bearing can be easier achieved than an equivalent translational bearing. Furthermore, having a rotational design, all deviations will reappear after each turn, what simplifies the identification, and the stroke length, which can influence the power absorption significantly [26], can easily be extended. For hassle free utilisation in wave tank tests, the PTO should be easy to install and operate and, regarding array tests, cost-efficient and easy to replicate. This is achieved by using mostly standard parts.

To get an accurate and cost-effective speed-proportional damping, different principles are examined:

- Viscous dampers create an accurate damping force by forcing a fluid through a small hole. The damping can be changed by varying the hole diameter.
- Eddy-current breaks provide a nearly ideal, contactless velocity proportional force by moving a conductive material through a magnetic field. The damping can be adjusted by varying the magnetic field.
- Small permanent electric generators, like automotive alternators or bicycle hub dynamos are cost effective and provide the absorbed power directly.

We choose the eddy current break, as it is, despite its simplicity, the most accurate principle and has been successfully used in scale models [27,28]. Viscous dampers were occasionally used to simulate PTO forces [29], but their damping depends on the temperature, as the viscosity of most fluids changes significantly with the temperature, so monitoring the temperature is necessary for accurate results. Using a real generator comes with the advantage, that the absorbed power can be measured directly, rather than be calculated from the velocity. On the other hand, the characteristics of bicycle dynamos or car alternators differs from the three phase synchronous generator used in many direct-driven full scale WECs; static and dynamic friction, cogging forces, hysteresis, saturation are individual parameters of a generator; for general research it is beneficial to use an ideal linear generator instead.

The final set-up developed consists of a bicycle wheel truing stand (Tacx T3175) screwed on a table; see the generalized sketch in Figure 1 and the a photo and sketch of the device in the wave tank test in Figure 6 later in this paper. It is holding a bicycle front hub with disc break mounting holes (Shimano XT HB-M756). The bicycle hub has a low friction ball bearing. Instead of a disc break, a 2 mm thick aluminium disc with 40 mm diameter is mounted. A vice (Clarke CSV4E 100 mm) is located on the table below the disc, the edge of the aluminium (AL1050) is positioned between its clamps. The movable clamp holds a set of magnets (5× Neodymium N42 $20 \times 20 \times 10$). Changing the gap between the clamps changes the magnetic flux through the disc and so the PTO damping d_{PTO}. An estimation of the magnetic flux in dependence of the air gap length z is given in Equation (1),

$$B = B_r/\pi \left[\arctan\left(\frac{LW}{2z\sqrt{4z^2 + L^2 + W^2}} \right) - \arctan\left(\frac{LW}{2(D+z)\sqrt{4(D+z)^2 + L^2 + W^2}} \right) \right] \quad (1)$$

with L, W and D being the length, width and thickness of the magnet and B_r its remanence field.

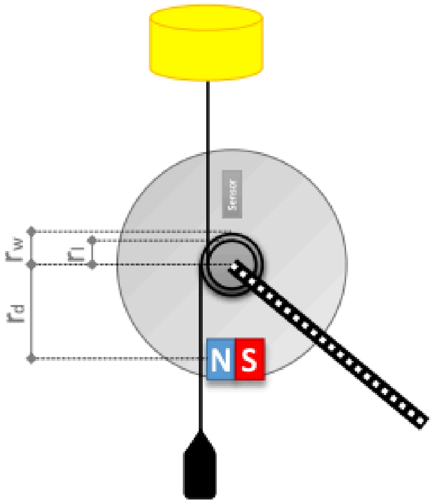

Figure 1. Simplified sketch of the PTO with relevant radii. Here r_d is the distance from the disc's centre to the magnets, r_w is the radius of the winch for the line leading to the weight, and r_l is the radius of the winch of the line leading to the buoys.

On the hub two ropes are installed, one is connected to the line going up to the buoy acting a positive moment on the hub, the other rope is connected to a weight acting as a counter moment on the hub. To capture the PTO position and speed, an Inertia Measurement Unit (IMU) based on the Intel Curie platform is mounted on the disc at distance r_S from the centre, recording acceleration in two directions and rotational speed. A similar position measurement system was used in [30]. Knowing acceleration (a_x, a_y) and rotational speed (ω), the angle α of the disc can be calculated:

$$\alpha = \arctan\left(\frac{a_x - r_S\omega^2}{a_y - \dot{\omega} r_S}\right) , \tag{2}$$

and so the power:

$$P = (\dot{\omega} r_s)^2 d_{PTO} \, . \tag{3}$$

A detailed overview over the processing done can be found in Figure 2.

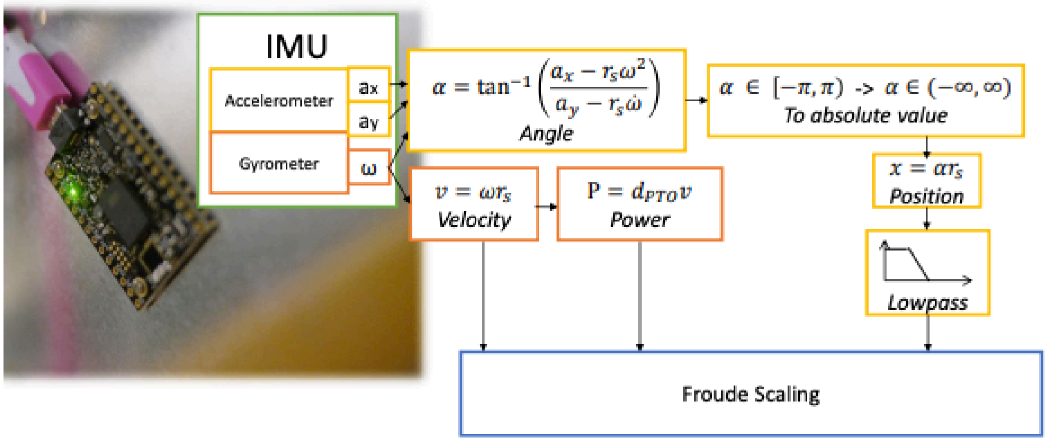

Figure 2. Processing of the measured data. Here v is the linearised velocity and x the linearised position.

2.1. Characteristics

A direct-driven linear generator, as used in many floating point absorbers wave energy converters is described by a mass-damper system. The force in the line F_l can be calculated as:

$$F_l = -\dot{x}_w d - m_w \ddot{x}_w - m_w g \,, \tag{4}$$

with x_w being the position of the weight, m_w the mass of the weight, d the overall damping and g the gravity acceleration.

The line force F_l of a rotational electric generator as described above can be expressed as:

$$F_l = (m_w r_w^2 / r_l + J / r_l)\ddot{\varphi} + (d_{PTO} r_d^2 / r_l)\dot{\varphi} + m_w g r_w / r_l \,, \tag{5}$$

with r_w being the radius the rope to the weight winds to the disc, r_l being the radius the line to the buoy winds on the disc, J is the moment of inertia of the rotor and g being acceleration. A sketch with all relevant radii can be found in Figure 1. Defining $x = r_l \varphi$ and $M = m_w (r_w / r_l)^2 + J / r_l^2$, we get:

$$F_l = M\ddot{x} + d_{PTO}(r_d / r_l)^2 \dot{x} + m_w g r_w / r_l \,, \tag{6}$$

where r_d is the distance between the centre of the disc and the magnets. Comparing Equation (4) with (6), the gearbox effect of the disc can be seen: The applied damping d_{PTO} is amplified by the ratio $(rd/r_l)^2$, thus for the 1:10 r_d/r_l ratio in the physical scale model the magnetic field can be 100 times weaker than for a linear generator. Unlike the linear generator the weight pulling downwards m_w and the inertia of the PTO M are not equal, latter includes also the disc inertia J/r_l^2. The inertia of a solid disc is:

$$J = 0.5 r_c^4 \pi \rho_c h_c \,, \tag{7}$$

with r_c being the radius of the disc, ρ_c being its density and h_c its thickness. By changing the ratio r_c^4/r_l, the disc can be designed to fit a specific inertia target.

2.2. Influence of Inertia on Absorbed Power

For simplification we assume the WEC to be a one body system with one degree of freedom (heave direction), assuming a stiff connection between buoy and the moving part of the PTO. In the presence of a flat water surface the system can be seen as an harmonic oscillator with the damped frequency:

$$\omega_d = \sqrt{k/M_t - (0.5d/M_t)^2} \,, \tag{8}$$

where k is the hydrostatic buoyancy stiffness of the buoy, M_t the total mass of inertia, including the mass and added mass of the buoy, the mass of the weights, the mass of the lines and the weight of the disc. The damping coefficient d is the sum of the electrical damping coefficient of the PTO d_{PTO} and the hydrodynamical damping coefficient of the buoy. The optimal d depends on the sea state [7]. As d has only a small influence compared to the natural frequency it is assumed to be fixed. Doing so the absorbed energy is proportional to the angular frequency respective velocity, and so:

$$\hat{E} \sim \hat{F} / (j\omega M_t + d - jk/\omega). \tag{9}$$

From Equation (9) follows that the most energy is absorbed when

$$M_t = k/\omega^2. \tag{10}$$

Controlling a WEC so that Equation (10) is always fulfilled, called complex conjugate control, requires an adjustable inertia or spring (an example for such and device can be found in [5]), or a reactive generator. In many cases it may be enough, if the WEC is designed so that we get close to the condition of Equation (10) for most sea states.

The hydrostatic buoyancy stiffness k depends on the shape of the buoy. For a cylindrical buoy with radius r, k is

$$k = r^2 \pi \rho g. \tag{11}$$

If we compare to a cylindrical buoy with a diameter of 5 m, which have been used by Uppsala University in the Lysekil project (UU-WEC) [31], k would be about 192.6 kN/m, according to Equation (10) the inertia should be around 48.15 t for the 3 s period and 102.5 t for the 12 s case. For most WECs with direct-driven linear generators the total moving mass is much less (about 10 tonnes for the mentioned UU-WEC), as a higher mass makes the system, especially the deployment, very expensive. Those devices can be controlled by changing the generator damping or by latching the translator (which can be seen as a extreme form of the former). Both, especially damping control, are not as efficient as complex-conjugate control.

With the generator presented in this paper, changing the mass is possible by changing r_m. Regarding the trend to simplify devices to cut costs and increase reliability, in wave climates where the region of high energy sea states is centred around one sea state, it might be sufficient, if the WEC is designed so that it fulfils Equation (10) only for this sea state.

Especially for direct-driven generators, changing the damped frequency of the system by changing the generator damping d_{PTO} is a cost effective way to adapt the WEC to different sea states [32], but not as effective as changing the natural frequency. However, to achieve the optimal power absorption, both the natural frequency and the damping have to match the sea state.

Buoy and generator are connected with a line, in case the line is loose, both bodies can move independently. In that case Equation (8) is not valid, as we have now two bodies with their own frequency. The linear approach is only valid if the line is stiff at all times.

2.3. Differences to Linear Generator

As a conclusion of this section, three differences between a rotational direct-driven generator compared to a linear one should be pointed out:

- The damping is increased by factor $(r_d/r_l)^2$ for the rotational direct-driven generator, less magnets/coils are needed for the same damping.
- If $r_c > r_l$, the inertia of the rotatory PTO can be much higher with the same weight. The eigenfrequency decreases with the inertia.
- The stroke length of the rotational PTO is not directly limited by the generator height.
- For a rotatory motor a good bearing (e.g., roller bearing) is much easier to design than for a translatory generator. On the other hand, the force acting on the rotatory bearing is much higher than on a linear generator bearing. Furthermore a winch based rotatory generator has friction due to the rope unwinding.

3. Theory of Wave Body Interactions

In this paper, linear potential theory is used to describe the wave-body interaction, assuming an irrotational, incompressible fluid and non-steep waves. This assumption is a reasonable approximation for the non-steep, operational waves considered here [33]. Using potential flow, a velocity potential ϕ can be defined fulfilling the Laplace equation. The free kinematic and dynamic free surface boundary condition are:

$$\frac{\partial^2 \phi}{\partial t^2} + g \frac{\partial \phi}{\partial z}\bigg|_{z=0} = 0\,, \tag{12}$$

$$\eta = -\frac{1}{g}\frac{\partial \phi}{\partial t}\bigg|_{z=0}\,, \tag{13}$$

where η is the surface elevation. The sea bed boundary condition is:

$$\left[\frac{\partial \phi}{\partial z}\right]_{z=-h} = 0 \,, \tag{14}$$

with h being the height of the water surface above the sea bed.

The interaction between a buoy and a wave can be described with three waves: The excitation wave induces a force on the body, the movement of the buoy causes a radiated wave and the presence of the buoy's shape is an obstacle for the incoming wave, resulting in a scattered wave.

The velocity potential is the sum of the undisturbed incident φ_0, the scattered φ_S and the radiated φ_R part. The latter can be calculated from the motion of the buoy:

$$\varphi_R = i\omega \sum_{j=1}^{6} x_{bj} \varphi_j \,, \tag{15}$$

where x_{bj} is the motion of the buoy in coordinate j and ω is the frequency of the wave. Integrating the velocity potential over the wetted surface S results in the excitation force acting on the buoy:

$$F_{e,j} = i\omega\rho \iint_S (\phi_0 + \phi_S) n_j dS \,, \tag{16}$$

with n_j being the normal vector in direction j [33,34].

4. Physical Experiments

4.1. Physical Model Set-up

The physical model presented in Section 2 is used, with a 40-mm wide and 2-mm thick aluminium discs (AL1050). Its weight is 0.660 kg, which is equivalent to a full scale linear translator with 47.5 t inertia. To consider also the inertia of the IMU and the bolts holding it, the rounded value 48 t is used. The weight of the PTO m_w refers to a full scale weight of 5 tonnes. Two discs can be mounted on the hub allowing the disc inertia to be 48 or 96 t. A overview over all relevant parameters can be found in Table 1.

The damping was examined with a "free fall" test, where only the force of the weight and no buoy as counter force is acting on the system. The damping coefficient can then be calculated from the steady state velocity and the weight.

Figure 3 shows the damping in this steady state condition. It is clearly visible that the damping is not constant over a period, the deviation from the mean velocity correlates well with the disc position. This may be explained that despite high-precision manufacturing methods, the disc is not completely plane, which results in a slight changing of the distance between disc and magnets. However, the divergence is within $\pm 5\%$ and thus relatively small.

Table 1. Parameters of the scale model and their Froude-scaled full scale equivalence.

Parameter	Model Scale Value	Full Scale Value
disc radius (r_s)	0.2 m	2 m
attachment radius (r_w and r_l)	10 mm	0.1 m
Mass weight (m_w)	5 kg	5000 kg
Mass buoy (m_b)	5 kg	5000 kg
Inertia disc (J)	48 kg	48, 000 kg
PTO damping (d_{PTO})	312 Nm/s	100 kNm/s
Sea state duration	6.5 min	20 min

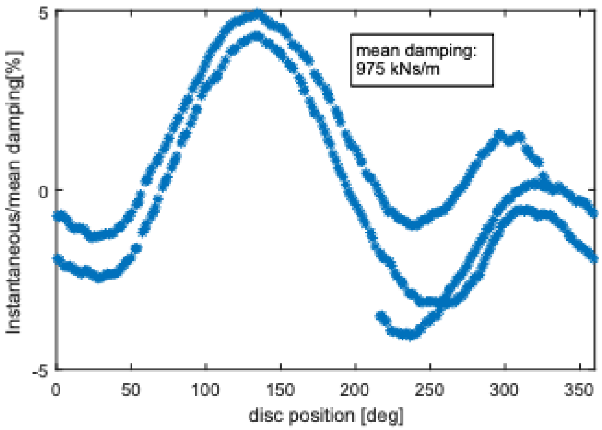

Figure 3. Instantaneous damping related to the mean damping, plotted over the disc position. The calculation is based on the disc rotational velocity after reaching constant velocity while a force of 12.5 N (model scale) is acting on the line. Mean damping is full scale equivalent. Graph shows one test with 2.25 revolutions.

The test was redone without damping and different weights (0.115, 0.5, 1 and 2 kg, model scale) to verify the inertia of the disc and measure the friction in the system, see Figure 4. The measured acceleration in steady state was compared to the theoretically value. From the graph the friction was estimated to about 0.6 N (model-scale). The heavy oscillation for the 0.5 kg and 0.115 kg cases can be explained with the weight of the IMU, that makes the disc slightly unbalanced. However this effect is very small.

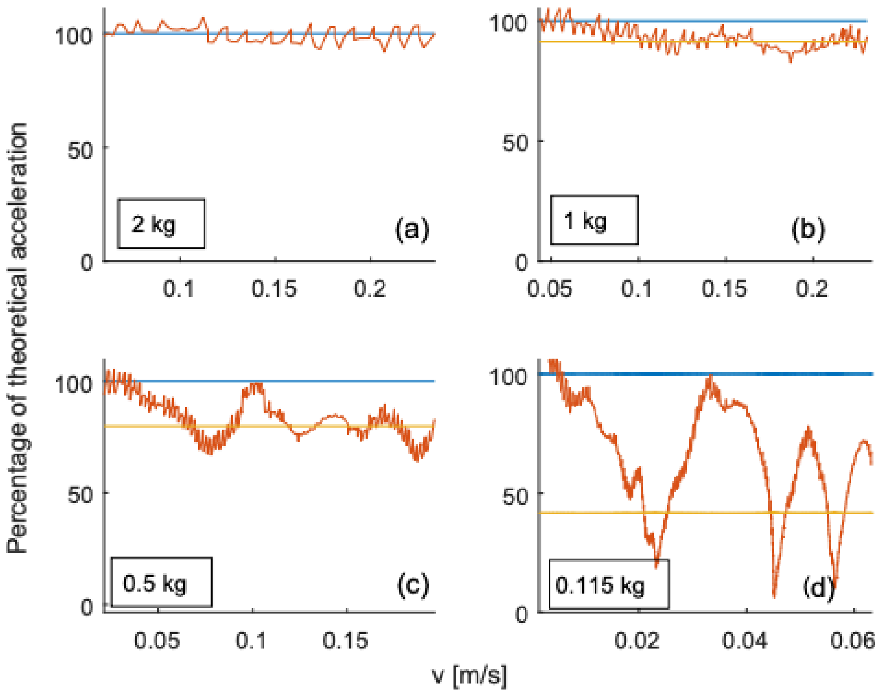

Figure 4. Acceleration measured and low pass filtered (orange) in relation to the theoretical acceleration (100%, blue line). The yellow line represents the value the measured acceleration tends to. Values are directly measured from the scale model.

The relation between clamp gap and damping from Equation (1) was verified once again with a "falling" weight, by changing the air gap of the vice (measured in lever turns). The results of this test are compared to Equation (1) in Figure 5. If v is constant, the damping is directly proportional to the magnetic flux B. In the figure the proportionality constant is chosen so that both graphs agree at clamp position '0'. The buoy is connected to the PTO with a line guided by a pulley system. The pulleys have a ball bearing and rotate nearly frictionless. From the PTO the line is guided over the gantry on which the PTO is placed, from there down to the floor of the wave basin and then to the buoy. The stiffness of the line between weight and buoy is estimated to 133.33 kN/m. The low stiffness is mostly caused by the knots and the aluminium profile the pulleys are mounted, rather by the line itself.

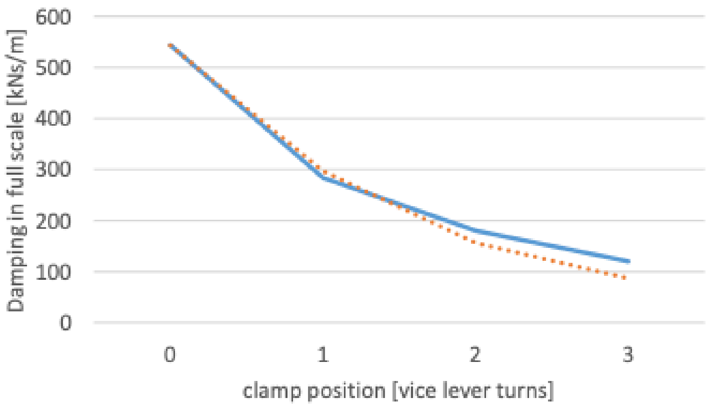

Figure 5. Measured damping of the PTO (blue) in relation to the gap width, measured in turns of the vice knob. The dotted line shows the trend of the magnetic flux according to Equation (1). The curve is scaled so that it matches with the measurement for the zero clamp position.

4.2. *Wave Tank Tests*

The wave tank tests were performed in the Ocean Basin in the COAST Laboratory at the University of Plymouth, a photo and sketch of the set-up can be found in Figure 6. The tests were conducted at a full-scale equivalent depth of 25 m.

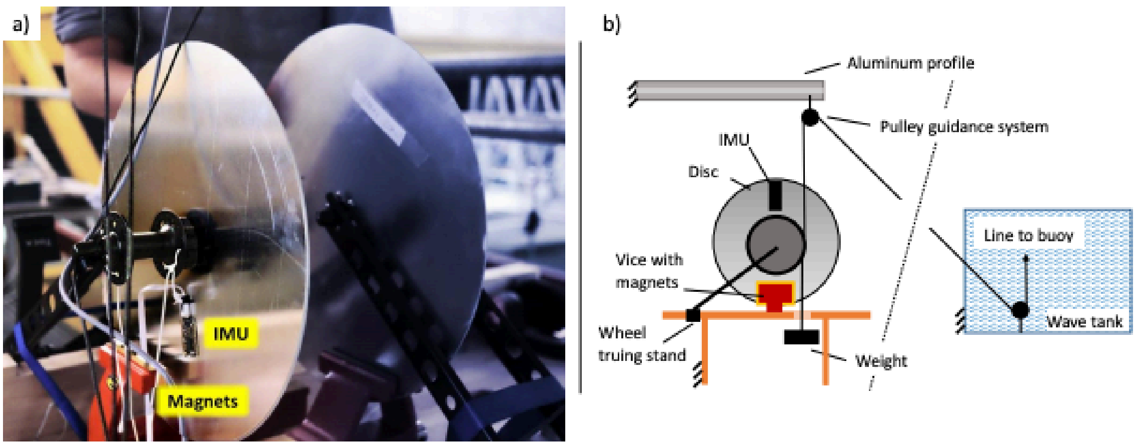

Figure 6. (**a**) Photo of the physical scale model; (**b**) Schematic of the set-up during the scale model testing in the wave tank.

The full-scale equivalent buoy measures 5 m in diameter and weights 5000 kg and can be in good agreement described as ellipsoidal shaped.

The eight 20 min long Brettschneider sea states performed in the tank tests form a 4×2 power matrix which consists of four wave periods ranging from $T_e = 3.5$ s to 9.5 s and two significant wave heights, $H_s = 0.75$ m and 1.75 m. Two matrices were performed for a PTO equipped with one disc and two discs respectively, leading to a total inertia of 53 t and 101 t.

5. Numerical Simulations

5.1. Numerical Model

The WEC was modelled as a two body system connected with the line force F_l. The total force on the buoy is:

$$F_B = F_e + F_r + F_h + F_{Gb} + F_l + m_b\ddot{x}(t): \tag{17}$$

The excitation force F_e is calculated as a convolution between the impulse response function $h_e(t)$ of the buoy and the incident wave elevation $\eta(t)$. The damping force F_r due to the radiated wave is obtained in a similar manner by convolution $h(t)$ with the velocity $\dot{x}(t)$. The hydrostatic force F_h of the buoy is the product of the buoyancy b_b at equilibrium and $x(t)$ the position of the buoy below the surface (draft). Furthermore the gravity force F_{Gb} is the product of the mass of the buoy m_b and the gravity acceleration.

The PTO is modelled as a linear translator with additional inertia, implying that $r_w = r_d = r_l$. The generator provides an ideal damping, so Equation (6) becomes:

$$F_{PTO}(t) = d_{PTO}\dot{y}(t) + M\ddot{y}(t) + F_l(t) + m_w g\,, \tag{18}$$

with y being the position of the weight. With its non-linear behaviour the line force is simulated with the following equation:

$$F_l(t) = \begin{cases} c_l(x(t) - y(t)) + d_l(\dot{x}(t) - \dot{y}(t)) & , x > y \\ 0 & , \text{else} \end{cases}\,, \tag{19}$$

with c_l and d_l being the line stiffness and damping. They were chosen to mimic an ideal line and at the same time avoid numerical oscillation. To obtain the hydrodynamic parameters the commercial software WAMIT [34] (based on the boundary elements method) was used. The hydrodynamic parameters were calculated for wave periods up to 16 s, with a resolution of 0.1 s and then inverse-Fourier transformed into time-domain. As solver a delayed-differential-equation solver (DDE) with 0.1 ms fixed step size is used. A flow chart of the solver can be found in Figure 7.

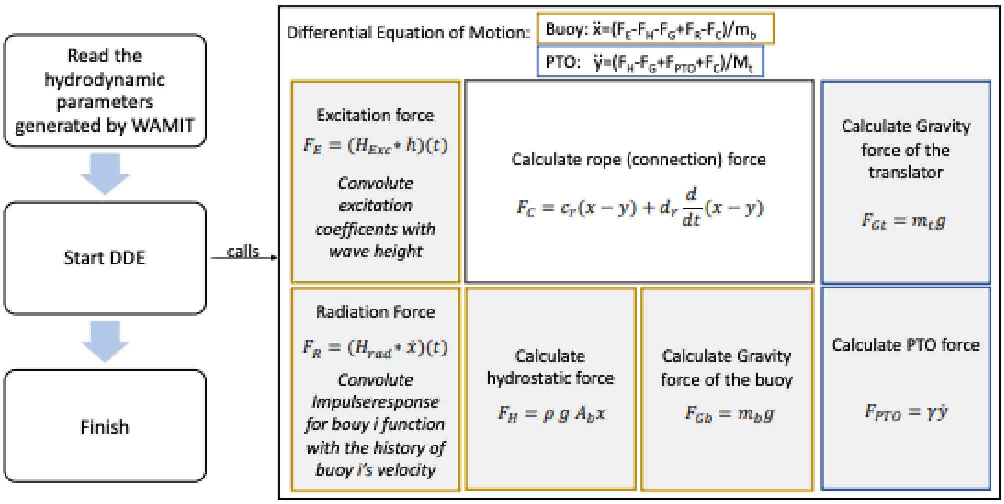

Figure 7. Diagram of the numerical simulation.

5.2. Parameters

Similar to the wave tank tests, a buoy measuring 5 m in diameter, but with a cylindrical shape, and a weight of 5000 kg is used. For different rotational inertiae mass (J) and generator damping coefficients (d_{PTO}), the performance of the PTO for a power matrix with wave energy periods ranging from $T_e = 3.5$ s to 9.5 s and significant wave height between $H_s = 0.75$ s and $H_s = 3.75$ s were tested. For $J = 0$, the rotational PTO and the linear PTO are identical, and therefore this configuration is used as reference. As in the wave tank test, each sea state had a duration of 20 min.

6. Results and Discussion

The simulated power matrix can be found in Figure 8. For each inertia, a matrix with a low generator damping of 75 kNs/m and a moderate damping of 125 kNs/m is simulated. The power output of the high-inertia PTOs were set in relation to a PTO with $M = m_w$, which can be seen as a linear generator. Figure 9 plots the velocity of the PTO with $M = 45$ t and $M = 120$ t.

M=120 t, m=5 t, d=75 kNs/m

Hs [m] \ T [s]	3.5	5.5	7.5	9.5
0.75	146%	239%	211%	162%
1.75	87%	147%	167%	159%
2.75	61%	111%	137%	143%
3.75		95%	124%	135%

M=45 t, m=5 t, d=75 kNs/m

Hs [m] \ T [s]	3.5	5.5	7.5	9.5
0.75	186%	139%	110%	95%
1.75	167%	139%	111%	95%
2.75	142%	138%	118%	101%
3.75		136%	124%	109%

M=120 t, m=5 t, d=125 kNs/m

Hs [m] \ T [s]	3.5	5.5	7.5	9.5
0.75	124%	193%	197%	177%
1.75	86%	133%	157%	163%
2.75	65%	104%	128%	141%
3.75		90%	113%	109%

M=45 t, m=5 t, d=125 kNs/m

Hs [m] \ T [s]	3.5	5.5	7.5	9.5
0.75	142%	139%	130%	123%
1.75	130%	130%	126%	122%
2.75	114%	120%	120%	119%
3.75		114%	116%	109%

Color key: 0%, 20%, 40%, 60%, 80%, 100%, 120%, 140%, 160%, 180%, 200%

Reference: M=m=5 t mass and d=125kNs/m

Figure 8. Matrix of power output for two direct-driven PTOs with different inertia, but the same weight, calculated by the numerical simulation and compared to a generator with $M = m_w$, so a linear generator.

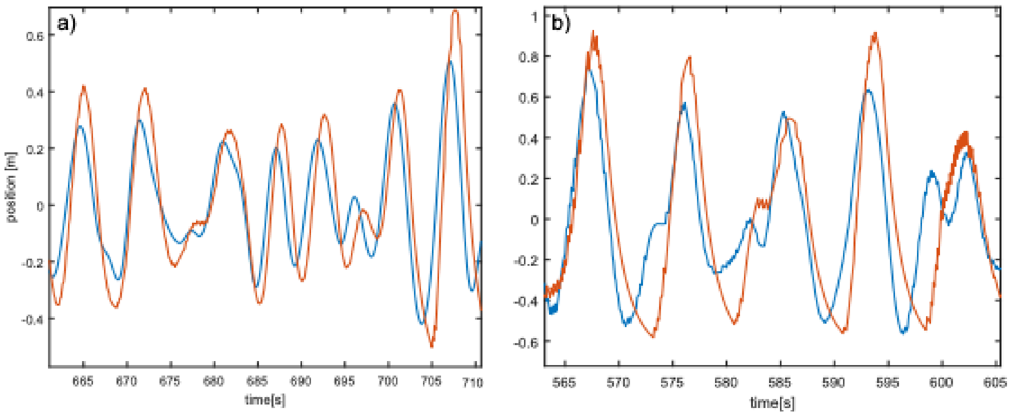

Figure 9. Position of the translator in the numerical simulation for Ts = 7.5 s and Hs = 0.75 m (**a**), and Hs = 1.75 m (**b**). The thin blue curve is from the PTO with low inertia (45 t), the thick orange curve with high inertia (120 t). The damping was set to 75 kNs/m. All values scaled to full scale equivalents.

Figure 10 shows the power matrices performed in the wave tank: The first matrix shows the absorbed power of the low inertia, the second matrix of the high inertia PTO; the third matrix shows the realtion between the low and high inertia PTO. The generator damping was fixed for all sea states to 100 kNs/m. The motion for both PTO in two sea states is plotted in Figure 11. The recorded PTO data from the wave tank tests can be found in the Supplementary Materials.

To compare the numerical simulation and physical wave tank test in Figure 12, the numerical simulation was executed for the $M = 53$ kg case with a damping of $d = 100$ kNs/m. For the line stiffness, firstly the nearly ideal parameter as used in the simulation of the power matrix are used and then the estimated parameter of the real line.

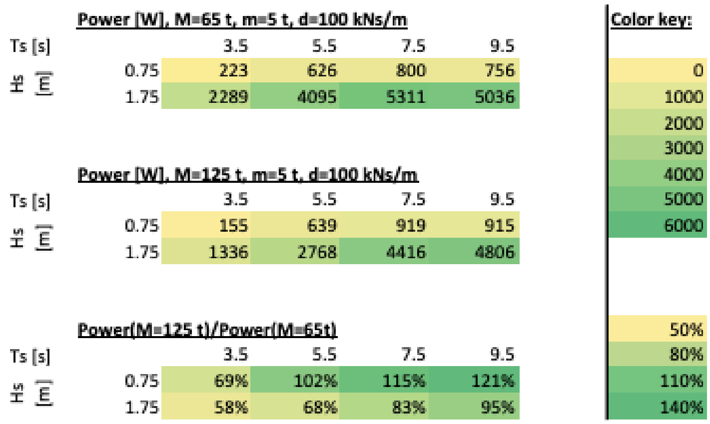

Power [W], M=65 t, m=5 t, d=100 kNs/m

Hs [m] \ Ts [s]	3.5	5.5	7.5	9.5
0.75	223	626	800	756
1.75	2289	4095	5311	5036

Power [W], M=125 t, m=5 t, d=100 kNs/m

Hs [m] \ Ts [s]	3.5	5.5	7.5	9.5
0.75	155	639	919	915
1.75	1336	2768	4416	4806

Power(M=125 t)/Power(M=65t)

Hs [m] \ Ts [s]	3.5	5.5	7.5	9.5
0.75	69%	102%	115%	121%
1.75	58%	68%	83%	95%

Color key:

0
1000
2000
3000
4000
5000
6000
50%
80%
110%
140%

Figure 10. Matrix of generated power ($d_{PTO}v^2$) for two direct-driven PTOs with different inertia, but same weight, results of the wave tank test.

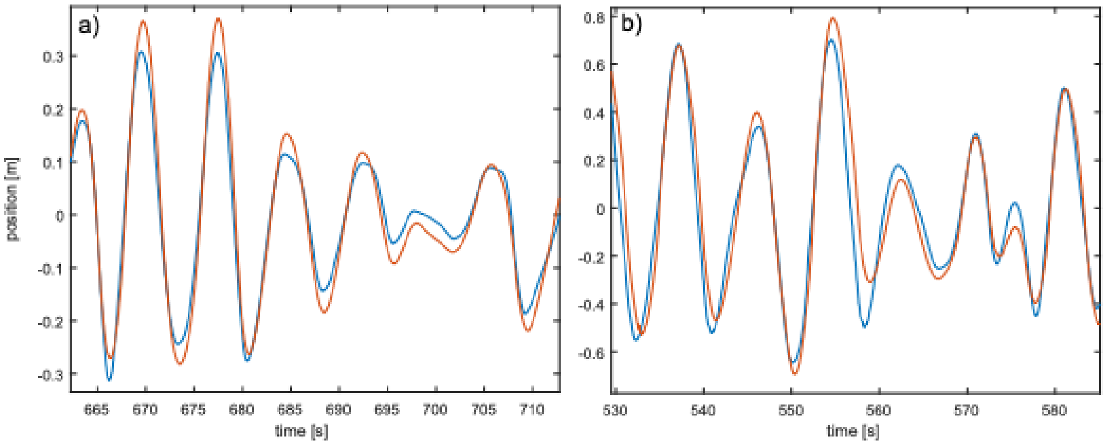

Figure 11. Position of the translator in the wave tank tests for Ts = 7.5 s and Hs = 0.75 m (**a**), and Hs = 1.75 m (**b**). The thin blue curve is from the PTO with low inertia (53 t), the thick orange curve with high inertia (101 t). The damping was set to 100 kNs/m. All values scaled to full scale equivalents.

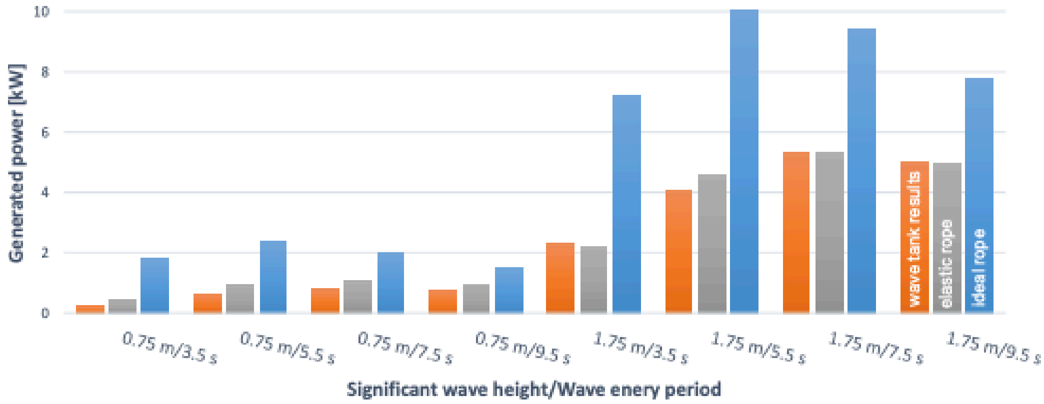

Figure 12. Comparison of the generated power in the physical wave tank tests (**orange**), the numerical simulation using a medium stiff line with $c_l = 133$ kN/m and $d_l = 10$ kN/m (**grey**) and the numerical simulation using an ideal stiff line with $c_l = 4$ GN/m and $d_l = 1$ kN/m (**blue**). The inertia was set to $M = 53$ kg.

6.1. Numerical Simulations

For nearly all sea states (80–100%) the higher inertia is beneficial (see Figure 8). Only for a few sea states with short periods and high waves, the linear reference PTO absorbs significantly more power. The predicted power increase when shifting the natural frequency towards the wave frequency, good to see for low sea states, with the power absorption increasing up to +139%. Outside the peak frequency the additional power is much less.

In the linear equation used in section 3, the wave height had no influence on the absorbed power. However, in the simulation the higher inertia PTOs advantage drops significantly when increasing the wave height. Here the non-linear effect of the line may play a role, limiting the downward speed of the PTO to $v = m_w g / d_{PTO}$. Figure 9 correspondents with this observation: For $H_s = 0.75$ m both PTOs show a smooth curve; the high inertia PTO shows a nearly ideal sinusoidal shape, indicating a good frequency match. The high inertia PTO reaches a faster speed in the downwards movement than the low inertia PTO. For $H_s = 1.75$ m, only the low inertia has a continuous movement, while the high inertia PTO has a sharp knick at the bottom position, caused by the frequency mismatch when the translator weight is still in the downwards movement, but the buoy, following the wave, is already moving upwards. The maximal downwards speed in this sea state is the same for both PTOs, it is limited by the generator damping and weight. A higher generator weight could reduce the negative effects on the absorbed power in higher sea states.

Focusing on the damping, the difference in the resonators bandwidth (characterized by the Q-factor) can be seen: The low damping leads to a higher Q-factor, and so to a higher peak power. While the peak power for the higher damping is smaller, the decrease in power off the resonance centre is smaller.

6.2. Numerical Simulations and Physical Tests

The results of the physical wave tank tests shown in Figure 8 are slightly different: For the low amplitude waves and long wave periods, the high inertia PTO has an advantage over the low inertia PTO. For short periods the low inertia PTO generates more power. However, for $H_s = 1.75$ m waves, the low inertia is beneficial for all tested periods. The difference is getting smaller as higher the wave period is, and for wave energy periods higher than 9.5 s the high inertia PTO may absorb more power. But comparing to the simulation power matrix in Figure 8, the higher inertia should perform better from $T_e = 5.5$ s upwards.

This may be explained with the ideal stiff line in the simulation. Figure 12 shows the influence of the line stiffness: While using the ideal line, the numerical simulation absorbs approximately 2 times, in low sea states up to 10 times of the power of the physical tests. While reducing the stiffness of the line, the power rapidly plunges very close to the wave tank test result. Also the peak period changes towards the higher wave energy periods. The line reduced stiffness used was with 133 kN/m very low. We assume that the low stiffness results primary from the knots connecting the different part together and that the line stiffness itself plays a secondary role. The low line stiffness may therefore only be valid for small displacements.

The differences between numerical simulations with the non-ideal line and physical wave tank tests are very small. For the low waves, the predicted power from the simulation is slightly higher, what might be a result of the friction in the system. For the 1.75 m waves, the agreement is very good, but the peak frequency for the simulation seems to be between 5.5 s and 7.5 s, while for the physical tests it seems to be between 7.5 s and 9.5 s. Differences may be caused by reflections in the wave tank, limits of the linear potential wave theory, the heave only simplification or inaccuracies of the PTO system. The cylindrical shape of the buoy in the simulation and the ellipsoidal shape in the wave tank test have nearly no influence on the results: In the numerical model the buoyancy stiffness is linearised at the steady state draft, where it is the same for both shapes.

Similar tests comparing a physical with a numerical point absorber WEC model were performed by [11]. The physical scale model uses a motor to mimic the PTO and is designed without using connecting lines. The measured data from the physical tests agrees very well with the model data, and no line elasticity has to be considered. However, while the motor allows a wide range of control strategies to be simulated, it results in a clearly visible noise in the passive damping mode especially for high and short period waves.

The time series of the physical experiments matches in general the observation from the numerical simulation: The high inertia PTO matches the wave frequency very well in the low amplitude waves, what can be seen in the higher peaks in Figure 11, but for the low inertia, the period is too high to catch all peaks.

In direct comparison with the numerical results of Figure 9, the experimental curves look smoother. The sharp knick as seen for the high inertia PTO in the high wave in the simulation does not exist in the experimental results. Here the line elasticity may have smoothed the results.

6.3. Overall

Despite the differences in simulation and physical test, mostly caused by the line stiffness, the overall characteristics are the same: The peak frequency for a PTO increases with its inertia, and the benefit from the frequency matching decreases with the wave height. With the damping the resonance bandwidth can be adjusted and so the ratio between absorbed peak power and power off the resonance centre. This is especially important as an uncontrolled PTO can not adjust its frequency.

The experiments showed that tuning the undamped eigenfrequency of the PTO towards the energy period of the sea state is not always beneficial. While in sea states with low wave height sea states, the natural frequency from the linear estimation agrees well with the real behaviour of the PTO, in higher and steeper waves it leads to a slack line, thus reducing the benefit of the frequency tuning. On the other side, compared to a traditional low inertia PTO, the absorbed power is for nearly all sea states in the power matrix in Figure 8 much higher. Control strategies, like latching or complex conjugate control, rely on a PTO with high frequency and may provide better results for a wider range of sea states, due to their ability to adapt to the sea state. But controllable PTO designs require additional electrical or mechanical mechanism, and suitable controller for real sea states are still a topic of ongoing research. For many wave climates, a well tuned, non adjustable frequency may be good enough. When designing the WEC converter to match a specific sea states, the energy adsorption for this sea state may increase significantly, however, on the other side, it will get out of tune for sea states far away. This can be used to automatically detune the device in storm conditions.

The results of the added inertia from Figures 8 and 10 agree well with the effect of an additional submerged added mass sphere in [8], where the absorbed power with the additional inertia sphere is increased up to the factor of 3 compared to the linear generator without the sphere. Even though the generator design was similar to the one used in this paper, the specific parametrization and sea states were different, so that the values can not be compared directly. In [22], while analysing the influence of inertia on a cylindrical bottom-hinged WEC, the absorbed power of the increased inertia WEC correlates with the wave period. However, it also increases if the wave amplitude gets higher, which opposes the finding in this paper and is a good example of the fact that the characteristics between different WEC types alter.

7. Conclusions

In this paper a new design of a physical model PTO with constant damping was presented, showing a simple and accurate way to get low friction PTO with a nearly ideal velocity dependent force.

The alternating rotatory design combines the simplicity of a direct-driven generator by having no gearbox, beside a disc, with the advantages of a rotational system such as a decoupling of stroke and generator length.

The additional inertia allows to design the device for specific sea states and the PTO damping can be used to adjust the degree of specialisation. This can be used to build a simple control-free WEC, tuned for the most significant sea state in a certain wave climate. Away from this sea state, for example in harsh, stormy conditions, the WEC will automatically detune.

In numerical simulations with an ideal connection line between buoy and PTO, the additional inertia provided up to 239% of the power of a similar generator where the inertia is equivalent to the weights (direct-driven linear generator). For the parametrisation with the smallest Q-factor 80% of the tested sea states still had an increase in power absorption compared to a linear generator. However, at lower wave energy periods and higher waves heights the advantage in power absorption of the high inertia PTO compared to the linear generator gets smaller.

The findings of the numerical simulation are confirmed in wave tank tests. Here, the stiffness of the line showed a big influence on the system. A low line stiffness decreases the absorbed power and increased the peak wave period.

Due to the simple design and the the good performance without control, alternating rotatory generators might also be an interesting option for full-scale devices operating in wave climates with small energy spectrum bandwidth.

Further improvements of the physical model could include a replacement of the permanent magnets with electro magnets as used in [27] which allow a quick and reliable change of the damping as well as adjustable damping control strategies.

Supplementary Materials: The position and velocity data of the physical scale tests are available online at http://www.mdpi.com/1996-1073/11/9/2332/s1.

Author Contributions: The general conceptualization and methodology were done by S.T. The conceptualization and methodology for the wave tank test were mostly done by S.T. and M.G. (Marianna Giassi) with help from M.G. (Malin Göteman), J.E., M.H. and E.R. Project administration, including supervision, was done by M.G. (Malin Göteman), J.E., M.H., E.R. and J.I., M.G. (Malin Göteman), J.E. and J.I. were furthermore responsible for the funding acquisition.

Funding: The authors want to thank the Swedish Energy Agency (project number 40421-1), the Swedish Research Council (VR, grant number 2015-04657) for funding this research and the Åforsk Foundation. This work was supported by Stand Up for Energy.

Acknowledgments: This paper would not exist in this form without the help of Tom Tosdevin who helped a lot preparing the physical PTO and adjusting the damping. With their fast and uncomplicated help the team of Plymouth University's coast lab, especially Kieran Monk, Alastair Reynolds, Hannah Poulson, Gregory Nash and Andy Oxenham played an important part in securing that the PTO was finished in time.

Conflicts of Interest: The authors declare no conflict of interest.

Abbreviations

The following abbreviations are used in this manuscript:

WEC	Wave energy converter
PTO	Power take-off
IMU	Inertia measurement unit
WAMIT	WaveAnalysisMIT; Wave interaction analysing tool
COAST laboratory	Coastal, ocean and sediment transport laboratory; Facility at the University of Plymouth containing the wave tank
Q-factor	quality factor
DDE	Delayed differential equation
g	gravity acceleration

References

1. Clément, A.; McCullen, P.; Falcão, A.; Fiorentino, A.; Gardner, F.; Hammarlund, K.; Lemonis, G.; Lewis, T.; Nielsen, K.; Petroncini, S.; et al. Wave energy in Europe: Current status and perspectives. *Renew. Sustain. Energy Rev.* **2002**, *6*, 405–431. [CrossRef]

2. Allan, G.; Gilmartin, M.; McGregor, P.; Swales, K. Levelised costs of wave and tidal energy in the UK: Cost competitiveness and the importance of "banded" renewables obligation certificates. *Energy Policy* **2011**, *39*, 23–39. [CrossRef]
3. Ocean Energy: Cost of Energy and Cost Reduction Opportunities. Available online: https://energiatalgud.ee/img_auth.php/1/10/SI_OCEAN._Ocean_Energy_-_Cost_of_Energy_and_Cost_Reduction._2013.pdf (accessed on 13 August 2018).
4. Lejerskog, E.; Strömstedt, E.; Savin, A.; Boström, C.; Leijon, M. Study of the operation characteristics of a point absorbing direct driven permanent magnet linear generator deployed in the Baltic Sea. *IET Renew. Power Gener.* **2016**, *10*, 1204–1210. [CrossRef]
5. Wang, W.; Wu, M.; Palm, J.; Eskilsson, C. Estimation of numerical uncertainty in computational fluid dynamics simulations of a passively controlled wave energy converter. *Proc. Inst. Mech. Eng. Part M J. Eng. Marit. Environ.* **2018**, *232*, 71–84. [CrossRef]
6. Valério, D.; Beirão, P.; da Costa, J.S. Optimisation of wave energy extraction with the Archimedes Wave Swing. *Ocean Eng.* **2007**, *34*, 2330–2344. [CrossRef]
7. Todalshaug, J.; Falnes, J.; Moan, T. A comparison of selected strategies for adaptive control of wave energy converters. *J. Offshore Mech. Arct. Eng.* **2011**, *133*, 031101.
8. Engström, J.; Kurupath, V.; Isberg, J.; Leijon, M. A resonant two body system for a point absorbing wave energy converter with direct-driven linear generator. *J. Appl. Phys.* **2011**, *110*, 124904, [CrossRef]
9. Yurchenko, D.; Alevras, P. Dynamics of the N-pendulum and its application to a wave energy converter concept. *Int. J. Dyn. Control* **2013**, *1*, 290–299. [CrossRef]
10. Göteman, M.; Engström, J.; Eriksson, M.; Leijon, M.; Hann, M.; Ransley, E.; Greaves, D. Wave Loads on a Point-Absorbing Wave Energy Device in Extreme Waves. *J. Ocean Wind Energy* **2015**, *2*, 176–181. [CrossRef]
11. Beatty, S.; Ferri, F.; Bocking, B.; Kofoed, J.; Buckham, B. Power Take-Off Simulation for Scale Model Testing of Wave Energy Converters. *Energies* **2017**, *10*, 973. [CrossRef]
12. Thomas, S.; Giassi, M.; Göteman, M.; Eriksson, M.; Isberg, J.; Engström, J. Optimal Constant Damping Control of a Point Absorber with Linear Generator In Different Sea States: Comparision of Simulation and Scale Test. In Proceedings of the 12th European Wave and Tidal Energy Conference, Cork, Ireland, 27 August 2017.
13. Ewart, L.B.; Thies, P.R.; Stratford, T.; Barltrop, N. Optimising structural loading and power production for floating wave energy converter. In Proceedings of the 12th European Wave and Tidal Energy Conference, Cork, Ireland, 27 August 2017.
14. Bosma, B.; Lewis, T.; Brekken, T.; von Jouanne, A. Wave Tank Testing and Model Validation of an Autonomous Wave Energy Converter. *Energies* **2015**, *8*, 8857–8872. [CrossRef]
15. Têtu, A.; Power Take-Off Systems for WECs. In *Handbook of Ocean Wave Energy*; Pecher, A., Kofoed, J.P., Eds.; Springer International Publishing: Cham, Switzerland, 2017; pp. 203–220.
16. Al-Habaibeh, A.; Su, D.; McCague, J.; Knight, A. An innovative approach for energy generation from waves. *Energy Convers. Manag.* **2010**, *51*, 1664–1668. [CrossRef]
17. Lok, K.; Stallard, T.; Stansby, P.; Jenkins, N. Optimisation of a clutch-rectified power take off system for a heaving wave energy device in irregular waves with experimental comparison. *Int. J. Mar. Energy* **2014**, *8*, 1–16. [CrossRef]
18. Polinder, H.; van der Pijl, F.F.A.; de Vilder, G.J.; Tavner, P.J. Comparison of direct-drive and geared generator concepts for wind turbines. *IEEE Trans. Energy Convers.* **2006**, *21*, 725–733. [CrossRef]
19. Cheng, M.; Zhu, Y. The state of the art of wind energy conversion systems and technologies: A review. *Energy Convers. Manag.* **2014**, *88*, 332–347. [CrossRef]
20. Rhinefrank, K.; Schacher, A.; Prudell, J.; Hammagren, E.; von Jouanne, A.; Brekken, T. Scaled development of a novel Wave Energy Converter through wave tank to utility-scale laboratory testing. In Proceedings of the 2015 IEEE Power Energy Society General Meeting, Denver, CO, USA, 26–30 July 2015; pp. 1–5.
21. Sjolte, J.; Tjensvoll, G.; Molinas, M. Power Collection from Wave Energy Farms. *Appl. Sci.* **2013**, *3*, 420–436. [CrossRef]
22. Flocard, F.; Finnigan, T. Increasing power capture of a wave energy device by inertia adjustment. *Appl. Ocean Res.* **2012**, *34*, 126–134. [CrossRef]
23. Sheng, W.; Lewis, T. Energy Conversion: A Comparison of Fix- and Self-Referenced Wave Energy Converters. *Energies* **2016**, *9*, 1056. [CrossRef]

24. Sidenmark, M.; Josefsson, A.; Berghuvud, A.; Broman, G. The Ocean Harvester: Modelling, Simulation & Experimental Validation. In Proceedings of the 8th European Wave and Tidal Energy Conference, Uppsala, Sweden, 7–10 September 2009.
25. Larsson, K. Investigation of a Wave Energy Converter with a Flywheel and a Corresponding Generator Design. Master's Thesis, Chalmers University of Technology, Goteborg, Sweden, June 2012.
26. Castellucci, V.; Eriksson, M.; Waters, R. Impact of Tidal Level Variations on Wave Energy Absorption at Wave Hub. *Energies* **2016**, *9*, 843. [CrossRef]
27. Lopes, M.; Henriques, J.; Lopes, M.; Gato, L.; Dente, A. Design of a non-linear power take-off simulator for model testing of rotating wave energy devices. In Proceedings of the 8th European Wave and Tidal Energy Conference, Uppsala, Sweden, 7–10 September 2009.
28. Payne, G.; Taylor, J.; Parkin, P.; Salter, S. Numerical modelling of the sloped IPS buoy wave energy converter. In Proceedings of the International Offshore and Polar Engineering Conference, Sapporo, Japan, 10–15 June 2006.
29. Yu, Y.H.; Lawson, M.; Li, Y.; Previsic, M.; Epler, J.; Lou, J. *Experimental Wave Tank Test for Reference Model 3 Floating- Point Absorber Wave Energy Converter Project*; Technical Report; National Renewable Energy Laboratory: Golden, CO, USA, 2015.
30. Mercadé Ruiz, P.; Ferri, F.; Kofoed, J.P. Experimental Validation of a Wave Energy Converter Array Hydrodynamics Tool. *Sustainability* **2017**, *9*, 115. [CrossRef]
31. Lejerskog, E.; Gravråkmo, H.; Savin, A.; Strömstedt, E.; Tyrberg, S.; Haikonen, K.; Krishna, R.; Boström, C.; Rahm, M.; Ekström, R.; et al. Lysekil Research Site, Sweden: A status update. In Proceedings of the 9th European Wave and Tidal Energy Conference, Southampton, UK, 5–9 September 2011.
32. Ekström, R.; Ekergård, B.; Leijon, M. Electrical damping of linear generators for wave energy converters—A review. *Renew. Sustain. Energy Rev.* **2015**, *42*, 116–128. [CrossRef]
33. Falnes, J. *Ocean Waves and Oscillating Systems: Linear Interactions Including Wave-Energy Extraction*; Cambridge University Press: Cambridge, UK, 2002.
34. WAMIT User Manual Version 7.0. Available online: http://www.engr.mun.ca/~bveitch/courses/8000/software/wamit/wamit.pdf (accessed on 13 August 2018).

Attachments 4 – 6

Additional reports from Uppsala University:

Cooling Strategies for Wave Power Conversion Systems

Baudoin, Antoine
Uppsala universitet, Teknisk-naturvetenskapliga vetenskapsområdet, Tekniska sektionen, Institutionen för teknikvetenskaper, Elektricitetslära.

http://uu.diva-portal.org/smash/get/diva2:1049240/FULLTEXT01.pdf

The comprehensive thermal study of the substation indicates that the rated power in the present configuration is around 170 kW

Layout design of wave energy parks by a genetic algorithm

https://www.sciencedirect.com/science/article/pii/S0029801818301045?via%3Dihub

MariannaGiassiMalinGöteman
Department of Engineering Sciences, Uppsala University, Uppsala, Sweden

---

Arrays of Point-Absorbing Wave Energy Converters in Short-Crested Irregular Waves

Malin Göteman [1,*],**Cameron McNatt** [2],**Marianna Giassi** [1],**Jens Engström** [1] and**Jan Isberg** [1]
1
Department of Engineering Sciences, Uppsala University, 75105 Uppsala, Sweden

https://www.mdpi.com/1996-1073/11/4/964

Attachment 7

Confidential and groundbreaking test results from Uppsala University which shows a production price of just 5 Eurocent per. kWh after measurements carried out in Scotland 2011/2012 with wave signatures equivalent to Agios Georgios Island.

In the production price, the acquisition cost and depreciation of the plant are calculated.

We got these calculations directly from Professor Mats Leijon at The Ångstrøm Laboratory at Uppsala University in 2014.

Engl 260 MW-Seabased/4800h

Produktionskostnad, real kalkyl

			INDATA:	
Installerad effekt vid inmatningspunkt			260 000 kW	
Investering			564 MEuro	2169
Avskrivningstid			24 år	Euro/kW
Fullastimmar baserad på installerad effekt (utan parkeffekt)			4 800	
Parkeffekt		95%	1090752 MWh	
Årlig produktion vid tillgänglighet =		92%	1 003 492 MWh	
Utnyttjningstid, baserad på 55 kW		90%	3860 tim	
Real kalkylränta	6,0%			
Drift och Underhåll	0,6 Eurocent/kWh		6 422 kEuro/år	
Nättariff	0,0 Eurocent/kWh		0 kEuro/år	
Kapitalkostnad	4,5 Eurocent/kWh			
Produktionskostnad	5,1 Eurocent/kWh		0,05 Eurocent/kWh	
Kapitalkostnad, realt, annuitet:		0,0797	44 939 kEuro/år	
Summa kostnader:			51 361 kEuro/år	

	RESULTAT:
	Produktionskostnad utan investeringsstöd: Brutto:
DoU	0,64 Eurocent/kWh
Nättariff	0,00 Eurocent/kWh
kapitalkost.	4,48 Eurocent/kWh
Produktionskostnad =	5,12 Eurocent/kWh Brutto
Investering, Euro / kW =	2 169 Euro/kW
Specifik prod-kostnad, Euro/kWh,år =	0,56 Euro/kWh,år

Attachment 8

The drawings on the balanced system from West Maritime.

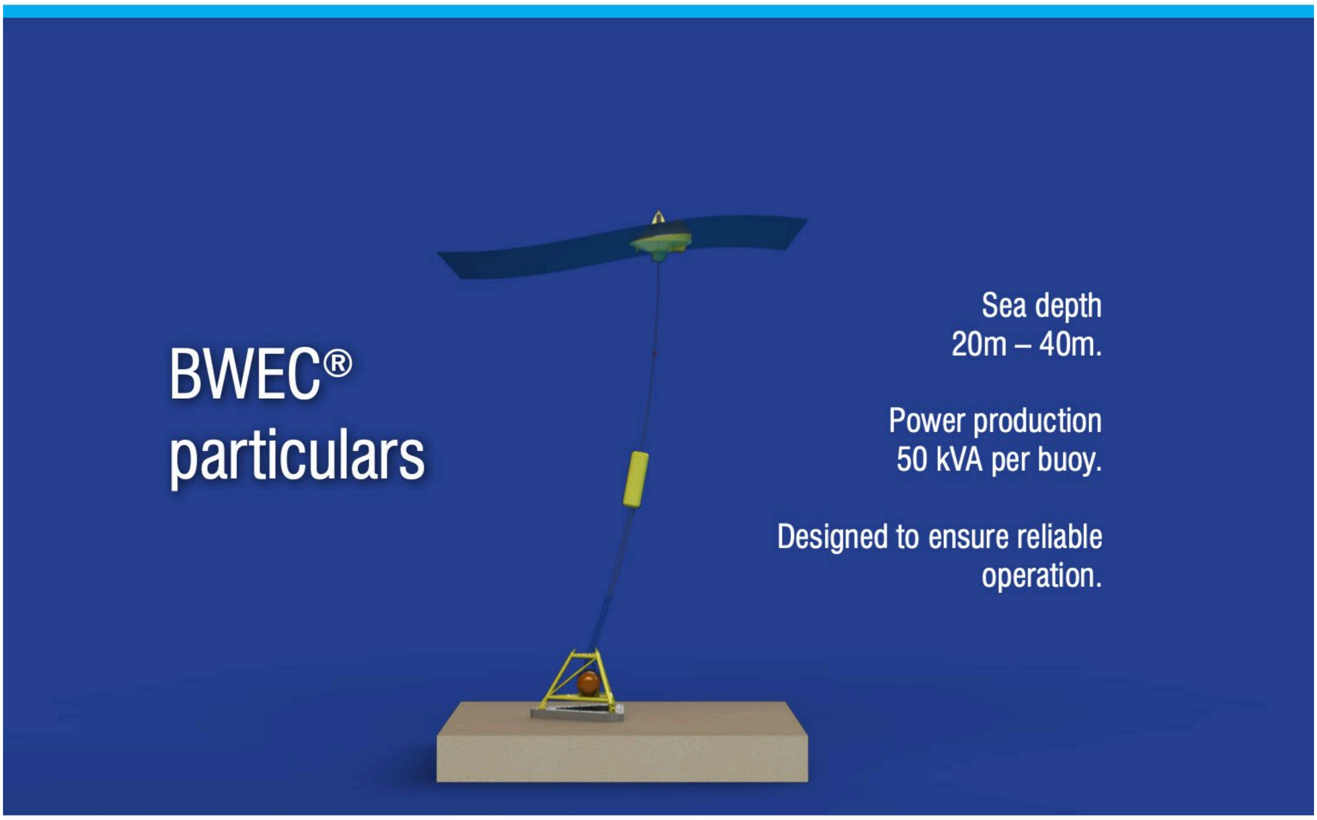

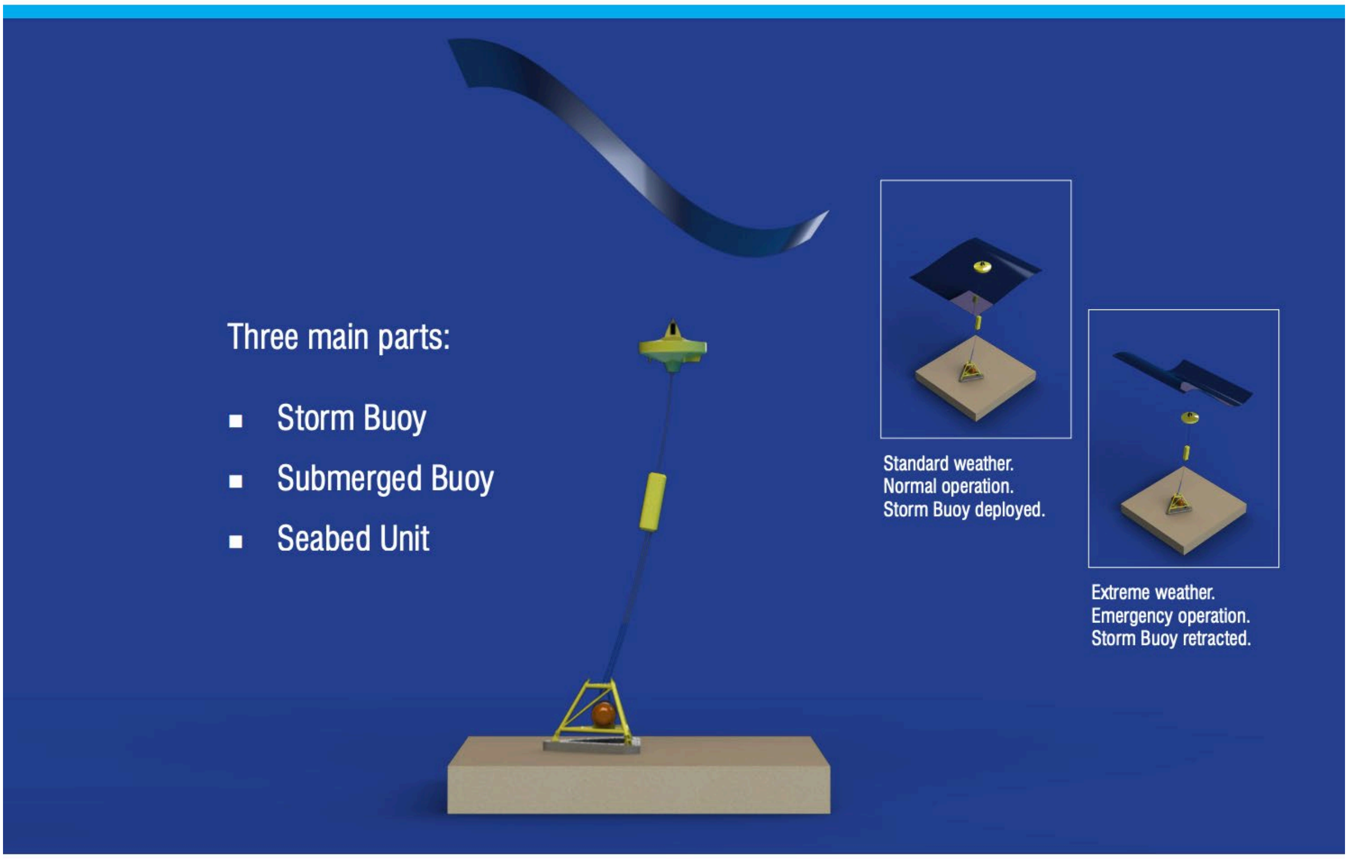
Three main parts:
Storm Buoy
Submerged Buoy
Seabed Unit
Standard weather.
Normal operation.
Storm Buoy deployed.
Extreme weather.
Emergency operation.
Storm Buoy retracted.

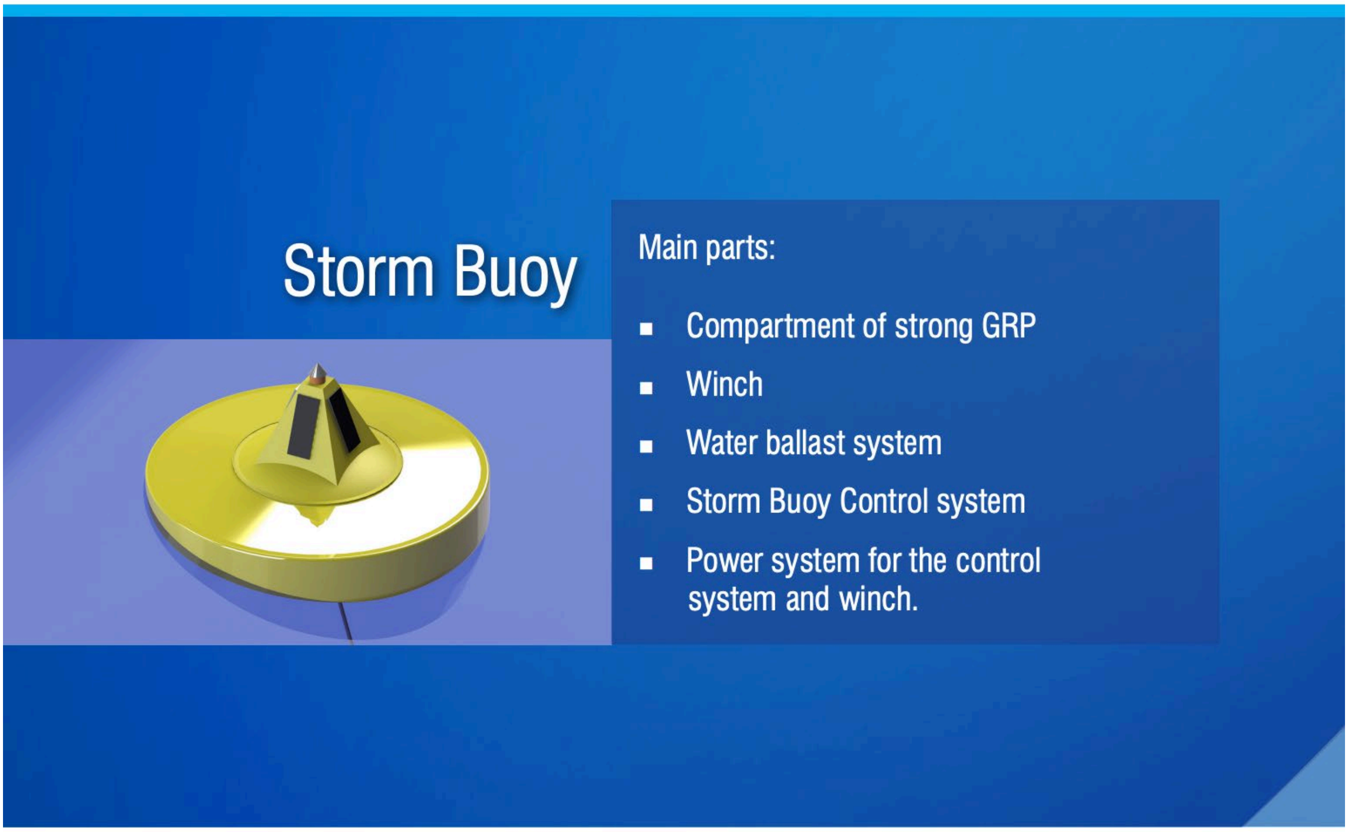
Storm Buoy
Main parts:
Compartment of strong GRP
Winch
Water ballast system
Storm Buoy Control system
Power system for the control system and winch.

Submerged Buoy

Main parts:

- Standard buoy approx. $3m^3$
- Modified to the concept

Seabed Unit

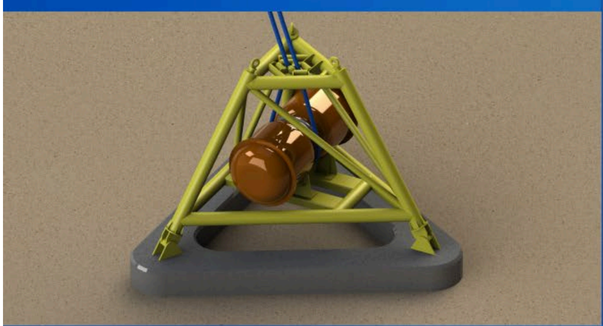

Main parts:

- Strong steel structure with quick release maintenance system.
- Concrete base foundation aprox. 30 tons.

- Two pressure compartments, each with a 25 kVA generator connected to a sheeve by a shaft.

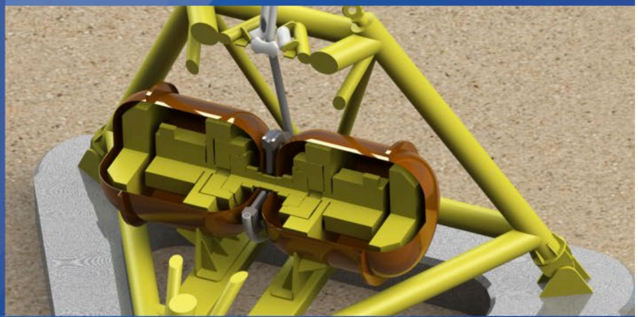

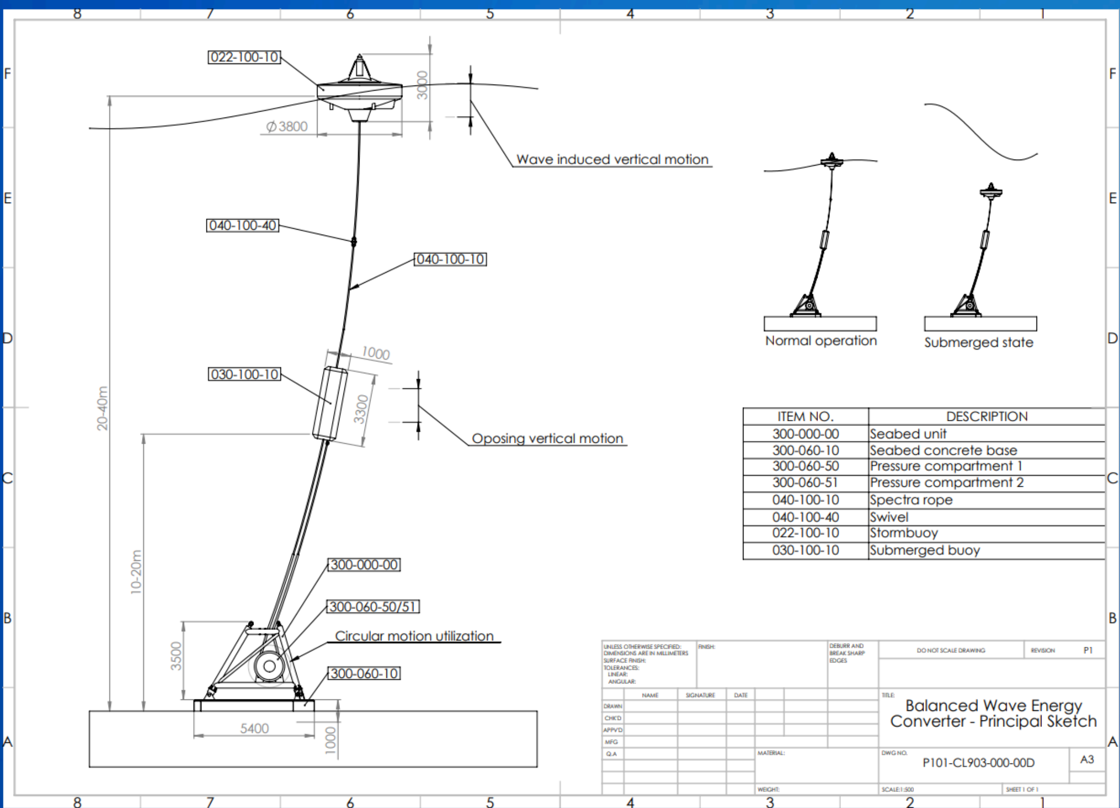

BWEC® system principal sketch

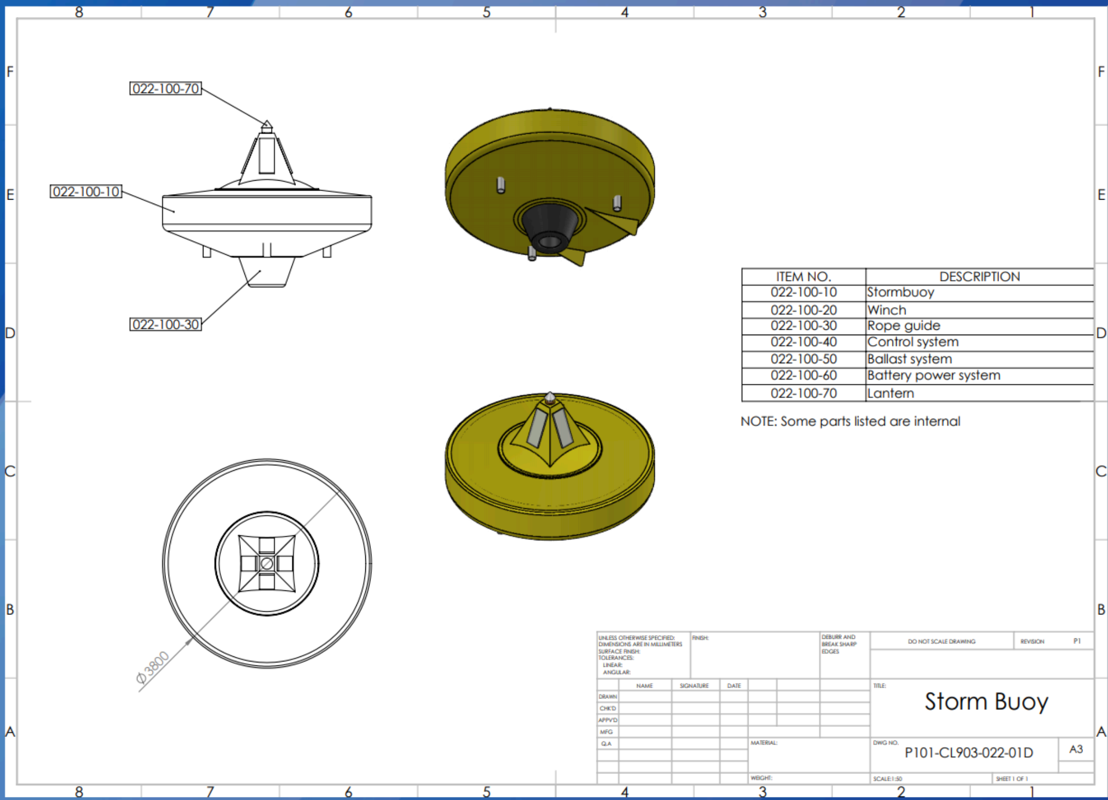

ITEM NO.	DESCRIPTION
022-100-10	Stormbuoy
022-100-20	Winch
022-100-30	Rope guide
022-100-40	Control system
022-100-50	Ballast system
022-100-60	Battery power system
022-100-70	Lantern

Storm Buoy outlines and systems

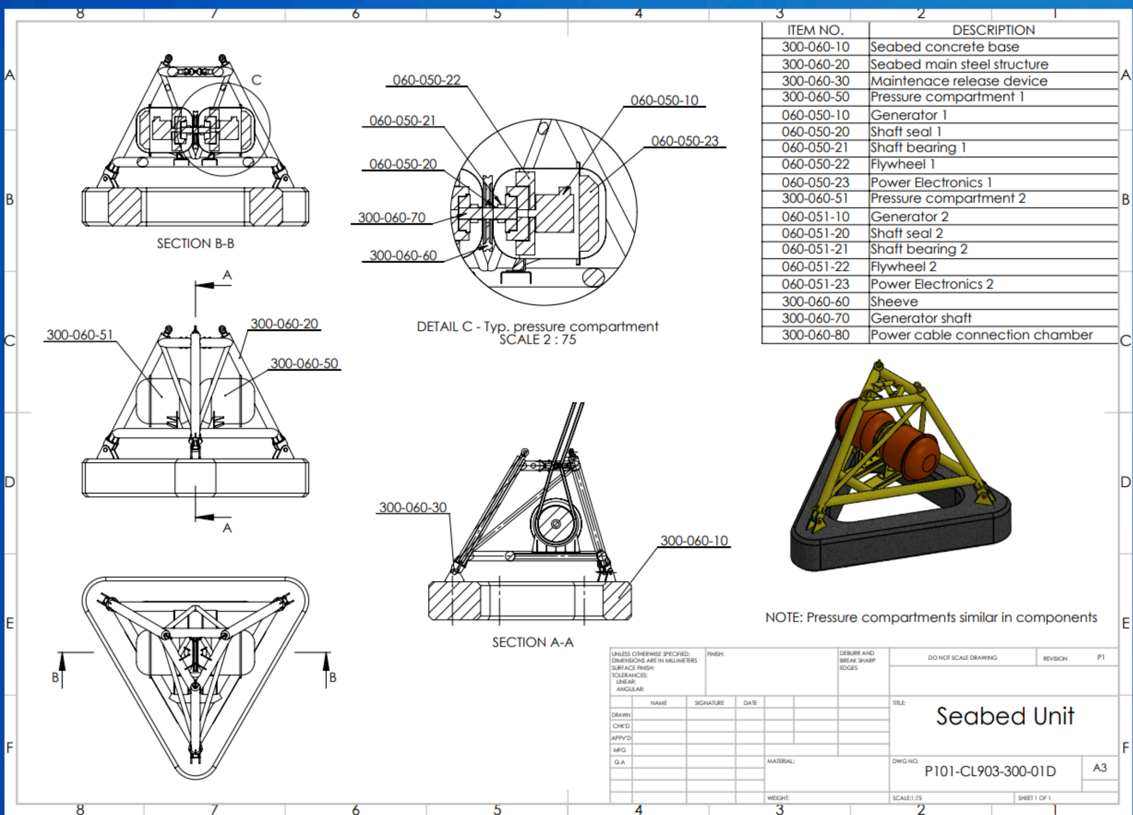

ITEM NO.	DESCRIPTION
300-060-10	Seabed concrete base
300-060-20	Seabed main steel structure
300-060-30	Maintenace release device
300-060-50	Pressure compartment 1
060-050-10	Generator 1
060-050-20	Shaft seal 1
060-050-21	Shaft bearing 1
060-050-22	Flywheel 1
060-050-23	Power Electronics 1
300-060-51	Pressure compartment 2
060-051-10	Generator 2
060-051-20	Shaft seal 2
060-051-21	Shaft bearing 2
060-051-22	Flywheel 2
060-051-23	Power Electronics 2
300-060-60	Sheeve
300-060-70	Generator shaft
300-060-80	Power cable connection chamber

Seabed Unit system components